Molecular mechanisms of coagulation across physiological and injury states

by

Chih-Jen Yang

A DISSERTATION

Presented to the Department of Biomedical Engineering

of the Oregon Health & Science University

School of Medicine

in partial fulfillment of the requirements for the degree of

Doctor of Philosophy

in Biomedical Engineering

March 2026

CERTIFICATE OF APPROVAL

This is to certify that the Ph.D. Dissertation of
Chih-Jen Yang
Molecular mechanisms of coagulation across physiological and injury states
has been approved

Mentor: Owen J. T. McCarty, Ph.D.
Professor of Biomedical Engineering

Member/Chair: Sandra Rugonyi, Ph.D.
Professor of Biomedical Engineering

Member: Zachary M. Working, M.D.
Associated Professor of Biomedical Engineering

Member: Belinda H. McCully, Ph.D.
Assistant Professor of Physiology,
Western University of Health Sciences

Member: Joseph J. Shatzel, M.D.
Associate Professor of Biomedical Engineering

Member: Lei Wang, Ph.D.
Assistant Professor of Biomedical Engineering

Acknowledgements

I would like to start by thanking my supervisor, Dr. Owen McCarty, for being my mentor during my PhD. He welcomed a student from far away and I am truly grateful for that. He has been a great mentor not only in science, but also in all aspects of life. His guidance has helped me become a better person.

Special thanks to my dissertation committee, Dr. Sandra Rugonyi, Dr. Zachary Working, Dr. Belinda McCully, Dr. Joseph Shatzel, and Dr. Lei Wang, for guiding my scientific career and helping bring my PhD to completion. I understand how it feels when listening to a young intern doctor present a case. Patience and kindness are essential.

Thanks to Dr. Joseph Aslan for all the interesting discussions on science. You are quite a different type of person compared to Owen. Yet your extensive knowledge of platelets and biochemistry is amazing and your questions during weekly lab meetings are something I enjoyed.

Special thanks to my mentor in the lab, Dr. Cristina Puy. I was truly amazed by your knowledge of the coagulation system, endothelial cells, and experimental design. Every time I shared a new idea, you could easily beat me. After years of training, I have grown from being shut down immediately to at least being able to defend my ideas for a few more minutes. For that, I am very grateful to be your student.

I would like to thank Jiaqing Pang (JP) for the countless Western blots you generated over the years! Many of the sticky notes on your bench were from me. Your knowledge in biochemistry is incredible. You are a fantastic cook, and I am also very impressed that you can read Traditional Chinese!

I thank Dr. André Lira Da Silva for the scientific input and discussions. Although you do not talk much in the lab, I have found that you are a fun person and a great cook, too.

I would also like to thank Dr. Aleksandr Shamanaev. Although I am about to leave as you joined this big family, I still learned a lot from our daily conversations. I wish I had more opportunities to ask you more questions.

I thank Dr. Jenny Wang. We come from the same place and share a similar background. It was always nice talking with you late in the evening, when it was already 7 pm and only the two of us were left in the lab.

I would like to thank my fellow lab members, Ethan Kelmser, Samantha Moellmer-Gomez, Yiheng Zhang, and Xu Zhang, for your companionship during my PhD. Every PhD student faces their own challenges and struggles through this journey, and I am glad we went through them together and supported each other. Especially Yiheng, you are a resilient girl I admire. Also thank you for listening to my moaning.

I would also like to thank former lab members Helen Vu and Alex Melrose, as well as the guy we currently rely on heavily, Vrishank Shivaprakash, for all the help in the lab. Alex, although I do not always agree with your political views and philosophy, I enjoyed the time hanging out with you. Also thanks to former lab members: Dr. Iván Parra-Izquerdo, Dr. Stéphanie Reitsma, Dr. Hari Hara Sudhan Lakshmanan, Dr. Tony Zheng, Dr. Tia Kohs, Dr. Helena Ventosa, Ting Liu, and Kelly Jordan. Every time I searched for information on PubMed and found papers with your names and our lab's, I felt a sense of pride. Your work paved the path for mine. I would also like to thank all the folks on the BME 13th floor for their contribution in donating blood. I especially want to thank the neighboring Hinds' lab, Nakayama's lab, and Yantansee's lab.

I would like to thank my undergraduate students, Amelia Rodolf from the University of California and Micki Geffert from the Rochester Institute of Technology, for their enthusiasm and for giving me the opportunity to share the curiosity of research with them.

Special thanks also go to my collaborators, Dr. Jamie Lo, Dr. Michael Hutchens, and Dr. Martin Schreiber. Without you, I would never have had the chance to work with non-human primates and pigs in a clinical setting. I also thank my collaborators at Vanderbilt University, Scripps Institute, and Aronora Inc. for your valuable insights into my research.

I would also like to thank the BME staff: Mr. Alex Breiding, Ms. Margaux Schwartz, and Ms. Alyssa Yadao. You have been exceptionally helpful from the very first day, from assisting with course registration, handling invoices for international conference travel, to coordinating room reservations for defense. I am deeply grateful for everything you have done to make my years in the program run so smoothly.

I would like to thank the hospital that supports me during this journey and that I will serve again soon, Tri-Service General Hospital, for guiding me through both this academic process and my experience in the United States. I am very fortunate to have the opportunity to bring what I have learned here back with me and to explore more exciting new science.

Last but not least, I would like to express my deepest gratitude and love to my beautiful wife, Tien-Yun. Throughout this long journey, you have been the one holding everything together when my time and energy were consumed by experiments and writing. Your patience, strength, and support made it possible for me to reach this milestone. You are my torch when the path feels dark, my pillar when things feel uncertain, and my constant source of warmth and encouragement. You remind me what truly matters in life. After all these years, you remain my love, my greatest blessing, and my wonderwall.

Table of contents

List of figures

List of tables

List of abbreviations

aPTT	activated partial thromboplastin time
BSA	bovine serum albumin
BK	bradykinin
CD62P	P-selectin
CTI	corn trypsin inhibitor
DAMP	Damage-associated molecular pattern
DIC	Disseminated intravascular coagulation
DNA	deoxyribonucleic acid
ECM	extracellular matrix
ELISA	Enzyme-Linked Immunosorbent Assay
FII	coagulation factor II (prothrombin)
FIIa	activated coagulation factor II (thrombin)
FV	coagulation factor V (zymogen)
FVa	activated coagulation factor V
FVII	coagulation factor VII (zymogen)
FVIIa	activated coagulation factor VII
FVIII	coagulation factor VIII (zymogen)
FIX	coagulation factor IX (zymogen)
FIXa	activated coagulation factor IX
FX	coagulation factor X (zymogen)
FXa	activated coagulation factor X
FXI	coagulation factor XI (zymogen)
FXIa	activated coagulation factor XI

FXII	coagulation factor XII (zymogen)
FXIIa	activated coagulation factor XII
HK	high-molecular weight kininogen
HKa	cleaved high-molecular weight kininogen
INR	International normalized ratio of PT values
LPS	lipopolysaccharide
NETs	neutrophil extracellular traps
NF-κB	nuclear factor kappa-light-chain-enhancer of activated B cells
PAR	protease-activated receptor
PBS	Phosphate-Buffered Saline
PK	prekallikrein
PKa	kallikrein
PolyP	polyphosphates
PPACK	Phe-Pro-Arg-chloromethylketone, protease inhibitor
PPP	platelet-poor plasma
PS	phosphatidylserine
PT	prothrombin time
TEG	thromboelastography
TF	tissue factor
tPA	tissue plasminogen activator
TIC	Trauma-induced coagulopathy
TRAP-6	thrombin receptor-activating peptide 6

Abstract

Molecular mechanisms of coagulation across physiological and injury states

Chih-Jen Yang

Department of Biomedical Engineering

School of Medicine

Oregon Health & Science University

February 2026

Thesis Advisor: Owen J. T. McCarty, Ph.D.

Coagulation is a tightly regulated biological process essential for maintaining hemostasis while preserving uninterrupted blood perfusion to vital organs. Dysregulation of this delicate balance contributes to several leading causes of morbidity, including cardiovascular disease, trauma, and stroke. Beyond clot formation, the coagulation system is also intricately linked to inflammation and immune responses, interacting with platelets, endothelial cells, biological surfaces, and damage-associated molecular patterns. The goal of this work is to define how coagulation is modulated across physiological and pathological contexts, and to identify mechanisms by which thrombosis and inflammation can be selectively targeted without compromising hemostasis.

The first chapter focuses on the contact pathway of coagulation, specifically investigating the interaction between activated factor XI (FXIa) and high-molecular-weight kininogen (HK). Both FXI and prekallikrein bind to HK and form stable complexes in the circulation. While HK cleavage by kallikrein is a well-established source of the proinflammatory mediator bradykinin, the fate of HK following FXI activation has remained poorly defined. Using biochemical assays, proteomic analyses, and monocyte-based inflammatory signaling studies, we demonstrate that FXIa cleaves HK in a

manner distinct from kallikrein and generates bradykinin more slowly, while preferentially releasing domain 5, a HK fragment that is implicated in monocyte activation, lipopolysaccharide spreading, and lymphocyte chemotaxis. Importantly, polyphosphates, an established molecule from bacteria and activated platelets in triggering contact pathway, bind to domain 5 of HK and selectively enhance FXIa-mediated HK cleavage within domain 5, suggesting a mechanism by which FXI-driven inflammation may be amplified during bacterial sepsis and platelet activation.

The second chapter extends to the characterization of the procoagulant phenotype of one of the most procoagulant body fluid, amniotic fluid, across gestation in human and rhesus macaque. Using untargeted proteomics, lipidomics, and functional coagulation assays, we show that amniotic fluid from both species exhibits a potent and dynamic procoagulant activity throughout gestation. This procoagulant activity is largely phospholipid-dependent, providing mechanistic insight into the wide-spread coagulation activation and consumptive coagulopathy observed in amniotic fluid embolism.

The third chapter examines how pathological conditions reshape the coagulation phenotype, focusing on post-trauma hypercoagulability. We identify skeletal muscle myosin as a previously underappreciated modulator of post-trauma coagulation. Skeletal muscle myosin has been shown to exert procoagulant activity by enhancing prothrombin activation. However, despite being released during tissue injury, circulating myosin levels paradoxically decrease after trauma. We demonstrate that skeletal muscle myosin binds directly to fibrin and becomes sequestered within the forming fibrin clot. This entrapment increases clot resistance to fibrinolysis and explains reduced plasma myosin levels, highlighting a novel mechanism contributing to post-trauma hypercoagulability.

Together, these three chapters establish a continuum from physiological regulation and pathological dysregulation of coagulation, highlighting how the coagulation system functions within a complex biological environment and plays essential roles in both health and disease.

Chapter 1. Introduction to Coagulation

1.1 Overview

Blood coagulation is a tightly regulated biological process that plays a central role in maintaining vascular integrity following injury. Under physiological conditions, coagulation activation rapidly generates a fibrin-rich clot that stabilizes platelet aggregates and limit blood loss, a process known as hemostasis. At the same time, coagulation must remain appropriately controlled to avoid pathological thrombus formation that can obstruct blood flow. Achieving this balance requires sophisticated coordination among plasma coagulation factors, surrounding molecules, and blood cells.

Most coagulation proteins circulate in plasma as zymogens. Upon vascular injury or exposure to foreign surfaces, these zymogens are sequentially activated through proteolytic cleavage, culminating in the generation of thrombin.[1] Thrombin is a central effector of coagulation. It converts soluble fibrinogen into insoluble fibrin, activates platelets, and amplifies its own generation by activating upstream coagulation factors (Figure 1.1). The formation of stable fibrin network provides mechanical strength to the developing clot.[2]

Traditionally, the coagulation process is described as a cascade initiated through intrinsic or extrinsic pathways that ultimately converge into the common pathway. While this framework remains useful for conceptual understanding, it is now clear that coagulation *in vivo* is a highly dynamic process that integrates signals from circulating inflammatory mediators, microvesicles, platelets, endothelial cells, immune cells, and even microorganism. For example, activation of coagulation enzymes leads to thrombin generation, which both potently converts fibrinogen into fibrin and activates platelets, thereby stabilizing platelet aggregates into a tightly packed clot.[3] In parallel, lipopolysaccharide, a bacterial membrane component, can act as a regulator of contact pathway activation during infection.[4]

Beyond its role in hemostasis, coagulation is closely intertwined with inflammation, innate immunity, and tissue repair.[5] Activated coagulation proteases can signal through protease-activated receptors on endothelial cells and leukocytes, thereby regulating vascular permeability, cytokine production, and leukocyte recruitment.[6] In this context, coagulation functions not only as a hemostatic mechanism but also as an integral component of host defense, a process often referred to as immunothrombosis.[7,8] Fibrin formation and localized thrombin generation can help confine pathogens and inflammatory cells within the vasculature, limiting microbial spreading and coordinating immune responses. Conversely,

inflammatory stimuli reciprocally affect coagulation by altering endothelial anticoagulant function, suppressing fibrinolysis, and enhancing procoagulant tissue factor expression on immune cells.

Subsequent sections will describe the coagulation cascade in greater detail, including the intrinsic, extrinsic, common pathways, fibrinolysis, platelet-coagulation interactions, and the interplay between coagulation and inflammation. Together, these concepts establish the foundation for understanding how coagulation functions in health and how its dysregulation contributes to disease.

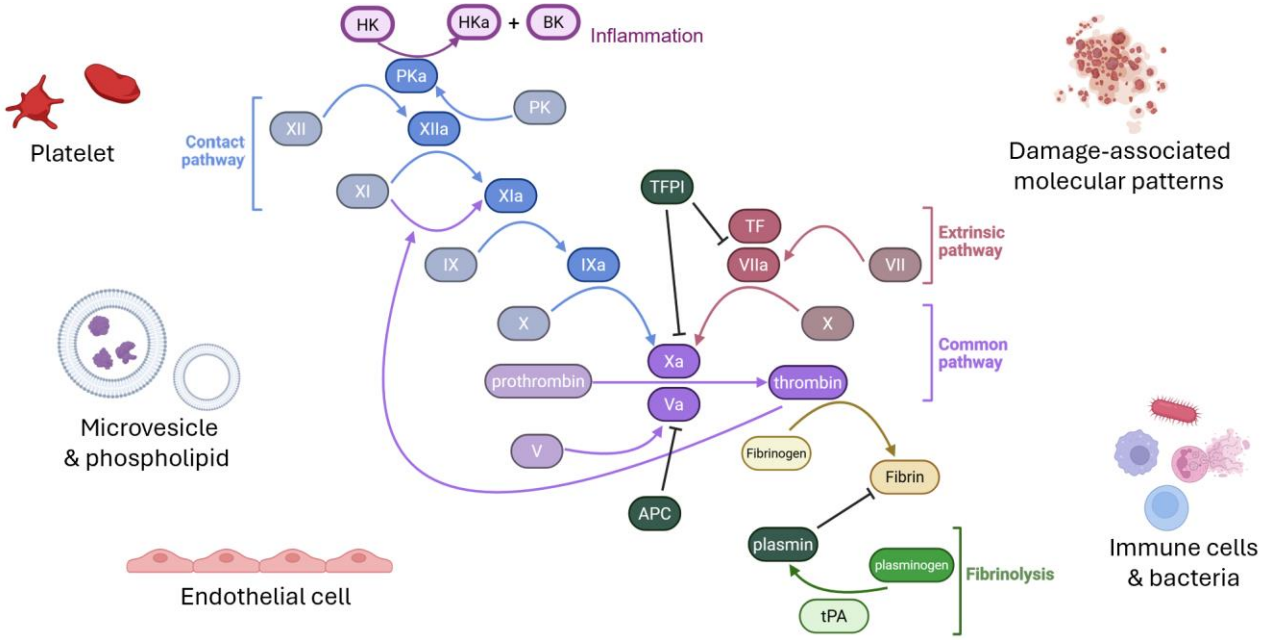

Figure 1.1 Schematic of coagulation cascade. Created with BioRender.com.

1.2 Coagulation in morbidity and mortality

Coagulation plays a central role in many of the leading causes of death worldwide and is a major determinant of both mortality and long-term morbidity.[9] Approximately one in three deaths is attributed to conditions such as heart disease, trauma, or stroke.[10] These conditions are closely linked to dysregulated coagulation, which bring a tremendous burden on the healthcare system. Current antithrombotic therapies target key enzymes in the coagulation cascade, such as thrombin and activated factor Xa (FXa), and have been highly effective in the prevention and treatment of

thrombotic disease.[11] However, as these coagulation enzymes are also essential for normal hemostasis, their inhibition is inherently associated with an increased risk of bleeding which might lead to severe and life-threatening hemorrhage. Although newly developed direct oral anticoagulants offer improved safety profiles compared with older therapies, clinically significant bleeding remains common and limits their use in many patients.[12] These challenges highlight the need for anticoagulant strategies that more precisely separate antithrombotic efficacy from bleeding risk.[13]

1.3 Coagulation Cascades

Blood coagulation is traditionally described as distinct pathways that ensure a rapid but regulated hemostatic response to vascular injury.

1.3.1 *Extrinsic pathway*

The extrinsic pathway of coagulation is initiated by the exposure of tissue factor (TF), a transmembrane glycoprotein that forms a complex with circulating factor VII/VIIa (FVII/FVIIa) to trigger thrombin generation following vascular injury.[14] Under physiological conditions, TF is expressed by cells in the subendothelial layer of the vessel wall and is physically separated from the circulation by endothelium. 1 %-4 % of FVII already circulates in plasma in the active form FVIIa ready to serve coagulation when TF is exposed**.**[15] Following endothelial injury, exposure of TF leads to formation of the TF-FVIIa complex, which initiates coagulation by activating both factor X (FX) and factor IX (FIX), resulting in the generation of trace amounts of thrombin. This initial thrombin production ignites the fuse of amplification phase by activating the cofactors factor V (FV) and factor VIII (FVIII), increasing thrombin generation by several orders of magnitude (Figure 1.2). In the presence of calcium and phospholipid surfaces, the tenase and prothrombinase complexes are subsequently assembled. The tenase complex, composed of activated FIX (FIXa), FX, and activated FVIII (FVIIIa), accelerates further activation of FX.[16] FXa then associates with prothrombin and

activated FV (FVa) to form the prothrombinase complex, which efficiently converts prothrombin into thrombin and drives robust clot formation.[3]

A hallmark of the extrinsic pathway coagulation enzymes is that they are vitamin K-dependent. Vitamin K is required for a post-translational γ-carboxylation reaction that converts specific glutamate (Glu) residues to γ-carboxyglutamate (Gla) residues within these coagulation enzymes.[17] This modification is essential for the formation of the Gla domain, which enables vitamin K-dependent coagulation factors to bind negatively charged phospholipid surfaces, such as phosphatidylserine (PS) to achieve optimal enzymatic activity.[18] The vitamin K-dependent coagulation factors include prothrombin (FII), FVII, FIX, FX, as well as the regulatory protein C and protein S. Deficiency of vitamin K disrupts this process and impairs coagulation function, a phenomenon similarly observed during warfarin therapy. Warfarin inhibits the vitamin K epoxide reductase complex in the liver and consequently limits the production of functional vitamin K-dependent coagulation factors in the liver.

During the amplification phase of thrombin generation, thrombin also activates factor XI (FXI), a component of the intrinsic pathway of coagulation. Activated factor XI (FXIa) subsequently activates FIX (Figure 1.2).[19] In contrast to the tenase and prothrombinase complexes, FIX activation by FXIa does not require a phospholipid surface. FIX is a 55 kDa protein composed of a heavy chain and a light chain. Deficiency of FIX results in the bleeding disorder hemophilia B, whereas deficiency of the tenase cofactor FVIII leads to hemophilia A.[20]

Regulation of the extrinsic pathway is primarily mediated by tissue factor pathway inhibitor, a Kunitz type protease inhibitor that suppresses the activity of the TF-FVIIa complex as well as FXa.[21] In addition, FVa and FVIIIa are inactivated by activated protein C, which is generated when thrombin binds thrombomodulin on the endothelial surface.[22]

The ultimate function of the extrinsic pathway is the rapid formation of a hemostatic clot that limits blood loss following endothelial barrier disruption. Thrombin, the final enzymatic product of both the extrinsic and intrinsic coagulation pathways, converts fibrinogen into fibrin fibers that provide structural stability to the clot. Fibrinogen is a large 340 kDa hexameric homodimer that circulates in plasma at concentrations of 2 to 4 mg per milliliter. The structure consists of two sets of three disulfide linked polypeptide chains, Aα, Bβ, and γ.[23] Thrombin-mediated proteolysis converts fibrinogen into fibrin, which is subsequently crosslinked and fortified by coagulation factor XIII.[24]

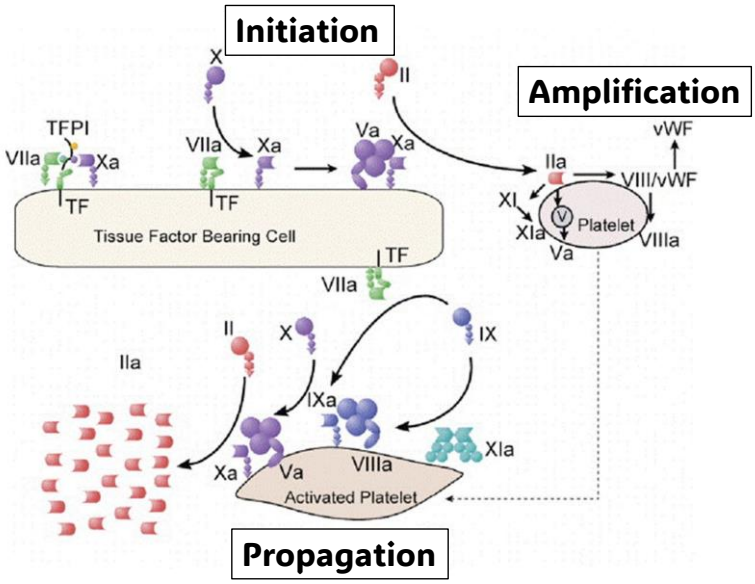

Figure 1.2 Cell-based model of coagulation.
A cell-based model of coagulation has three distinct phases: initiation, amplification and propagation.
Adapted from Becker. Factor Xa inhibitors: critical considerations for clinical development and testing. J Thromb Thrombolysis (2021). Reprinted with permission.

1.3.2 *Intrinsic pathway*

While the extrinsic pathway of coagulation triggers a rapid response and drives early fibrin formation, an alternative pathway can also be activated to generate FXa and thrombin. The intrinsic pathway of coagulation, also known as the contact pathway, is initiated by surface-dependent activation of factor XII (FXII), leading to activation of prekallikrein and FXI and subsequent amplification of thrombin

generation.[13,25] Although long considered dispensable for normal hemostasis given the absence of spontaneous bleeding in FXII deficiency and only mild bleeding phenotype associated with FXI deficiency, growing evidence demonstrates that this pathway plays an indispensable role in pathological thrombosis.[26,27] Contact pathway components can be activated on a variety of biologically relevant surfaces, including foreign biomaterials, activated platelets, neutrophil extracellular traps, extracellular nucleic acids, bacterial products, and polyphosphates, enabling coagulation to be triggered in inflammatory and infectious settings.[28] In parallel, activation of FXII and prekallikrein engages the kallikrein-kinin system, resulting in bradykinin release, vascular permeability increase, leukocyte recruitment, and proinflammatory cytokine production.[29] These interconnected mechanisms establish the intrinsic pathway functions as a molecular link between coagulation and inflammation and contribute to thromboinflammatory disease states such as sepsis and device-associated thrombosis. Importantly, inhibition of contact pathway coagulation factors markedly attenuates inflammation and improves survival in preclinical models of sepsis. This finding identifies the intrinsic pathway as a promising therapeutic target in sepsis.[30] The following sections of this thesis will introduce the individual coagulation enzymes of the contact pathway in detail.

Factor XII

FXII is a 80 kDa glycoprotein synthesized in the liver and circulates in plasma at a concentration of about 400 nM. Within the coagulation system, the primary function of FXII is to initiate the intrinsic pathway through activation of FXI. In addition to FXI, activated FXII (FXIIa) cleaves several other substrates, including plasma prekallikrein, plasminogen, and the complement components C1r and C1s, thereby linking coagulation with fibrinolytic and complement pathways.[29,31,32]

FXII zymogen can undergo autoactivation upon exposure to negatively charged surfaces or be cleaved by plasma kallikrein. Proteolytic cleavage at arginine 353 generates α FXIIa which consists of a heavy

and light chain connected by disulfide bonds and retains the ability to support contact dependent coagulation.[33] Further cleavage at arginine 334 produces β FXIIa, a truncated form that no longer binds negatively charged surfaces. Although β FXIIa lacks procoagulant activity via FXI activation, it remains enzymatically active and promotes kallikrein generation and thus amplifies inflammatory signaling. In plasma, FXIIa activity is tightly regulated by C1 inhibitor and antithrombin.[34] Upon binding to either inhibitor, FXIIa forms a stable complex that leads to loss of its enzymatic activity.[31]

Notably, congenital FXII deficiency does not result in a bleeding phenotype, indicating that FXII is dispensable for physiological hemostasis. Nonetheless, dysregulated FXII activation has been strongly linked to inflammatory diseases. Gain of function mutations in FXII are a known cause of hereditary angioedema which results in excessive bradykinin generation and vascular permeability.[35] In sepsis, FXII holds a critical upstream position in the contact pathway where it can be triggered by bacterial surfaces, polyphosphates, extracellular nucleic acids, and damaged host cells.[4,36,37] Experimental models of sepsis demonstrate that FXII driven-contact activation contributes to thrombin generation, proinflammatory cytokine release, hypotension, and organ injury, whereas inhibition or genetic deletion of FXII attenuates inflammation and improves survival without increasing bleeding risk.[32]

Factor XI

FXI is a structurally unique protease zymogen that circulates as a homodimeric glycoprotein of approximately 160 kDa.[19] FXI shares ~60% sequence homology with plasma prekallikrein (PK), reflecting its evolutionary origin from duplication of the KLKB1 gene during mammalian evolution, which distinguishes FXI from other coagulation proteases (Table 1.1).[38,39] FXI is synthesized predominantly by hepatocytes and secreted into circulation. It is present at a plasma concentration of approximately 30 nM. Structurally, each FXI monomer consists of four N-terminal apple domains (A1-A4) and a C-terminal serine protease domain, with the two subunits covalently linked via a

disulfide bond at Cys321, forming a stable homodimeric complex (Figure 1.3).[40,41] The apple domains serve as platforms for protein-protein interactions, mediating binding to substrates, cofactors, and cellular surfaces, while the catalytic serine protease domain contains the active site required for proteolytic activity.[42]

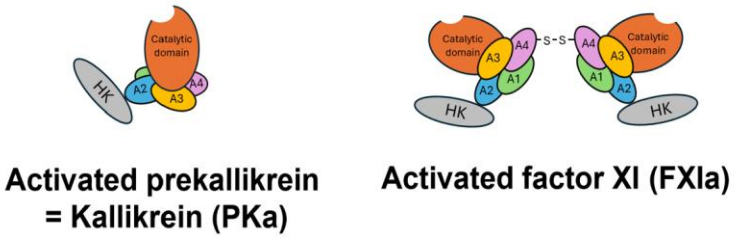

Domain	Identities	Positives	Gaps
Apple 1	47/84 (56%)	64/84 (76%)	0/84 (0%)
Apple 2	45/84 (54%)	60/84 (71%)	0/84 (0%)
Apple 3	45/84 (54%)	60/84 (71%)	0/84 (0%)
Apple 4	44/84 (52%)	55/84 (65%)	0/84 (0%)
Catalytic	161/236 (68%)	194/236 (82%)	0/236 (0%
Average	**342/572 (60%)**	**433/572 (75%)**	**0/572 (0%**

Figure 1.3 & Table 1.1 Structure of contact pathway proteins PK and FXI. Comparison of sequences in different domains between PK and FXI
There is 60% sequence homology between FXI and PK. Both consists of 4 apple (A) domains combined with a catalytic domain. However, FXI zymogen circulates in circulation as a dimer. Protein sequence data were obtained from UniProt, and sequence alignments were performed using the NIH BLAST database.

Activation of FXI to the active protease FXIa occurs through proteolytic cleavage at Arg369-Ile370, a process that induces significant conformational rearrangements within the dimer.[38] In plasma, the majority of FXI circulates in complex with high-molecular-weight kininogen (HK), which facilitates localization to negatively charged surface and cellular interface, thereby promoting efficient activation.[43] Upon conversion to FXIa, it dissociates from HK and initiate downstream substrate activation. Functionally, FXI plays a central role in the amplification phase of thrombin generation.[44] FXI can be activated by FXIIa within the intrinsic pathway or by thrombin generated through the extrinsic pathway, a process referred as the FXI-thrombin feedback loop.[45] Through these activation mechanisms, FXI serves as a molecular link between coagulation initiation and propagation (Figure 1.2).[13] The principal physiological substrate of FXIa is FIX; however, FXIa has also been shown to activate FX *in vitro*, enhance thrombin generation through activation of the cofactors FV and FVIII, and promote coagulation by proteolytic inactivation of TFPI, linking intrinsic and extrinsic pathways.[46-48]

Clinically, FXI deficiency is named hemophilia C.[49,50] In contrast to hemophilia A or B, FXI deficiency is associated with a relatively mild bleeding diathesis and spontaneous bleeding being uncommon.[51] Instead, bleeding typically manifests following surgical or traumatic challenges, particularly in tissues with high fibrinolytic activity, such as the nasal mucosa, oral cavity, and urinary tract.[51,52] This clinical phenotype underscores the concept that FXI is also dispensable for baseline hemostasis but becomes increasingly important for thrombin amplification and clot stabilization under hemostatic stress.[13]

Beyond hemostasis, growing evidence implicates FXI as a mediator of thromboinflammation during sepsis, a pathological state of excessive activation of coagulation and inflammation that culminates in organ dysfunction.[7,8] In experimental models of sepsis, pharmacological inhibition of FXI or FXIa attenuates coagulation activation and inflammatory injury, improving survival and reducing organ damage in preclinical sepsis models without causing significant bleeding.[27] These findings support the concept that targeting FXI may provide a safer antithrombotic and anti-inflammatory strategy in sepsis with the potential to selectively suppress pathological coagulation and inflammation while preserving physiological hemostasis.[53,54]

It is also worth noting that recent studies have associated FXI with cardiac homeostasis and heart failure.[55,56] Preclinical studies in murine models of heart failure suggest that FXI may play a cardioprotective role. In contrast, large-scale human genetic and Mendelian randomization analyses do not support a causal association between reduced FXI levels and an increased risk of heart failure.[57] These findings are reassuring for the development of FXI-targeted therapies, yet the potential cardiac effects of pharmacologic FXI inhibition, particularly in older patients or those with established heart failure, warrant further clinical evaluation.

1.3.3 *The Kallikrein-Kinin system*

As discussed previously, the contact pathway is closely linked to inflammatory processes and contributes to host defense as well as pathological inflammation.[8,29] The kallikrein-kinin system constitutes another major inflammatory arm of the contact pathway and the generation of the well-recognized proinflammatory peptide bradykinin (BK).[58] BK is produced through reciprocal activation of FXIIa and plasma kallikrein (PKa), with PKa cleaving HK to release BK (Figure 1.4A). Structurally, HK serves as a multifunctional scaffold in the contact system, with domain 6 of HK binding FXI and PK to form stable plasma complexes, while domain 5 mediates HK binding to negatively charged cellular or extracellular surfaces, facilitating the assembly and localization of contact pathway components.[59] Bradykinin signals through two G protein-coupled receptors, B2R and B1R, expressed primarily on the endothelial surface and immune cells.[60] The activity of bradykinin is tightly regulated by rapid enzymatic degradation by angiotensin-converting enzyme (Figure 1.4B). Dysregulated bradykinin generation is a hallmark of hereditary angioedema, characterized by recurrent episodes of localized mucosal and cutaneous edema.[61,62] Although HK is primarily cleaved by PKa, other proteases, including plasmin, FXIa, thrombin, and mannose-binding lectin-associated serine protease-1have also been reported to cleave HK.[63-65]

(A) **(B)**

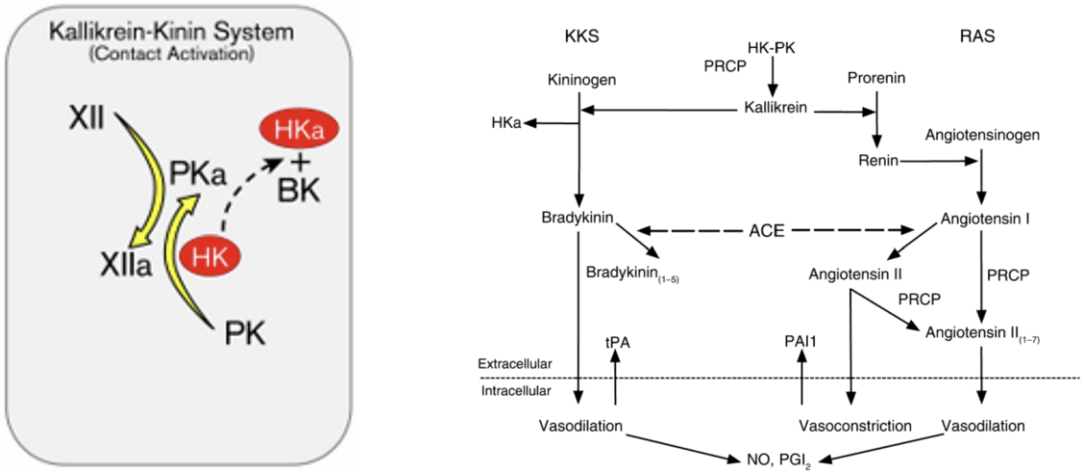

Figure 1.4 Kallikrein-kinin system.
Generation of the vasoactive peptide bradykinin (BK) is mediated by the proteolytic conversion of HK by PKa. The reciprocal activation between FXII and PK will lead to PKa. (A) was from Ponczek et al., The evolution of factor XI and the kallikrein-kinin system. Blood advances (2020). (B) was from Schmaier. The plasma kallikrein-kinin system counterbalances the renin angiotensin system. J Clin Invest (2002). Reprinted with permission.

1.3.4 *Fibrinolysis*

Once a hemostatic plug has formed, it is essential to appropriately dissolve the clot to restore vascular patency and initiate wound healing after the initial vascular breach has been repaired.[66,67] The fibrinolytic system is responsible for fibrin clot remodeling and lysis, with plasmin serving as its central effector enzyme (Figure 1.5).[68,69] Plasmin is produced from its zymogen plasminogen, through proteolytic activation by tissue-type plasminogen activator (tPA) and urokinase-type plasminogen activator (uPA), as well as PKa and FXIIa.[70] Localization of plasminogen to the fibrin surface markedly enhances plasmin generation, thus confining fibrinolysis to sites of clot formation.[71,72]

As mentioned above, the principal function of plasmin is degradation of fibrin, which maintains vascular patency and prevents excessive clot persistence. In addition, plasmin degrades components of the extracellular matrix and basement membrane, contributing to tissue remodeling and wound repair.[73,74] Given its broad proteolytic activity, plasmin is tightly regulated to prevent excessive tissue damage. Once generated, plasmin is rapidly inhibited and cleared from the circulation by α2-

antiplasmin and α2-macroglobulin.[75,76] In parallel, upstream modulation of plasmin is achieved through inhibition of tPA and uPA by plasminogen activator inhibitor-1 and -2, providing an additional layer of regulation over fibrinolytic activity (Figure 1.5).[77] Dysregulation of this finely balanced system can lead to either hyperfibrinolysis, contributing to bleeding, or fibrinolysis shutdown, which promotes pathological thrombosis.[78,79]

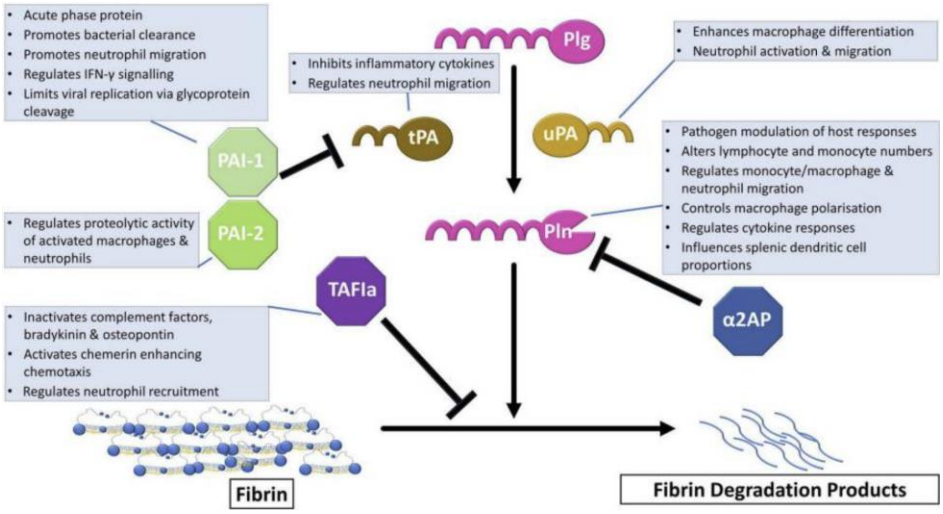

Figure 1.5 Overview of the fibrinolytic system and its regulation.
Plasminogen (Plg) is converted to the active enzyme plasmin (Pln) through cleavage by tPA or uPA. This activation step is regulated by plasminogen activator inhibitor-1 (PAI-1), the primary physiological inhibitor, as well as plasminogen activator inhibitor-2 (PAI-2). Plasmin degrades crosslinked fibrin into fibrin degradation products that are cleared from the circulation. Plasmin activity is further controlled by α2-antiplasmin (α2AP), which inhibits plasmin through formation of an inhibitory complex. Activated thrombin-activatable fibrinolysis inhibitor (TAFIa) suppresses fibrinolysis by removing C-terminal lysine residues required for plasminogen binding to fibrin. Boxes indicate additional roles of fibrinolytic components in immune regulation. From Whyte et al. All tangled up: interactions of the fibrinolytic and innate immune systems. Frontiers in Medicine (2023). Reprinted with permission.

1.4 Platelet Biology Overview

Besides the coagulation system, platelets are also a key component of the hemostatic response and contribute to inflammatory and thrombotic processes.[80,81] Platelets are small, anucleate fragments derived from bone marrow megakaryocytes that rapidly accumulate at sites of

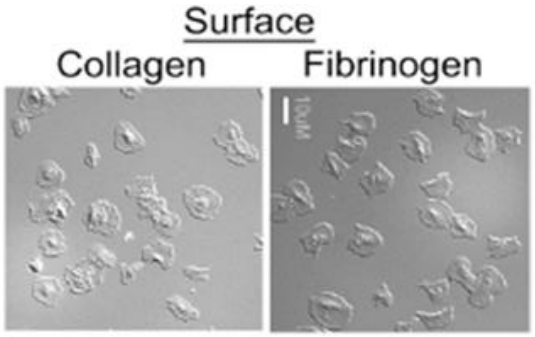

Figure 1.6 Static adhesion of platelets.
Platelets were then immobilized on fibrinogen- or collagen-coated coverslip surface.

vascular injury.[82] In primary hemostasis, platelets adhere to exposed subendothelial matrix proteins, aggregate to form a platelet plug, and provide a membrane surface that supports coagulation reactions, thereby stabilizing the developing clot (Figure 1.6).[83,84] Although traditionally viewed mainly in bleeding control, platelets are now recognized as active regulators of immune and inflammatory responses.[85,86]

Platelet activation is initiated by endothelial disruption and exposure of extracellular matrix components such as collagen and von Willebrand factor.[87] Adhesion and aggregation are mediated by platelet surface receptors, including GPIbα and integrins, followed by cytoskeletal reorganization and granule secretion.[88,89] Activated platelets then externalize phosphatidylserine, creating a procoagulant membrane that supports assembly of the tenase and prothrombinase complexes and promotes thrombin generation.[90,91] Through these mechanisms, platelets not only limit blood loss but also enhance fibrin formation and clot stability.[71]

In addition to their hemostatic function, platelets participate directly in inflammatory and immune responses. The multifunctional roles of platelets have evolved under selective pressures to protect against hemorrhage and infection.[92] Organisms with circulatory systems face the dual challenge of preventing blood loss while limiting microbial invasion following tissue injury. Despite lacking a nucleus, platelets retain immune sensing and effector capabilities.[93,94] Platelets express pattern recognition receptors that enable detection of microbial components and signals associated with tissue damage.[95] Upon activation, they release bioactive mediators, including chemokines, cytokines, growth factors, and antimicrobial peptides.[96] Platelets also interact with leukocytes and endothelial cells through adhesion molecules such as P-selectin, facilitating leukocyte recruitment and modulating vascular inflammation.[97,98]

The coordinated activation of platelets, coagulation factors, and immune cells underlies immunothrombosis, a condition where localized thrombus formation contributes to host defense by limiting pathogen spreading.[8,99] While protective when the pathogens are restricted, excessive or dysregulated platelet activation can promote pathological thrombosis, disseminated intravascular coagulation, and organ dysfunction, particularly in severe infection and sepsis.[7,8,100]

1.5 Coagulation-inflammation crosstalk

Inflammation is a core component of the innate immune response and represents the body's earliest reaction to tissue injury or infection.[101] Through coordinated changes in vascular permeability, leukocyte recruitment, and the release of soluble mediators, inflammation contains damage, eliminates pathogens, and supports tissue repair.[102,103] When properly regulated, these responses remain localized and resolve once the inciting stimulus is removed. In contrast, excessive or sustained inflammation, such as that seen in severe infection or trauma, disrupts endothelial function, impairs microvascular perfusion, and contributes to organ dysfunction.[104] In this context, inflammatory responses function in concert with other vascular regulatory systems to optimize host protection.[7,105]

A key molecular link between inflammation and coagulation lies in the contact activation system.[32] Rather than being driven mainly by tissue injury, this system responds to danger-associated signals associated with infection, cellular damage, or exposure to foreign surfaces.[106] Once activated, it couples coagulation and inflammation by driving thrombin generation while simultaneously promoting inflammatory signaling through bradykinin release.[29,58] The resulting increase in vascular permeability, leukocyte recruitment, and cytokine production directly links coagulation initiation to inflammatory amplification.[61] Beyond this initial interaction, inflammation and coagulation further reinforce one another through bidirectional feedback mechanisms. Pro-inflammatory cytokines such as tumor necrosis factor-α and interleukin-6 shift the hemostatic balance toward coagulation by increasing tissue

factor expression, weakening endogenous anticoagulant pathways, and limiting fibrinolysis.[7,107] At the same time, coagulation proteases, including thrombin and FXa, signal through protease-activated receptors on endothelial cells, platelets, and leukocytes, promoting endothelial activation, cytokine release, and leukocyte adhesion.[6,108] Together, these processes form a self-amplifying cycle that increases the risk of pathological thrombosis during systemic inflammation (Figure 1.7).[109,110]

Platelets represent another critical interface between inflammation and coagulation, acting not only as mediators of hemostasis but also as active participants in innate immunity.[8] In addition to forming the primary hemostatic plug, platelets express pattern-recognition receptors, directly interact with microbial components, and regulate leukocyte recruitment.[111] Interactions between platelets and neutrophils promote the formation of neutrophil extracellular traps, which contribute to pathogen containment while providing a procoagulant scaffold that enhances thrombin generation.[112,113] From an evolutionary standpoint, similar to coagulation system, this dual functionality of platelets reflects an adaptation that enables platelets to address the concurrent challenges of bleeding and infection.

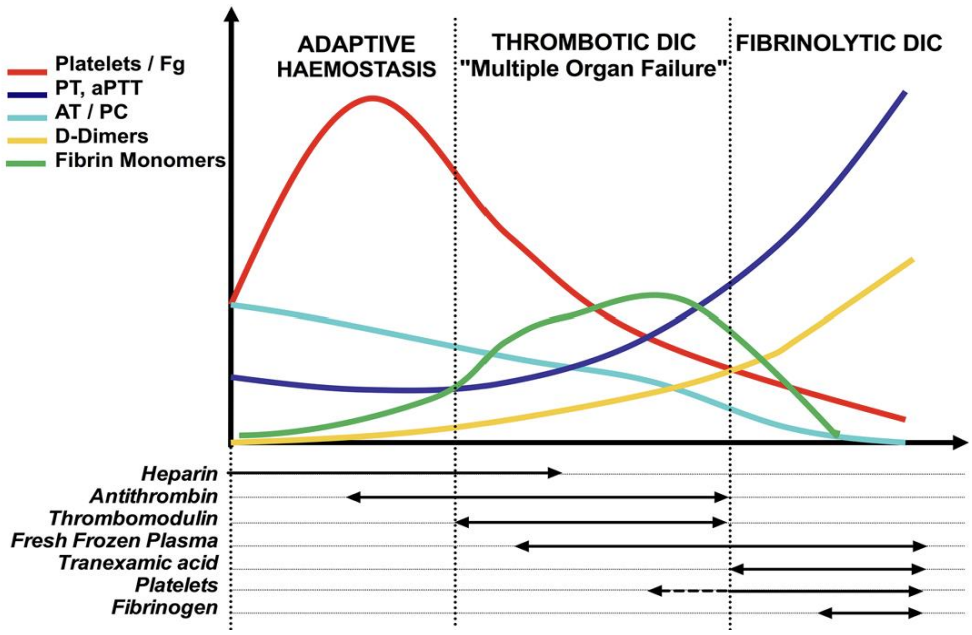

Figure 1.7 Natural history of coagulation during infection and potential therapeutics.
Early infection is characterized by adaptive haemostasis, with increased platelet counts and fibrinogen production, mild thrombin generation, shortened PT/aPTT, reduced natural anticoagulants, and suppressed fibrinolysis with low D-dimer levels; With sustained thrombin generation and anticoagulant consumption lead to a prothrombotic, organ failure–associated DIC state marked by platelet and fibrinogen consumption, impaired fibrin stabilization, and increased D-dimers. In late stages, global consumption of coagulation factors and platelets results in fibrinolytic DIC, with prolonged PT/aPTT, severe hypofibrinogenemia, marked hyperfibrinolysis, and bleeding. From Delabranche et al. Immunohaemostasis: a new view on haemostasis during sepsis. Ann. Intensive Care (2023). Reprinted with permission.

The pathological impact of coagulation-inflammation crosstalk is evident in sepsis and critical illness, where contact pathway activation, platelet consumption, endothelial dysfunction, and cytokine release drive disseminated intravascular coagulation and organ failure.[7,109] Studies in murine and nonhuman primate models show that inhibition of FXI or FXII reduces inflammatory cytokine production and consumptive coagulopathy while improving survival without a significant bleeding risk, suggesting that the intrinsic pathway contribute more to pathological inflammation than to essential hemostasis.[27,114]

Together, these observations highlight coagulation as an active regulator of inflammation and support therapeutic strategies aimed at limiting pathological thrombosis and inflammation while preserving physiological hemostasis (Figure 1.7).

1.6 Coagulation disorders & anticoagulant therapies

Congenital coagulation disorders

Congenital coagulation disorders comprise a heterogeneous group of inherited conditions that alter hemostatic balance through quantitative or qualitative abnormalities in coagulation factors, regulatory proteins, or their functional interactions. These conditions disrupt the finely regulated coagulation system, leading to either bleeding or thrombotic phenotypes depending on the affected component, the nature of the defect. As a result, congenital coagulation disorders provide important clinical and biological insight into the individual role of coagulation cascade.

The most prevalent congenital bleeding disorders are hemophilia A and hemophilia B, caused by deficiencies of FVIII and FIX, respectively.[115,116] Impaired downstream FX function that further leads to spontaneous bleeding, hemarthroses, and excessive hemorrhage following trauma or surgical procedures. In contrast, deficiencies of other intrinsic pathway components, such as FXI, are typically associated with a milder and more variable bleeding phenotype, often becoming clinically apparent only under hemostatic stress. Notably, deficiency of FXII does not result in a bleeding tendency despite marked prolongation of laboratory coagulation assays, emphasizing the discrepancies between *in vitro* clotting measurements and *in vivo* hemostatic requirements.[26,66]

Congenital disorders affecting common pathway factors, including FII, FV, FX, and fibrinogen, are rare but associated with severe bleeding due to their central roles in thrombin generation and fibrin formation.[117,118] Disorders of fibrinogen may present as afibrinogenemia, hypofibrinogenemia, or dysfibrinogenemia, with clinical manifestations ranging from life-threatening hemorrhage to paradoxical thrombosis.[119] In contrast, inherited defects in natural anticoagulants such as protein C, protein S, and antithrombin predispose individuals to venous thrombosis, highlighting the importance of regulatory pathways in limiting excessive coagulation.[120-122]

Beyond factor deficiencies, prothrombotic congenital disorders also include gain-of-function mutations such as factor V Leiden, which confers resistance to activated protein C, and the prothrombin G20210A variant, which increases prothrombin levels and thrombin generation.[123] These genetic alterations shift the hemostatic balance toward a hypercoagulable state and contribute to inherited thrombotic risk (Table 1.2).[124]

Disorder	Primary defect	Pathophysiology	laboratory findings	Clinical phenotype
Hemophilia A	Factor VIII deficiency	Impaired intrinsic pathway → reduced thrombin generation	↑ aPTT, normal PT; ↓ FVIII	Severe bleeding, hemarthrosis
Hemophilia B	Factor IX deficiency	Impaired intrinsic pathway	↑ aPTT, normal PT; ↓ FIX	Severe bleeding
Hemophilia C	Factor XI deficiency	Impaired thrombin amplification	Mild ↑ aPTT; ↓ FXI	Mild-moderate post-surgical bleeding
von Willebrand disease	Quantitative/qualitative VWF defect	Impaired platelet adhesion & FVIII reduction	↑ aPTT; abnormal VWF assays	Mucocutaneous bleeding
Congenital hypofibrinogenemia	Fibrinogen deficiency	Impaired clot formation	↑ PT, ↑ aPTT; ↓ fibrinogen	Bleeding, poor wound healing
Factor XIII deficiency	FXIII deficiency	Impaired fibrin cross-linking	Normal PT/aPTT; ↓ FXIII	Delayed bleeding, poor clot stability
Antithrombin deficiency	Reduced AT activity	Impaired inhibition of thrombin/FXa	Normal PT/aPTT; ↓ AT	Venous thrombosis
Protein C deficiency	Reduced APC activity	Impaired FVa/FVIIIa inactivation	Normal PT/aPTT; ↓ protein C	Venous thrombosis
Protein S deficiency	Reduced APC cofactor	Impaired anticoagulant pathway	Normal PT/aPTT; ↓ protein S	Venous thrombosis
Factor V Leiden	APC-resistant factor V	Prolonged FVa activity	Normal PT/aPTT ↑ APC resistance	Venous thrombosis
Prothrombin G20210A mutation	Increased prothrombin levels	Excess thrombin generation	Normal PT/aPTT; ↑ thrombin	Venous thrombosis

Table 1.2 Congenital coagulation disorders
Overview of inherited deficiencies or functional abnormalities of coagulation factors, fibrinolytic proteins, or natural anticoagulants. PT: prothrombin time; aPTT: activated partial thromboplastin time; VWF: von Willebrand factor.

Acquired coagulation disorders

Acquired coagulation disorders arise from pathological conditions that interfere with normal hemostatic regulation rather than inherited defects in coagulation proteins. These disorders commonly develop secondary to systemic illness, inflammation, organ dysfunction, or pharmacologic intervention. Of note, disseminated intravascular coagulation (DIC) is characterized by widespread activation of coagulation, leading to excessive thrombin generation and fibrin deposition within the microvasculature.[109] Continued coagulation activation results in consumption of platelets and clotting factors, which predisposes patients to bleeding despite widespread ongoing thrombus formation. DIC most frequently occurs in conditions such as sepsis, severe trauma, burn injury, heatstroke, malignancy, and obstetric complications, where inflammatory signaling further amplifies coagulation activation and contributes to organ dysfunction.[109,125]

Other acquired coagulation disorders include vitamin K deficiency, liver disease, and the presence of circulating anticoagulants or factor inhibitors, emphasizing the close relationship between coagulation function and overall health (Table 1.3).

Disorder	Primary cause	Pathophysiology	Laboratory findings	Clinical phenotype
Liver disease-associated coagulopathy	Reduced synthesis of clotting factors & inhibitors	↓ most coagulation factors & inhibitors	↑ PT/INR, ↑ aPTT, ↓ fibrinogen	Bleeding or thrombosis
Vitamin K deficiency	Impaired γ -carboxylation	↓ FII, FVII, FIX, FX	↑ PT > aPTT	Bleeding
Disseminated intravascular coagulation	Systemic coagulation activation	Consumptive coagulopathy	↑ PT, ↑ aPTT, ↓ platelets, ↑ D-dimer	Bleeding + microthrombosis
Antiphospholipid syndrome	Anti-phospholipid antibodies	Endothelial & coagulation activation	↑ aPTT (LA); positive aPL	Arterial & venous thrombosis
Acquired hemophilia A	Autoantibodies to FVIII	Neutralization of FVIII	↑ aPTT not corrected by mixing	Severe spontaneous bleeding
Heparin-induced thrombocytopenia	Anti-PF4 antibodies	Platelet activation → thrombosis	↓ platelets; positive PF4 Ab	Thrombosis

Table 1.3 Acquired coagulation disorders
Overview of Acquired coagulation disorders arising from immune-mediated, inflammatory, metabolic, or consumptive processes.
PT: prothrombin time; aPTT: activated partial thromboplastin time; aPL: antiphospholipid antibodies.

Anticoagulant therapies

Anticoagulant therapy is a fundamental strategy in the prevention and treatment of thromboembolic disease and has substantially reduced morbidity and mortality across a wide range of cardiovascular conditions.[67,126] Traditional anticoagulants include vitamin K antagonists such as warfarin, which reduce hepatic synthesis of multiple coagulation factors, and heparin, which enhances antithrombin-mediated inhibition of thrombin and FXa.[127] More recently, direct oral anticoagulants that selectively inhibit thrombin or FXa have become widely adopted because of their predictable pharmacokinetics, fewer food and drug interactions, and lower need for routine laboratory monitoring.[11,128,129] These agents have simplified anticoagulation management and expanded access to anticoagulant therapies. Despite their proven efficacy, all currently available anticoagulants interfere with key components of hemostasis and therefore carry an inherent risk of bleeding (Table 1.4).[130,131]

Concern over bleeding complications remains a major factor influencing clinical decision-making.[132] Fear of serious hemorrhagic events, particularly intracranial or other vital organ bleeding, often forces clinicians to prescribe reduced doses, shorten treatment duration, or avoid anticoagulation even in patients with a clear indication for therapy.[133,134] This risk-benefit dilemma is especially pronounced in older, those with renal impairment, a prior history of bleeding, or concomitant antiplatelet therapy.[135] As a result, anticoagulant therapy remains suboptimally prescribed in routine practice, leaving a substantial proportion of patients inadequately protected from thrombotic events.[136]

These limitations have driven ongoing efforts to identify new alternative anticoagulant targets that are more selective to pathological thrombosis while preserving normal hemostasis. In this context, FXI has emerged as a promising candidate.[13] FXI functions primarily as an amplification factor within the intrinsic pathway, sustaining thrombin generation during clot propagation rather than initiation.[19] Epidemiological studies suggest that congenital FXI deficiency is associated with a reduced risk of

venous thromboembolism and ischemic stroke.[137,138] Based on these observations, several FXI-directed anticoagulant strategies, including antisense oligonucleotides, monoclonal antibodies, and small-molecule FXIa inhibitors, are under active development for indications such as venous thromboembolism prophylaxis following orthopedic surgeries, ischemic stroke and atrial fibrillation.[139] Early clinical studies suggest that FXI inhibition may provide effective antithrombotic protection with a lower risk of bleeding in selected clinical settings.[54,140]

Class	Drug name	Year	Mechanism of action	Clinical indications
Unfractionated heparin	Heparin	1930s	Antithrombin-mediated inhibition of FXa & thrombin	Acute VTE, ACS, perioperative anticoagulation, dialysis
Low-molecular-weight heparins	Enoxaparin	1987	Antithrombin-mediated inhibition of FXa	VTE treatment and prophylaxis, ACS
	Dalteparin	1985	Antithrombin-mediated inhibition of FXa	VTE, cancer-associated thrombosis
Synthetic pentasaccharide	Fondaparinux	2001	Antithrombin-mediated inhibition of FXa	VTE, HIT
Vitamin K antagonists	Warfarin	1954	Inhibits vitamin K epoxide reductase → ↓ thrombin, FVII, FIX, FX	AF stroke prevention, mechanical valves, VTE
Direct thrombin inhibitors (parenteral)	Argatroban	2000	Directly inhibits thrombin	HIT
	Bivalirudin	2000	Direct thrombin inhibition	PCI, HIT
Direct thrombin inhibitors (oral)	Dabigatran	2010	Direct thrombin inhibition	AF, VTE
Direct FXa inhibitors (DOACs)	Rivaroxaban	2008	Direct FXa inhibition	AF, VTE, CAD/PAD
	Apixaban	2012	Direct FXa inhibition	AF, VTE
	Edoxaban	2015	Direct FXa inhibition	AF, VTE
	Betrixaban	2017	Direct FXa inhibition	Extended VTE prophylaxis[141]
FXI/XIa inhibitors (emerging)	Abelacimab	~2020s	Blocking FXI/FXIa	VTE prevention (trials)[142]
	Asundexian	~2020s	Oral FXIa inhibition	Stroke, AF (trials)[143]
	Milvexian	~2020s	Oral FXIa inhibition	VTE, AF (trials)[139]

Table 1.4 Overview of Anticoagulant Therapies
Overview of anticoagulant therapies, ranging from conventional agents to emerging FXI/XIa inhibitors. VTE: venous thromboembolism; ACS: acute coronary syndrome; HIT: heparin-induced thrombocytopenia; AF: atrial fibrillation; PCI: percutaneous coronary intervention

1.7 Thesis Overview

This thesis explores how the coagulation system interacts with its surrounding biological environment to shape hemostatic and thrombotic outcomes. Coagulation has long been viewed primarily as a mechanism for prevention of blood loss and vascular repair, but growing evidence indicates that coagulation factors also actively participate in regulating inflammatory signaling, vascular permeability, and immune responses. These functions place coagulation at the intersection of hemostasis and innate immunity. When this balance is disrupted, dysregulated coagulation contributes to thromboinflammatory disease states, including sepsis, trauma-induced coagulopathy, and even obstetric complications. The studies presented in this dissertation focus on identifying cofactors of coagulation activation and defining how intrinsic pathway components and tissue-derived factors influence clot formation and associated inflammatory responses.

In Chapter 2, the reagents, experimental systems, and analytical methods used throughout this dissertation are described. In Chapter 3, we investigate the role of FXIa-mediated HK cleavage as a mechanistic link between coagulation and inflammation. Using purified protein systems, plasma-based assays, and biochemical analyses, we characterize the capacity of FXIa to process HK and engage in kinin system. Importantly, HK cleavage by FXIa generates cleaved HK fragments that can activate immune cells. These studies demonstrate that FXIa extends beyond its established role in thrombin amplification to regulate kinin system, providing insight into how intrinsic pathway activation contributes to vascular dysfunction in inflammatory conditions such as sepsis.

In Chapter 4, we examine the procoagulant properties of amniotic fluid and its effects on plasma coagulation using a combination of proteomic analyses and functional biological assays. Our results demonstrate that amniotic fluid possesses strong procoagulant activity, which is predominantly driven by phospholipid components. These findings provide mechanistic insight into the severe hemostatic

disturbances observed in amniotic fluid embolism and suggest potential therapeutic strategies aimed at targeting common pathway in this setting.

In Chapter 5, we look into the contribution of skeletal muscle-derived myosin to trauma-induced coagulopathy by examining its interaction with fibrin. Although tissue injury releases muscle components into the circulation, their effects on coagulation remain incompletely understood. Using samples from clinical trauma patients, animal injury models, and *in vitro* biochemical assays, we show that circulating skeletal muscle myosin levels are paradoxically reduced after injury despite increased myoglobin release. Mechanistically, we demonstrate that skeletal muscle myosin binds directly to fibrin and becomes incorporated into fibrin clots, thereby enhancing clot stability and resistance to fibrinolysis. These findings provide a mechanistic explanation for the reduced plasma levels of skeletal muscle myosin observed after trauma and identify this muscle-derived protein as an active contributor to the altered coagulation phenotypes following tissue injury.

Taken together, the studies presented in this thesis define a continuum linking molecular-level interactions to complex coagulation phenotypes observed in inflammatory and traumatic disease states. By elucidating how intrinsic pathway proteases, physiological body fluid, and tissue-derived components shape coagulation and inflammation, this work advances our understanding of thromboinflammation and highlights potential therapeutic strategies aimed at selectively targeting pathological coagulation while preserving hemostasis.

Chapter 2. General Materials and Methods

2.1 Overview

To investigate the complex interplay in coagulation, this dissertation employs multi-faceted experimental approaches that evaluate how contact pathway components and tissue-derived factors influence coagulation across various biological contexts. While each subsequent chapter addresses a distinct biological question, they share a foundational common toolkit of reagents, biological samples, and analytical techniques. This chapter summarizes the standardized procedures used throughout the studies, ranging from fundamental biochemical analyses, such as western blotting and functional assessments of clot dynamics, including recalcified clotting time, thromboelastography, fibrin generation assay, and platelet activation measurements. These core methodologies provide the technical framework necessary to address the specific research aims, while other unique, experiment-specific procedures are detailed within their respective chapters.

2.2 Ethical considerations

All procedures involving human participants were conducted in accordance with the ethical standards of the institutional and/or national research committees and with the principles of the Declaration of Helsinki and its later amendments or comparable ethical standards. For studies utilizing human blood, written informed consent was obtained from healthy volunteers under an Oregon Health & Science University (OHSU) Institutional Review Board (IRB)-approved protocol, and no demographic information was collected. All participants provided informed consent prior to inclusion in the study.

All animal studies were performed in accordance with the Guide for the Care and Use of Laboratory Animals and the Animal Research: Reporting of *In vivo* Experiments (ARRIVE) guidelines. Experimental protocols were reviewed and approved by the appropriate Institutional Animal Care and Use Committees (IACUCs) prior to study initiation. Animals were housed and cared for in AAALAC-

accredited Category I facilities, with veterinary oversight to ensure humane treatment throughout the study. All experimental procedures were conducted in compliance with institutional, federal, and national regulations governing the ethical use of animals in research.

2.3 Common reagents

Human plasma-purified FXIa, FXI, FX, FXa, prothrombin, and α-thrombin were from Haematologic Technologies (Essex Junction, VT, USA). Plasma kallikrein, α-FXIIa, high molecular weight kininogen (HK) and fibrinogen were from Enzyme Research Laboratories, Inc. (South Bend, IN, USA). Chromogenic substrates S-2366, S-2302, S-2765, S-2388 were from Diapharma Group, Inc (West Chester, OH, USA). Tissue factor (TF; Innovin® PT reagent) was purchased from Siemens (Munich, Germany). Ellagic acid (aPTT reagent) was purchased from Thermo Fisher (Waltham, MA). Polyphosphate molecules of the size produced by bacteria (long-chain polyP, >595 phosphate units in length) and platelet (Short-chain polyP, 50-70 phosphate units in length) were a kind gift from Dr. James Morrissey of University of Michigan. Cross-linked collagen-related protein/CRP-XL was purchased from University of Cambridge (Cambridge, England). Thromboxane A_2 analog/U46619 and PAR1 agonist/TRAP6 were from Tocris (Bristol, England). Fibrinogen was purchased from Enzyme Research Laboratories (South Bend, IN). Anti-PK function-blocking antibodies (lanadelumab) were purchased from MCE (Monmouth Junction, NJ). Anti-FXI function-blocking antibodies (14E11) were generated as described. Corn trypsin inhibitor was purchased from Enzyme Research Laboratories (South Bend, IN). Hirudin was purchased from Hyphen Biomed (Neuville-sur-Oise, France). Phe-Pro-Arg-chloromethylketone (PPACK) was purchased from Santa Cruz (Dallas, TX).

2.4 Blood collection

Venous whole blood was obtained from healthy volunteers in accordance with an Oregon Health & Science University (OHSU) Internal Review Board (IRB)-approved protocol. After sterilization of the

decubitus field, blood was obtained by venipuncture with 19G butterfly needle and manually drawn into either empty syringe or a syringe with an appropriate anticoagulant.

2.5 Plasma preparation

Plasma was obtained by centrifugation of whole blood anticoagulated with sodium citrate (0.32% w/v) at 2,000 × g for 10 min at room temperature and subsequently stored at −80 °C.

2.6 Washed platelet preparation

Whole blood was collected from healthy adult donors by venipuncture into sodium citrate (0.38% w/v). Warmed acid-citrate-dextrose solution (85 mM sodium citrate, 100 mM glucose, 71 mM citric acid; 30 °C) was added to the anticoagulated blood, which was then centrifuged at 200 × g for 20 min to obtain platelet-rich plasma (PRP). The PRP was further centrifuged at 1,000 × g for 10 min in the presence of prostacyclin (PGI_2, 0.1 μg/mL) to collect platelets. Purified platelets were resuspended in modified HEPES/Tyrode buffer (129 mM NaCl, 0.34 mM Na_2HPO_4, 2.9 mM KCl, 12 mM $NaHCO_3$, 20 mM HEPES, 1 mM $MgCl_2$, pH 7.3) supplemented with 5 mM glucose and 0.1 μg/mL PGI_2. Platelets were washed once by centrifugation at 1,000 × g for 10 min and finally resuspended in HEPES/Tyrode buffer at the indicated concentrations.

2.7 Flow cytometry

Platelet activation was assessed by measuring surface expression of P-selectin and activated integrin GPIIb/IIIa using flow cytometry. Adult whole blood anticoagulated with sodium citrate was diluted in modified HEPES/Tyrode's buffer, and platelets were isolated and washed as described above. Washed platelets (2×10^8 platelets/mL) were incubated at room temperature for 20 min with antibodies against P-selectin (APC-CD62P) and activated GPIIb/IIIa (FITC-PAC-1) at a 1:25 dilution, together with the indicated agonists or vehicle control (HEPES/Tyrode's buffer). Reactions were stopped by fixation

with 2% paraformaldehyde for 10 min. Samples were then diluted in PBS, acquired on a flow cytometer, and analyzed using FlowJo.

2.8 Clotting assays

To measure prothrombin time (PT), 50 µL plasma was incubated with 100 µL Innovin (Thermo Fisher, Waltham, MA) and the time to clot formation was determined using a KC4 Coagulation Analyzer (Trinity Biotech, Ireland). For activated partial thromboplastin time (aPTT), 50 µL plasma was incubated with 50 µL aPTT reagent (Thermo Fisher, Waltham, MA) for 3 min. Clotting was initiated with $CaCl_2$ (50 µL, 8.3 mM final) and the time to clot formation was measured. For recalcified clotting time, 50 µL plasma was incubated with 50 µL of HBS buffer (25mM HEPES, 150 mM NaCl, pH 7.4). Clot formation was initiated with $CaCl_2$ (50 µL, 8.3 mM final) and the time to clot formation was recorded.

2.9 Fibrin generation assay

Pooled normal plasma (50 µL) was incubated with tested samples at different gestational time points followed by incubation with 50 µL of HBS for 3 minutes. $CaCl_2$ (50 µL, 8.3 mM final) was added to each plasma mixture. Fibrin generation was quantified by measuring changes in turbidity at an absorbance of 405 nm at 30-second intervals for 30-min using an Infinite M200 spectrophotometer (Tecan, CH). The lag time and time to reach half of maximum turbidity were obtained.

2.10 Western blot

Protein samples were separated by SDS-PAGE and transferred onto polyvinylidene difluoride membranes. Membranes were blocked and then incubated with the indicated primary antibodies, followed by horseradish peroxidase-conjugated secondary antibodies. Immunoreactive proteins were

visualized using enhanced chemiluminescence and detected using ProteinSimple FluorChem and Jess Imaging system (Biotechne, Minneapolis, MN).

2.11 Thromboelastography

Viscoelastic properties of citrated whole blood were analyzed using a TEG® 5000 hemostasis analyzer system (Haemonetics, Boston, MA). The initiation phase of clot formation was measured as R time, defined as the time from test until clot formation begins. The degree of fibrinolysis was quantified as LY30 (%), defined as the percentage reduction in clot amplitude 30 min after reaching maximum clot strength.

2.12 Statistical analysis

Statistical analyses were performed using GraphPad Prism 10.0 (GraphPad Software Inc., La Jolla, CA) and R version 4.2.2 for proteomic and network-based analyses where indicated. Unless otherwise specified, data are presented as mean ± standard deviation (SD). Individual data points represent independent biological replicates, defined as samples derived from distinct human donors, animals, or independent experimental preparations. When technical replicates were performed, values were averaged prior to statistical analysis to avoid pseudo-replication.

Data distributions were evaluated for normality using the Shapiro-Wilk test. For paired comparisons between two timepoints or conditions within the same biological group, the Wilcoxon signed-rank test was used. Comparisons between two independent groups were performed using the Mann-Whitney U test when data did not meet assumptions for parametric testing. For comparisons involving three or more groups, one-way analysis of variance (ANOVA) was applied when data were approximately

normally distributed. When normality assumptions were violated, the Kruskal-Wallis test followed by Dunn's post hoc multiple-comparison test was used.

For experiments involving multiple experimental conditions or pharmacologic inhibitors, statistical tests were selected based on the experimental design and data distribution and are specified in the corresponding figure legends. Where appropriate, post hoc corrections for multiple comparisons were applied to control for type I errors. All statistical tests were two-sided, and a p value < 0.05 was considered statistically significant.

Correlation analyses were performed using Pearson correlation for normally distributed data and Spearman rank correlation for non-parametric data. Linear regression models were used where indicated to assess associations between continuous variables. For proteomic analyses, linear modeling and empirical Bayes moderation of standard errors were applied as described in the relevant methods sections. False discovery rate correction was used for enrichment analyses where applicable.

Chapter 3. Polyphosphate Enhances Activated Factor XI-Mediated Kininogen Cleavage to Promote Bradykinin-Independent Inflammatory Signaling

Chih Jen Yang, Jiaqing Pang, Aleksandr Shamanaev, André L. Lira, Ashok P. Reddy, Keith D. Zientek, Joseph J. Shatzel, Christina U. Lorentz, Erik I. Tucker, Cristina Puy, Joseph E. Aslan, David Gailani, Owen J. T. McCarty

This work will be submitted to Arteriosclerosis, Thrombosis, and Vascular Biology or Journal of Thrombosis and Haemostasis.

3.1 Abstract

Background: Inhibition of factor XI (FXI) reduces cytokine and inflammatory markers in sepsis models, but the mechanisms remain elusive. Activated FXI (FXIa) cleaves high-molecular weight-kininogen (HK), generating bradykinin at slower rates and different cleavage sites compared to kallikrein. Bradykinin, released following cleavage of HK, is an established proinflammatory molecule. Other cleaved HK products including cleaved HK and free domain 5 are found to modulate immune responses. While polyphosphates (PolyP) is a potent cofactor for the proteolytic activity of FXIa and is implicated in inflammation during sepsis, its role in FXIa-mediated HK cleavage is less defined.

Aim: To define the role of PolyP in regulating the enzymatic susceptibility of HK to contact pathway proteases.

Methods: Cleavage of HK by contact pathway proteases including FXIa and kallikrein was analyzed by electrophoresis with Coomassie blue staining and Western blotting. Bradykinin levels were measured by ELISA. Cleaved HK fragment peptide sequences were identified by proteomic analysis. Interactions between PolyP and HK were assessed by pull-down assay. Inflammatory signaling pathway in THP-1 cells was detected by Western blotting.

Results: FXIa cleaved HK at different sites compared to kallikrein and proteolytically released HK domain 5. PolyP bound to HK domain 5 and significantly enhanced FXIa-mediated HK cleavage, selectively accelerating the cleavage steps within HK domain 5. This process resulted in increasing generation of cleaved HK and free domain 5, while having no impact on bradykinin generation. Conversely, PolyP did not appreciably affect kallikrein-mediated HK cleavage or bradykinin generation by kallikrein. FXIa-mediated HK cleavage products activated inflammatory signaling pathways in THP-1 cells. Inhibition of FXIa reduced the enhanced effect of PolyP on cleavage of HK. ***Conclusions:*** PolyP amplifies FXIa-mediated HK cleavage in a manner unrelated to bradykinin generation. However, the resulting cleaved HK products promote inflammatory signaling pathway activation in immune cells. These findings highlight a potential new mechanism by which FXIa contributes to inflammation.

3.2 Introduction

Despite substantial advances in antimicrobial therapy and supportive care, sepsis remains a leading cause of morbidity and mortality worldwide, driven largely by dysregulated inflammation and coagulation.[144,145] Increasing evidence suggests that activation of the contact pathway coagulation is critical to the propagation of pathological thrombotic and inflammatory responses during sepsis.[30] Among contact pathway components, coagulation factor(F) XI has emerged as a promising therapeutic target. Inhibition of FXI reduces coagulopathy, inflammation, endotheliopathy, organ injury, and mortality in multiple preclinical sepsis models without increasing bleeding risk, indicating that FXI participates in sepsis pathogenesis through inflammatory mechanisms beyond thrombin generation.[27,146-148]

High-molecular-weight kininogen (HK), is a multifunctional protein that serves as both a scaffold and a proteolytic substrate in the contact pathway. HK binds to FXI or its homolog prekallikrein (PK) and

form stable complexes in circulation.[38,149,150] Altered levels of intact and cleaved HK are frequently observed in inflammatory disease states, including sepsis, and are consistent with sustained contact pathway activation.[151-154] HK cleavage has classically been attributed to plasma kallikrein (PKa), resulting in liberation of bradykinin, a potent vasoactive and proinflammatory peptide.[29] Activated FXI (FXIa) has been reported to cleave HK at a slower rate than PKa, producing a different cleavage pattern that includes release of HK domain 5 (D5) and is associated with loss of HK procoagulant activity.[63,155] Accumulating evidence suggests that D5 is not an inert cleavage byproduct. D5 released from intact HK and cleaved HK have been shown to activate mononuclear cells, facilitate endotoxin dissemination, and promote lymphocyte chemotaxis.[156-158] These observations raise the possibility that FXIa-mediated HK cleavage also contributes to inflammatory signaling in sepsis.

Polyphosphates (PolyP), the polyanionic molecule derived from activated platelets and bacteria, is a potent cofactor for FXI activation and FXIa enzymatic activity.[159,160] PolyP enhances FXIa-mediated proteolysis on several substrates and modulates inflammatory responses during sepsis.[161,162] Whether PolyP influences FXIa-mediated HK cleavage and the generation of proinflammatory HK fragments have not been defined. Here, we demonstrate that PolyP directly binds D5 and selectively enhances FXIa-mediated cleavage within this domain, promoting generation of cleaved HK and free D5. These findings identify a mechanism linking FXI to inflammation and provide mechanistic insight into the anti-inflammatory effects of FXI inhibition in sepsis.

3.3 Materials and methods

3.3.1 Reagents

FXIa and PKa were from Haematologic Technologies (Essex Junction, VT). Single-chain HK (intact HK), two-chain HK (cleaved HK), and corn trypsin inhibitor were from Enzyme Research Laboratories (South Bend, IN). Chromogenic substrate S-2366 was from DiaPharma (West Chester,

OH). Recombinant human D5 was from R&D (Minneapolis, MN). FXI-depleted plasma was from Affinity Biologicals (Ancaster, ON). Bradykinin ELISA kit was from Enzo (Long Island, NY). Lanadelumab, exopolyphosphatase, and bradykinin were from MCE (Monmouth Junction, NJ). Laemmli sample buffer was from Bio-Rad (Hercules, CA). Ellagic acid (APTT-XL), anti-kininogen light chain antibody (pa5-98322), and NeutrAvidin Agarose beads were from Thermo Fisher Scientific (Waltham, MA). The anti-FXI antibody, 14E11, was generated as previously described.[163] Anti-HK antibody was from Nordic MUbio (Susteren, The Netherlands). Anti-transferrin antibody was from Santa Cruz Biotechnology (Dallas, TX). Anti-p65 antibody, anti-phospho-p65 antibody, and anti-tubulin antibody were from Cell Signaling (Danvers, MA). THP-1 cell line (human monocyte) was from ATCC (Manassas, VA). Long chain and short chain polyphosphates (LC-PolyP and SC-PolyP), and biotinylated LC-PolyP were kind gifts from Dr. James Morrissey of University of Michigan. All other reagents were obtained from Sigma-Aldrich (St. Louis, MO).

3.3.2 HK cleavage in purified system

HK was incubated with FXIa or PKa in the presence or absence of PolyP in HBS at 37°C for 0-2 hours. Samples were analyzed by SDS-PAGE under reducing conditions, followed by Coomassie blue staining. Images were captured with FluorChem E System (ProteinSimple).

3.3.3 Recombinant FXI monomer

Complementary DNAs encoding wild-type FXI containing Cys321→Ser and Leu284→Ala substitutions (FXI monomer) in the pJVCMV vector were expressed in HEK293 cells and purified by antibody-affinity chromatography as previously described.[164] Recombinant FXI monomer was then dialyzed and further purified by gel filtration on a Superose-12 column equilibrated with 50 mM sodium phosphate and 150 mM NaCl. FXI monomer was adjusted to 200 nM subunits and incubated

with FXIIa (100 nM) overnight at 4°C. Activation was terminated by addition of corn trypsin inhibitor, and FXIa activity was measured using chromogenic substrate S-2366.

3.3.4 Amino acid sequencing

HK was incubated with FXIa, separated by SDS–PAGE under reducing conditions, and protein bands corresponding to approximately 10–15 kDa were excised from the gel, and in-gel digested with trypsin in 0.01% ProteaseMAX (Promega, Madison, WI) at 50°C for 3 hours. Peptides were extracted using Promega protocol, samples filtered w Millipore 0.22 um filters, dried, dissolved in 20 ul of 5 % formic acid. Protein digests were separated by liquid chromatography using a NanoAcquity UPLC system (Waters) and introduced into a Q Exactive HF mass spectrometer (Thermo Fisher Scientific) via electrospray ionization using an EasySpray ion source (Thermo Fisher Scientific). Instrument control and data acquisition were performed using Xcalibur software (version 4.0).

Survey mass spectrometry (MS) spectra were acquired over an m/z range of 375–1400 at a resolution of 120,000 (at m/z 200). Data-dependent acquisition was employed to select the top 10 most abundant precursor ions for higher-energy collisional dissociation tandem mass spectrometry using an isolation width of 1.2 m/z, normalized collision energy of 30, and a resolution of 30,000. Dynamic exclusion was enabled, with charge states from +2 to +7 selected for MS/MS. The maximum ion injection time was set to 100 ms, with automatic gain control targets of 3×10^6 for MS1 and 5×10^3 for MS2. Raw data were analyzed using Comet (version 2016.01, rev. 3) against an April 2024 canonical FASTA database containing human UniProt sequences, supplemented with sequence-reversed entries for false discovery rate (FDR) estimation and 179 common contaminant sequences and their reversed counterparts.[165] Searches were performed with trypsin specificity, a monoisotopic precursor mass tolerance of 1.25 Da, and a fragment ion mass tolerance of 1.0005 Da. A static modification of +45.9877 Da was applied to cysteine residues, and a variable modification of +15.9949 Da was

applied to methionine residues. A linear discriminant transformation was used to enhance peptide identification sensitivity from the Comet analysis.[166,167] Separate score histograms were generated for matches to forward and reversed sequences for peptides of seven amino acids or longer. Reversed-sequence matches were used to estimate peptide-level FDRs and establish score thresholds for each peptide class. The resulting protein-level FDR was 1.6%.

3.3.5 Normal pooled plasma preparation

Human venous blood was collected in accordance with an IRB–approved protocol. Pooled normal plasma was prepared by centrifuging citrated whole blood (0.32 % w/v sodium citrate) from 12 donors without known hematological disorders or taking any medications, at 2150 × g for 10 minutes twice.

3.3.6 HK cleavage in plasma

Normal pooled plasma preincubated with lanadelumab was treated with varying concentrations of ellagic acid with or without contact pathway inhibitor or anti-FXI antibody (14E11) for 2 hours. In alternative experiments, FXI-depleted plasma preincubated with 40 μg/mL corn trypsin inhibitor was supplemented with different concentrations of FXIa for 2 hours. Plasma samples were separated by SDS-PAGE under reducing conditions, transferred to PVDF membrane and immunoblotted with an anti-HK antibody followed by an HRP-conjugated secondary antibody. Transferrin was served as a loading control.

3.3.7 Bradykinin measurement

HK (800 nM) was incubated with FXIa or PKa at 37°C for 2 hours. Under specific conditions, different polyanions were added to the reaction. At various time points, 10-μL aliquots were transferred into 90 μL of ice-cold ethanol and stored at −80°C overnight. Samples underwent clarification by centrifugation at 10,000 × g for 1 hour and subsequently analyzed by ELISA.

3.3.8 Pull-down assay for domain 5 of HK

Biotinylated PolyP was immobilized on NeutrAvidin agarose beads and incubated with Zn^{2+} and recombinant D5 for 2 hours at 4°C with gentle mixing. The bead mixture was then transferred to centrifuge columns (~30 μm pore size, Thermo Fisher Scientific) and washed three times to remove unbound protein. Bound proteins were eluted with 1 M NaCl and Laemmli 2X sample buffer with dithiothreitol, and the elution fractions were analyzed by western blotting using an anti-HK light chain antibody to detect D5.

3.3.9 Lipopolysaccharide preparation

Lipopolysaccharide chemotype E. coli O111:B4 (1 mg/mL) was solubilized in 20 mM HEPES buffer containing 150 mM NaCl, pH 7.4, and extensively vortexed for 10 minutes. The suspension was then sonicated in a 60°C water bath for 30 minutes and subjected to multiple temperature cycles between 4°C and 60°C. Finally, the lipopolysaccharide aggregate suspension was incubated at 4°C for at least 12 hours before use in experiments.

3.3.10 THP-1 cell signaling pathway

THP-1 cells (passages 5–25) were suspended in Hanks' balanced salt solution. The cells (1.5×10^6/mL) were incubated at 37°C for selected times with HK + FXIa, D5, or LPS. After incubation, the cell lysates were collected for western blot analysis.

3.4 Result

3.4.1 Cleavage of HK by FXIa or PKa

We first evaluated the proteolytic cleavage of HK by contact pathway protease FXIa and PKa. FXIa is known to cleave HK in a manner distinct from plasma kallikrein. Based on the SDS–PAGE under

reducing conditions, incubation of HK with FXIa resulted in loss of the ~110 kDa intact HK band and the appearance of HK fragments at 75 kDa, 65 kDa, and 45 kDa, a cleavage pattern that differed from kallikrein, which generated bands at 55 kDa, 55 kDa, and 45 kDa at a higher rate than cleavage by FXIa (Figure 3.1A). To determine whether the dimeric structure of FXIa affects HK cleavage, recombinant FXIa monomer was generated. Cleavage of HK was at comparable rates and similar cleavage patterns by wild type dimeric FXIa and monomeric FXIa. (Figure 3.2) Notably, FXIa-mediated cleavage produced additional fragments at 15 kDa and 11 kDa that were not observed following PKa treatment (Figure 3.1B). Peptide sequence analysis by mass spectrometry confirmed that these 15 kDa and 11 kDa fragments predominantly originated from D5 (Figure 3.1C). These findings indicated that FXIa-mediated HK cleavage resulted in the release of free D5. A schematic illustration summarizing HK cleavage by FXIa and PKa is shown in Figure 3.1D.

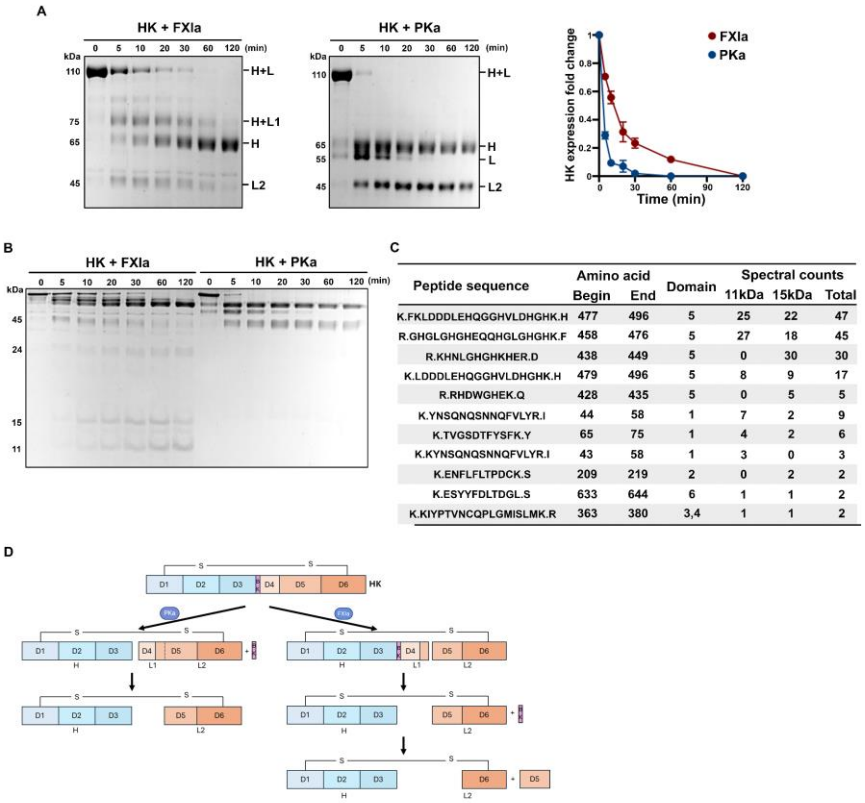

Peptide sequence	Amino acid Begin	Amino acid End	Domain	Spectral counts 11kDa	Spectral counts 15kDa	Spectral counts Total
K.FKLDDDLEHQGGHVLDHGHK.H	477	496	5	25	22	47
R.GHGLGHGHEQQHGLGHGHK.F	458	476	5	27	18	45
R.KHNLGHGHKHER.D	438	449	5	0	30	30
K.LDDDLEHQGGHVLDHGHK.H	479	496	5	8	9	17
R.RHDWGHEK.Q	428	435	5	0	5	5
K.YNSQNQSNNQFVLYR.I	44	58	1	7	2	9
K.TVGSDTFYSFK.Y	65	75	1	4	2	6
K.KYNSQNQSNNQFVLYR.I	43	58	1	3	0	3
K.ENFLFLTPDCK.S	209	219	2	0	2	2
K.ESYYFDLTDGL.S	633	644	6	1	1	2
K.KIYPTVNCQPLGMISLMK.R	363	380	3,4	1	1	2

Figure 3.1 Cleavage of HK by FXIa or PKa. (A) HK (800 nM) was incubated with FXIa (10 nM) or PKa (2 nM) in HBS for selected time (0-2 hours) at 37°C. Samples were analyzed by SDS-PAGE under reducing conditions, followed by Coomassie blue staining. (B) HK (3 μM) was incubated with FXIa (30 nM) or PKa (5 nM) in HBS for selected time (0-2 hours) at 37°C. (C) The low-molecular-weight bands of the gel (11–15 kDa) were excised and subjected to mass spectrometry analysis. (D) Schematic presentation of distinct HK cleavage patterns mediated by FXIa and PKa.

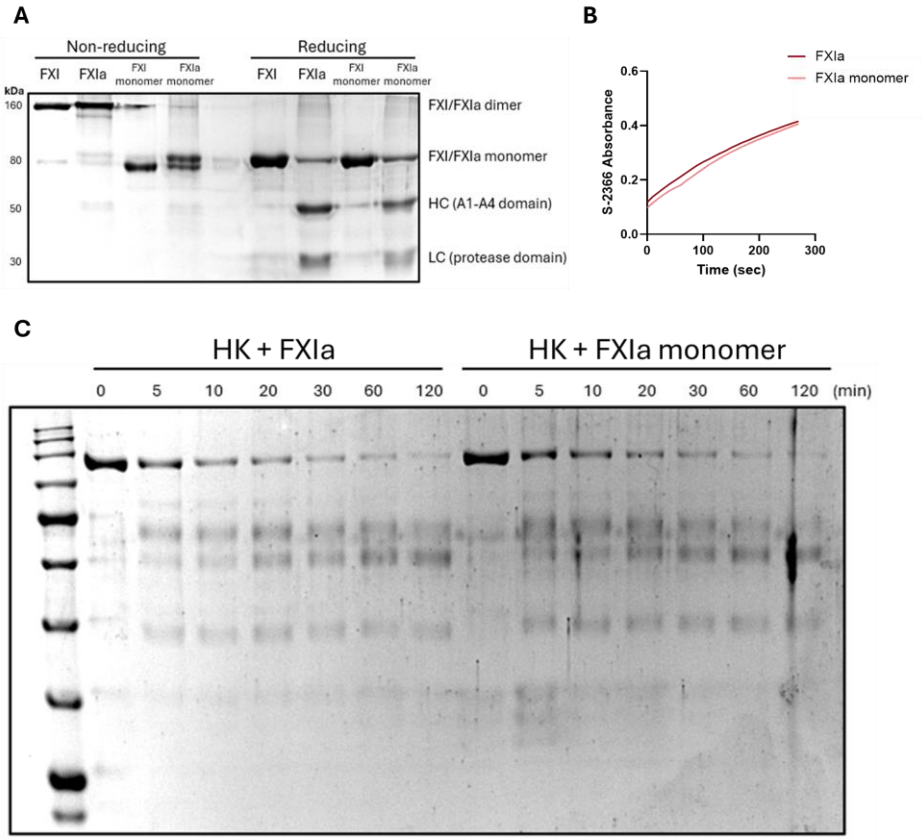

Figure 3.2 Recombinant FXI monomer preparation and HK cleavage by FXIa monomer. (A) SDS-PAGE analysis of wild-type FXI and recombinant FXI monomer in both zymogen and activated forms under non-reducing and reducing conditions. (B) Enzymatic activities were normalized prior to substrate incubation. (C) HK was incubated with the indicated enzymes for 2 hours.

3.4.2 Cleavage of HK by FXIa in plasma

We next examined whether FXIa-mediated cleavage of HK occurs in a plasma setting. As shown in Figure 3.3A, intact HK progressively disappeared following contact pathway activation by ellagic acid in a dose-dependent manner. Notably, this assay was performed in the presence of lanadelumab, an antibody that inhibits the enzymatic activity of PKa. The HK cleavage was reversed by either corn trypsin inhibitor or the anti-FXI antibody 14E11, which inhibits FXI activation by FXIIa. Furthermore, supplementation of FXI-deficient plasma with FXIa resulted in loss of intact HK (Figure 3.3B). These findings indicate that HK could be cleaved by FXIa under plasma conditions.

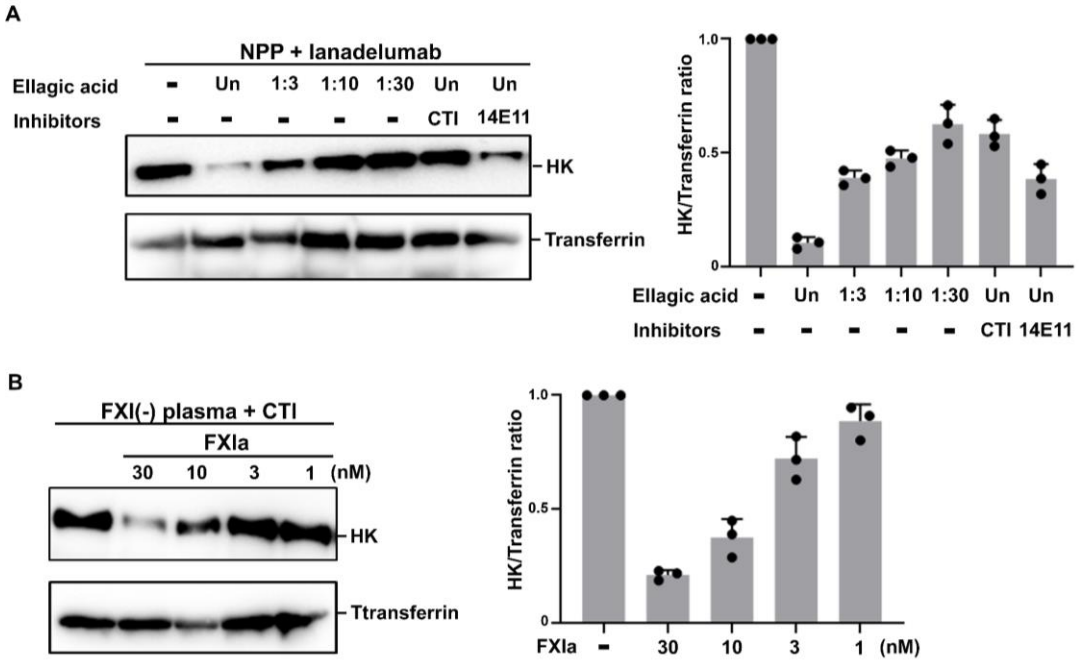

Figure 3.3 Cleavage of HK by FXIa in plasma. (A) Normal human pooled plasma was preincubated with lanadelumab (1 μM) and then stimulated with increasing dilution ratios of ellagic acid in the presence or absence of corn trypsin inhibitor (50 μg/mL) or an anti-FXI antibody, 14E11 (20 μg/mL) for 2 hours. HK cleavage was analyzed by SDS-PAGE followed by Western blotting. (B) FXI-deficient plasma pretreated with corn trypsin inhibitor was supplemented with increasing concentrations of FXIa (0-30 nM) for 2 hours. HK cleavage was analyzed by SDS-PAGE and Western blotting. NPP: normal human pooled plasma. FXI(-) plasma: FXI-depleted plasma.

3.4.3 Cleavage of HK by FXIa or PKa in the presence of PolyP

FXI contains anion-binding sites that are able to interact with polyanions such as heparin and PolyP.[168] Moreover, PolyP has been shown to enhance the enzymatic activity of FXIa for tissue factor pathway inhibitor and complement factor H proteolysis, as well as the FV activation.[161,162,169] We then investigated whether PolyP increases the rate of FXIa-mediated HK cleavage. SDS-PAGE analysis of HK incubated with FXIa in the presence of either LC-PolyP, as found in bacteria, or SC-PolyP, as primarily released from activated platelets, revealed an accelerated rate of HK cleavage. Notably, PolyP selectively enhanced the generation of the 75 kDa fragment and the 45 kDa fragment, corresponding to the heavy chain plus light chain 1 and light chain 2 as depicted in Figure 3.1D, while having minimal effect on the appearance of the 65 kDa fragment (heavy chain alone) (Figure 3.4A). Moreover, PolyP also promoted the appearance of 11 kDa fragment and enhanced FXIa-mediated HK cleavage in a dose-dependent manner (Figure 3.4B). The enhancing effect of PolyP was abolished by

the serine protease inhibitor PPACK (Figure 3.4C). In contrast, the presence of PolyP did not significantly alter the rate of HK cleavage by PKa (Figure 3.4D).

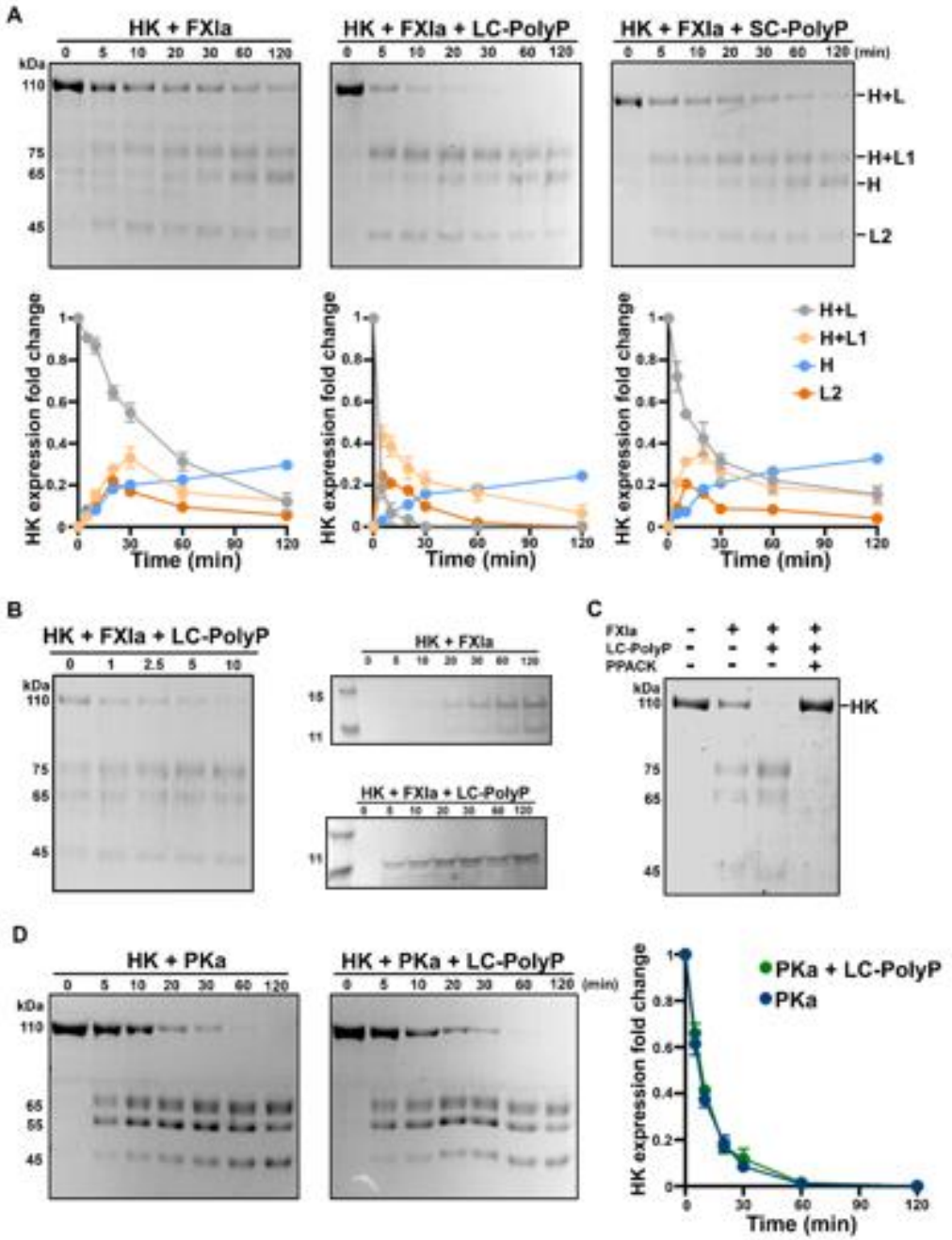

Figure 3.4 Cleavage of HK in the presence of PolyP. (A) HK (800 nM) was incubated with FXIa (10 nM) in the presence of long-chain polyphosphates or short-chain polyphosphates (10 μM) for selected time (0-2 hours) or (B) with increasing concentrations of long-chain polyphosphates (0-10 μM) for 30 mins, or (C) with PPACK (10 μM) followed by SDS-PAGE under reduced conditions and analyzed by Coomassie blue staining. (D) HK (3 μM) was incubated with FXIa (30 nM) in the presence of long-chain polyphosphate for selected time (0-2 hours). Only the low-molecular-weight bands of the gel (11–15 kDa) was shown. (E) HK (800 nM) was incubated with PKa (2 nM) in the presence of long-chain polyphosphates for selected time (0-2 hours).

3.4.4 Bradykinin generation from FXIa or PKa-mediated HK cleavage

To assess bradykinin generation by contact pathway protease, HK was incubated with FXIa or PKa and bradykinin levels were measured at multiple time points. Bradykinin generation from FXIa-mediated HK cleavage was markedly slower and reached lower levels than that by PKa-mediated cleavage. Bradykinin generation by FXIa was abolished by PPACK, indicating the bradykinin generation could be resulted from the proteolytic activity of FXIa (Figure 3.5A). In addition, FXIa-mediated bradykinin generation increased in a dose-dependent manner (Figure 3.5B). However, the presence of polyanions, including LC-PolyP, SC-PolyP, dextran sulfate, and heparin, did not accelerate or increase bradykinin generation by either FXIa or PKa (Figure 3.5C–F).

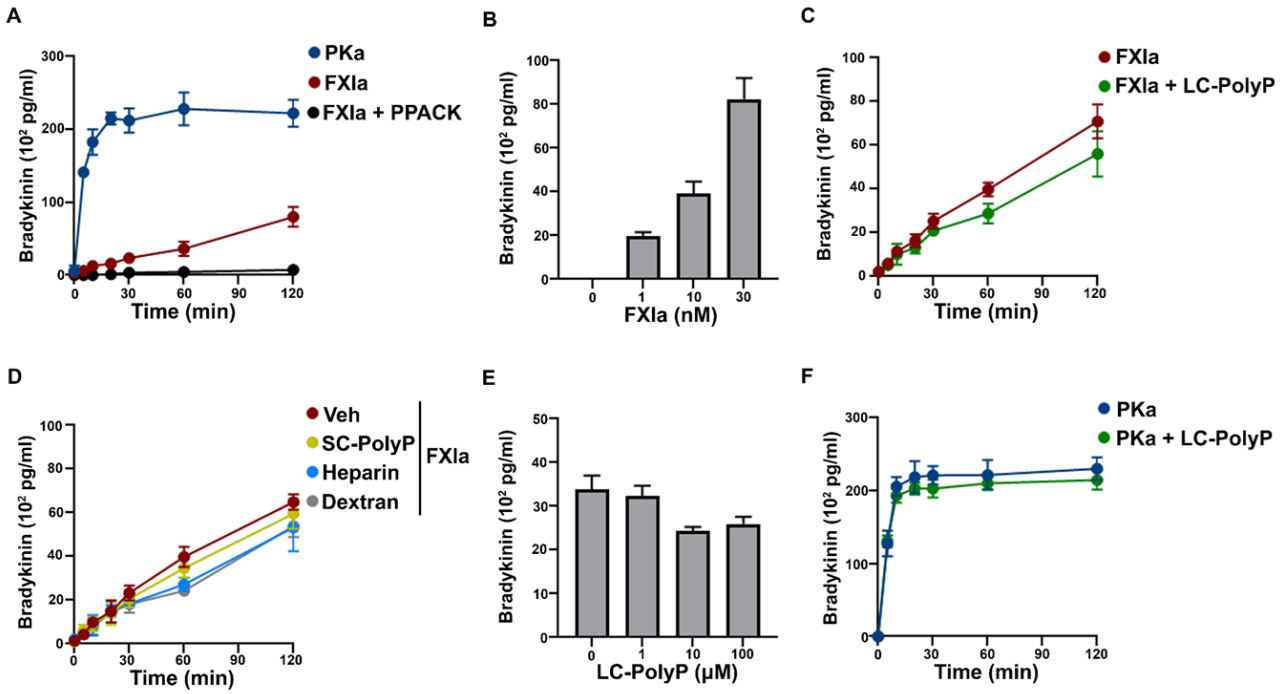

Figure 3.5 Bradykinin generation from FXIa-mediated HK cleavage. (A) HK (200 nM) was incubated with FXIa (10 nM) or PKa (2 nM) in the presence or absence of PPACK (10 μM) for selected time (0-2 hours) or (B) with increasing concentrations of FXIa (0-30 nM) for 1 hour followed by bradykinin measurement using ELISA. (C) HK (200 nM) was incubated with FXIa (10 nM) and 10 μM of long-chain polyphosphates, 10 μM of short-chain PolyP, heparin (10 U/mL), and dextran sulfate (10 μg/mL); or with (D) increasing concentrations of long-chain polyphosphates (0-100 μM), or (D) other polyanions (short-chain PolyP, heparin, and dextran sulfate). (E) HK (200 nM) was incubated with PKa (2 nM) in the presence of 10 μM of long-chain polyphosphates for selected time (0-2 hours).

3.4.5 Binding of PolyP to domain 5 of HK

Because D5 contains an anion-binding site for heparin binding and PolyP selectively enhanced FXIa-mediated HK cleavage within D5,[170,171] we examined whether PolyP directly binds to D5, thereby

facilitating FXIa-mediated proteolysis of this domain. A pull-down assay was performed using streptavidin-agarose beads and biotinylated LC-PolyP. As shown in Figure 3.6, D5 was detected in samples containing streptavidin beads with biotinylated LC-PolyP, but not in control samples containing beads alone or biotinylated bovine serum albumin. Addition of unconjugated LC-PolyP reduced D5 recovery, consistent with competitive inhibition of binding (Figure 3.6). However, polybrene, a positive-charged molecule, did not prevent D5 recovery. To determine whether the PolyP-D5 interaction is primarily electrostatic or also involves hydrophobic forces, the bead-bound complex was first eluted with 1 M NaCl, followed by elution with 2X Laemmli sample buffer containing dithiothreitol. Only a trace amount of D5 was eluted with 1 M NaCl, whereas the majority of D5 was recovered in the Laemmli-eluted fraction, suggesting that the PolyP-D5 interaction is not driven primarily electrostatic, but instead likely involves hydrophobic and/or conformationally dependent contacts.

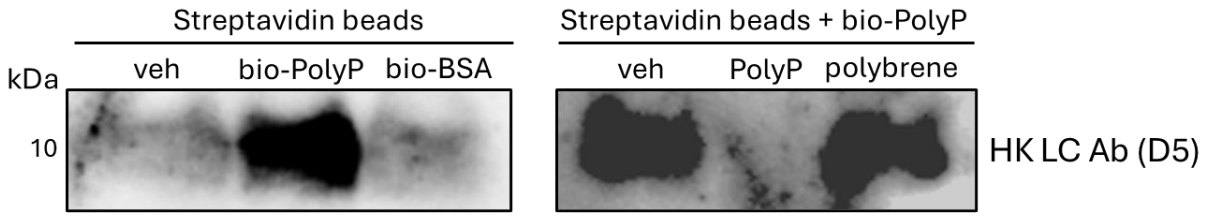

Figure 3.6 PolyP directly binds to HK domain 5. (A) LC-PolyP (100 μM) was immobilized on streptavidin-agarose beads for 1 hour, or beads alone were used as a control, prior to overnight incubation with D5 (1 μg). Bead-bound complexes were sequentially eluted with 1 M NaCl followed by 2X Laemmli sample buffer containing dithiothreitol. Elution fractions were analyzed by SDS-PAGE and immunoblotting using an anti-kininogen light-chain (HK LC) antibody. (B) In selected experiments, unconjugated LC-PolyP and polybrene was added during incubation.

3.4.6 Activation of immune cells by cleaved HK products

As PKa-cleaved HK and D5 have been reported to activate mononuclear cells and induce proinflammatory cytokine secretion,[156,172] we next examined whether FXIa-cleaved HK products exert similar effects. As shown in Figure 3.7A, incubation of THP-1 cells with FXIa-cleaved HK and recombinant D5 resulted in activation of NF-κB signaling pathways in THP-1 cells as evidenced by increased phospho-p65/total p65 ratios over time.

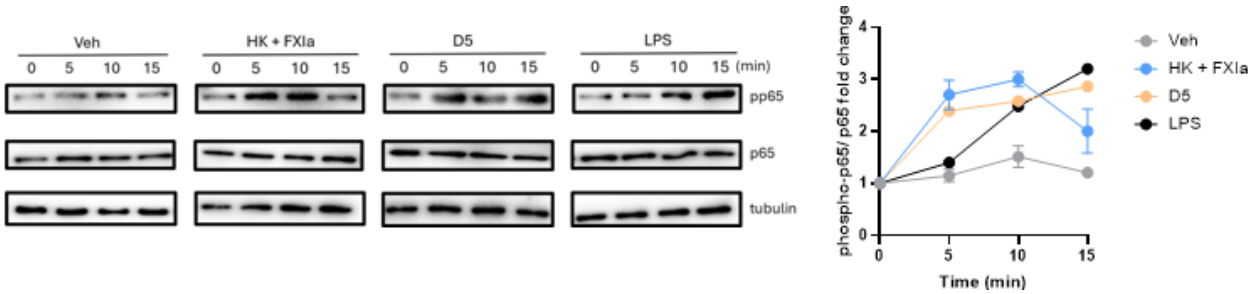

Figure 3.7 NF-κB signaling in THP-1 cells. THP-1 cells were suspended in Hanks' balanced salt solution and adjusted to 1.5 × 10^6 cells/mL. Cells were incubated at 37°C for the indicated times with HK (3 μM) plus FXIa (30 nM), D5 (800 nM), or LPS (100 ng/mL). Following incubation, cell lysates were collected and analyzed by western blotting.

3.5 Discussion

Elucidating the mechanisms by which inhibition of FXI attenuates inflammation is essential for understanding how FXI-targeted therapies improve outcomes in sepsis. In current study, we identify a previously unrecognized, bradykinin-independent mechanism by which FXIa contributes to inflammatory signaling. Although FXIa-mediated cleavage of HK is slower than that mediated by PKa and is associated with loss of procoagulant activity in HK, the release of free D5 triggers proinflammatory signaling in immune cells. Importantly, we found that PolyP directly binds D5 and markedly enhances FXIa-mediated cleavage within this domain.

HK is a multifunctional plasma protein that serves both as a non-enzymatic cofactor and a proteolytic substrate in the contact pathway of coagulation. Structurally, HK has six domains that confer distinct molecular functions (designated D1 to D6, respectively). D4 contains the bradykinin sequence, a well-established vasodilatory and proinflammatory peptide that is liberated following proteolytic cleavage. The C-terminal D6 mediates binding to FXI and PK, enabling formation of circulating complexes.[173] In parallel, D5 functions as a surface-interacting region that bridges HK-bound FXI and HK-bound PK to FXIIa bound on the surface, thereby promoting activation of FXI and PK.[174] While PKa is the principal enzyme responsible for HK cleavage within the contact system that results in bradykinin release,[29] HK can also be cleaved by several other proteases, including FXIa, neutrophil elastase,

plasmin, and mannose-binding lectin–associated serine protease-1.[63,65,175,176] Studies examining HK cleavage by FXIa are limited, likely due to the relatively inefficient proteolysis of HK and associated loss of procoagulant activity in HK following release of D5 by FXIa. However, increasing evidence over the past two decades indicates that D5 plays an active role beyond coagulation. Free D5 has been shown to stimulate mononuclear cells, facilitate lipopolysaccharide dissemination, and induce lymphocyte chemotaxis.[156-158] These observations raise the possibility that HK fragments from FXIa-mediated cleavage may have underappreciated immunoregulatory roles in settings involving concurrent contact pathway and immune activation.

Beyond bradykinin release, cleavage of HK generates cleaved HK, a two-chain, kinin-free form of HK in which the heavy chain (domains 1-3) and light chain (domains 5 and 6) remain linked by a disulfide bond. In contrast to the rapid degradation of bradykinin, cleaved HK persists in circulation for several hours, making it a useful end-point marker of contact pathway activation.[177-179] Cleaved HK has been reported to exhibit antimicrobial, anti-angiogenic, pro-apoptotic, and anti-adhesive properties.[180-182] Furthermore, cleaved HK has been shown to activate mononuclear cells.[156,172] The acquisition of these properties by cleaved HK, which are not observed in intact HK, can be ascribed to the conformational changes that expose previously buried peptide regions, particularly within D5, following cleavage.[183]

The majority of HK circulates in complex either with FXI or PK in plasma. Despite being homologous proteins, FXI and PK interact differently with HK. HK D6 adopts distinct conformations upon binding to FXI or PK, with FXI favoring a straightened conformation and PK promoting a bent double configuration. These conformational differences and associated exosite interactions likely reflect the divergent functional relationships between HK and PK versus FXI.[184] A key difference between FXI and PK is that FXI forms a homodimer, whereas PK exists as a monomer. The dimeric structure of FXI positions two HK molecules in closer proximity, potentially requiring an alternate conformation

of HK to accommodate binding to the dimerized FXI.[184,185] However, we found that monomeric FXIa cleaved HK in a manner that is comparable to that observed with dimeric FXIa. Analysis of sequential HK fragments in purified systems suggested that FXIa preferentially cleaves HK first at proximal D5, followed by D4 and then distal D5, ultimately liberating D5. In contrast, PKa initially cleaves D4 before targeting proximal D5 (Figure 3.1D). PolyP, an established molecule derived from bacteria or activated platelets that is integral to contact pathway coagulation, selectively enhanced FXIa-mediated cleavage at proximal and distal D5. This was reflected by accelerated appearance of the 75 kDa heavy plus light chain 1 fragment, the 45 kDa light chain 2, and the 11 kDa D5 fragment, respectively. In contrast, PolyP did not enhance the D4 cleavage step that produces the heavy chain (65 kDa). Furthermore, PolyP did not significantly affect HK cleavage by PKa. The D5-selective effect of PolyP on FXIa is consistent with direct D5-PolyP binding and may at least partially explain why PolyP did not enhance bradykinin generation by FXIa, since PolyP does not promote the D4 cleavage required for bradykinin release. The lack of effect of PolyP on PKa-mediated HK cleavage is not clear but may reflect the absence of an anion-binding site on the A3 domain of PKa or the possibility that the reaction already proceeds at its maximal rate.

In inflammatory disease states such as sepsis, HK consumption is frequently observed and low HK levels are associated with poor outcomes.[151-154] Modulation of HK cleavage and subsequent bradykinin generation may therefore influence inflammatory responses in these settings. Pharmacological inhibition and genetic deletion of FXI have been shown to reduce inflammation and improve outcomes in sepsis models.[27,146-148] The underlying mechanisms are complex. Beyond effects on downstream thrombin generation and consumptive coagulopathy, FXIa is also implicated in regulation of the complement system and vascular permeability.[161,186] Of note, inhibition of FXI activation in sepsis settings is associated with reduced HK cleavage.[147] It remains unclear whether reduced HK cleavage results directly from inhibition of FXIa-mediated HK cleavage, from reduced feedback activation of

FXII by FXIa, or from other unrecognized mechanisms. Identification of HK fragments specific to FXIa-mediated cleavage may help clarify it. Furthermore, antibody targeting D5 has been shown to reduce inflammatory cytokine levels and mortality in an endotoxemia model,[157] which is consistent with our finding that blocking FXIa-mediated HK cleavage attenuates inflammatory signaling in THP-1 cells. This observation underscores a potential role for FXIa-mediated HK cleavage in sepsis. Given the complexity and heterogeneity of sepsis, the role of HK is unlikely to be uniform across all clinical contexts.[157,187-190] A better understanding of how HK cleavage and its fragments regulate inflammation and coagulation may help define its overall contribution to disease pathogenesis.

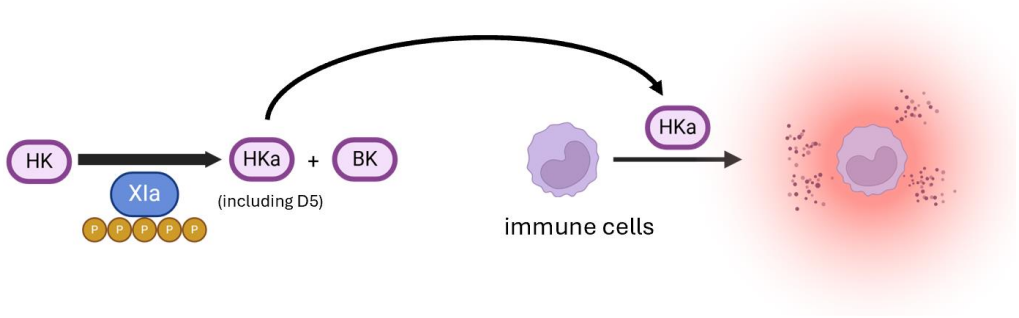

Figure 3.8 Schematic of conclusion. Created with BioRender.com.

Chapter 4. Characterization of the Procoagulant Phenotype of Amniotic Fluid Across Gestation in Rhesus Macaques and Humans

Chih-Jen Yang, Lyndsey E. Shorey-Kendrick, Cristina Puy, Ashley E. Benson, Phillip A. Wilmarth, Ashok P. Reddy, Keith D. Zientek, Kilsun Kim, Adam Crosland, Chaevien S. Clendinen, Lisa M. Bramer, Olivia L. Hagen, Helen H. Vu, Joseph E. Aslan, Owen J.T. McCarty, Joseph J. Shatzel, Brian P. Scottoline, Jamie O. Lo.

This work was originally published by Res Pract Thromb Haemost 2025 Jan 9;9(1):102676.

4.1 Abstract

Background: Amniotic fluid (AF) plays a key role in fetal development, yet the evolving composition of AF and its effects of hemostasis and thrombosis are poorly understood.

Objectives: Characterize the procoagulant properties of AF as a function of gestation in humans and non-human primates.

Methods: We analyzed the proteomes, lipidomes and procoagulant properties of AF obtained by amniocentesis from rhesus macaque and human pregnancies at gestational-age matched timepoints.

Results: When added to human plasma, both rhesus and human AF accelerated clotting time and fibrin generation. We identified proteomic modules associated with clotting time and enriched for coagulation-related pathways. Proteins known to be involved in hemostasis were highly correlated with each other and their intensity of expression varied across gestation in both rhesus and humans. Inhibition of contact pathway did not affect the procoagulant effect of AF. Blocking tissue factor

pathway inhibitor reversed the ability of AF to block the generation of activated factor X. The prothrombinase activity of AF was inhibited by phospholipid inhibitors. The levels of phosphatidylserine in AF were inversely correlated with clotting time. AF promoted platelet activation and secretion in plasma.

Conclusions: The addition of AF to plasma enhances coagulation in a manner dependent on phospholipids as well as the presence of proteases and other proteins that directly regulate coagulation. We describe a correlation between clotting time and expression of coagulation proteins and phosphatidylserine in both rhesus and human AF, supporting the use of rhesus models for future studies of AF biology.

4.2 Introduction

While the coagulation cascade is classically viewed as a blood-restricted hemostatic system, accumulating evidence indicates that coagulation factors are broadly distributed beyond the circulation and are present in different physiological fluids. Moreover, coagulation proteases and cofactors exert functions that extend beyond clot formation, including roles in innate immunity, inflammation, and cell signaling. These observations suggest that coagulation is a more ubiquitous and pleiotropic system than traditionally appreciated. In this chapter, we investigate one of the most pro-coagulant fluids in human body, amniotic fluid (AF). AF is comprised of a complex and dynamic milieu that serves to support fetal development throughout gestation. Despite the ubiquitous presence of AF in gestation, the dynamical role of AF in physiology remains largely undefined. It has long been suspected that the molecular constituents of AF facilitate delivery and maternal survival by contributing to hemostasis during birth.[191] This hypothesis gains support from the hemostatic challenge posed by delivery, as postpartum hemorrhage accounts for a significant portion of maternal morbidity and mortality; it would be natural to assume that evolution favors such a styptic.[192]

Diametrically opposed to the benefits of limiting maternal bleeding, AF induced coagulation is surmised to be the main driver of consumptive coagulopathy and mortality associated with AF embolism.[193] *In vitro* experiments have confirmed the procoagulant nature of AF to some extent, affirming that AF accelerates thrombin production, shortens clotting time, and activates platelet aggregation when exposed to blood.[194,195] AF has also been shown to contain procoagulant extracellular vesicles and increasing quantities of tissue factor over gestation, with data suggesting that extrinsic pathway proteins in AF play a role in regulating barrier function in fetal skin during development.[196-198]

Beyond these initial observations however, the nature and content of AF hemostatic proteins, how they may change throughout gestation, and their potential role in processes such as hemostasis, postpartum hemorrhage prevention, and the prothrombotic phenotype of pregnancy remain poorly understood. There may be limited transfer of proteins from AF to the maternal circulation, in particular during vaginal delivery,[199] but how this might contribute to thrombosis in pregnancy remains undefined, especially considering that thrombosis is the leading cause of maternal mortality in developed nations. Similarly, the role by which AF may safeguard against fetal loss, maintain the subchorionic space, and prevent subchorionic bleeding are unknown.[200,201]

The study of potential biological roles of human AF has been impeded by the practical challenges associated with obtaining AF from human pregnancies, especially longitudinal samples throughout gestation, and the lack of a close and suitable animal model for AF research. We have recently shown that the rhesus AF proteome is very similar to the human AF proteome throughout pregnancy and have established a reference AF proteome across gestation.[202] This work established the non-human primate (rhesus macaques, macaca mulatta) as a relevant model of human AF biology.

In this study, we examine the molecular profile of AF in both rhesus macaque and human samples in order to better understand the procoagulant effects of AF across gestation.[203,204] We established parallels between non-human primate and human AF on coagulation, and, for the first time, employed analysis of the defined AF proteome to quantify shifts in AF coagulation protein levels over the course of gestation. Ultimately, we align these findings with *in vitro* studies directed at furthering our understanding of the physiology of AF during pregnancy.

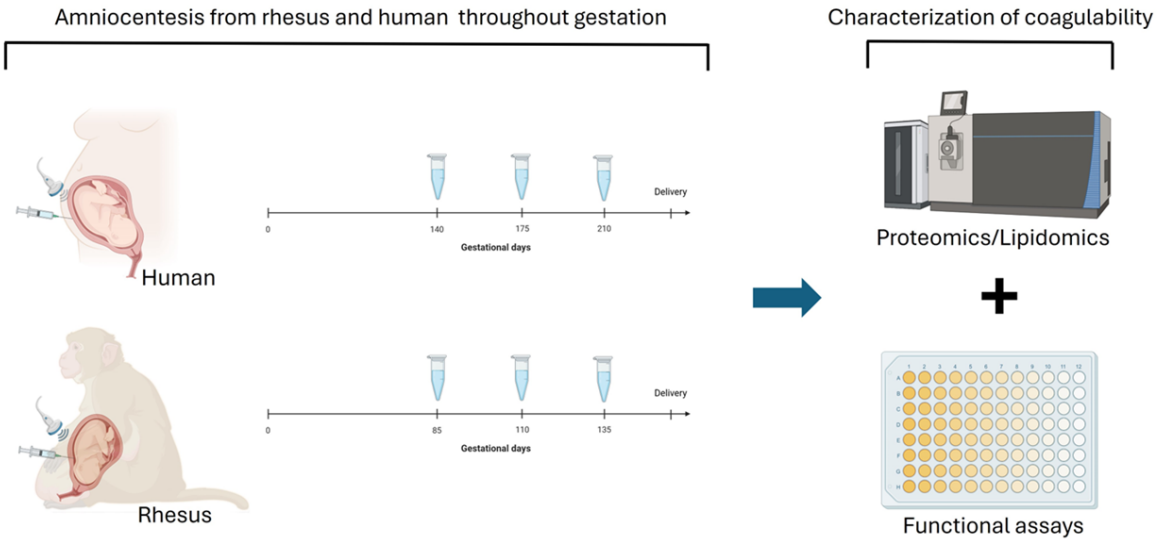

Figure 4.1 Schematic of the study design. Created with BioRender.com.

4.3 Materials and methods

4.3.1 *Reagents*

Factor (F) XII depleted plasma, FXI-depleted plasma, FIX-depleted plasma, and prekallikrein-depleted plasma were from Affinity Biologicals (Ancaster, ON). FX, FXa, FVIIa, FVa, prothrombin, GLA-domainless prothrombin, and α-thrombin were from Haematologic Technologies (Essex Junction, VT). Corn trypsin inhibitor was from Enzyme Research Laboratories (South Bend, IN, USA). Antibodies against tissue factor pathway inhibitor K1 and K2 domains were from MyBiosource (San Diego, CA). Innovin was from Siemens Healthcare Diagnostics (Deerfield, IL). Chromogenix S-2302, S-2765, and

S-2238 were from Diapharma (West Chester, OH). Annexin V (A13201) was from Thermo Fisher Scientific (Waltham, MA). APC anti-human CD62P was from BioLegend (San Diego, CA), FITC mouse anti-human PAC-1 was from BD Biosciences (Franklin Lakes, NJ). Phosphatidylserine Assay Kit (ab273295) was from Abcam (Cambridge, UK). All other reagents were obtained from Millipore Sigma (St. Louis, MO).

4.3.2 *AF collection and proteomics*

Rhesus and human AF samples were obtained as previously described.[202] Briefly, the rhesus sample group was comprised of 7 pregnant animals longitudinally sampled at 3 gestational time points (in days): gestational day (G)85, G110, and G135 (21 samples total, term is approximately 168 days). These gestational time points were matched by percentage completed gestation with 7 human samples at each time point (21 samples total). The comparable human gestational time point for G85 is approximately 20 weeks (G140), for G110 is approximately 25.5 weeks (G175), and for G135 is approximately 31.5 weeks (G210). Human samples were selected from pregnancies with the least pathological fetal indications (e.g., genetic testing with normal fetal anatomy on ultrasound). Determination of the overall AF proteomes at each gestational time point (rhesus G85, 110, and 135, and the comparable human gestational age time points: approximately 140, 175, and 210), was performed as previously described.[202]

4.3.3 *Recalcified clotting time*

Human venous blood was drawn in accordance with an IRB-approved protocol. Pooled normal plasma was prepared via centrifugation of citrated whole blood (in 0.32 %w/v sodium citrate) from four separate donors at 2150 × g for 10-min twice. Pooled normal plasma or factor-depleted plasma (50 µL) was incubated with vehicle control or 1:10 AF samples followed by a 3-min incubation with 50µL of 25 mM HEPES, 150 mM NaCl, pH 7.4 (HBS) in the absence or presence of selected inhibitors. Clot

formation was initiated with $CaCl_2$ (50 µL, 8.3 mM final) and the time to clot formation was determined on an KC4 Coagulation Analyzer (Trinity Biotech, Ireland). The clotting time measurement concluded when it reached 2000 sec. Clotting time was measured using individual rhesus AF samples from G85, G110, and G135 gestational time points, and individual human AF samples from equivalent gestational time points (G85, ~20 weeks, G110, ~25.5 weeks, and G135, ~31.5 weeks).

4.3.4 *Fibrin generation*

Pooled normal plasma (50 µL) was incubated with 1:10 AF at different gestational time points followed by incubation with 5 0µL of HBS for 3-min. $CaCl_2$ (50 µL, 8.3 mM final) was added to each plasma mixture. Fibrin generation was quantified by measuring changes in turbidity at an absorbance of 405 nm at 30-second intervals for 30-min using an Infinite M200 spectrophotometer (Tecan, CH). The lag time and time to reach half of maximum turbidity were obtained.

4.3.5 *FXIIa generation*

To measure the activation of factor (F) XII or prekallikrein in plasma, pooled normal plasma was incubated with pool samples of 1:10 AF at different gestational time points or 1:100 ellagic acid in the absence of $CaCl_2$ for 5-min. To measure the activation of FXII or prekallikrein in the AF, pool samples of 1:10 AF were incubated with 1:100 ellagic acid. The rate of hydrolysis of a FXIIa and kallikrein chromogenic substrate (2 mM Chromogenix S-2302) was measured at 405nm.

4.3.6 *FXa generation*

Innovin (1:100) was incubated with 50 pM FVIIa and 100nM FX in the presence of 10 µL of pooled AF at different gestational time points in HBS containing 5 mM $CaCl_2$ and 0.3 % bovine serum albumin for 15-min (final volume, 100 µL). In selected experiments, samples were incubated with the

anti-TFPI K1 and K2 domain antibodies (10 μg/mL respectively). 10μL of 100mM EDTA was added to quench the reaction. The rate of substrate hydrolysis of 1 mM Chromogenix S-2765 was measured at 405nm and then converted to FXa concentrations using a standard curve.

4.3.7 *Activation of prothrombin by prothrombinase complex*

5nM FVa and 0.2 nM FXa were incubated with 0.75 μM prothrombin in the presence of 10μL of pooled AF at different gestational time points in HBS containing 5mM $CaCl_2$ for 15-min (final volume, 100 μL). The reaction was stopped by 10 μL of 100 mM EDTA, and the rate of thrombin formation was determined by measuring thrombin concentration through the rate of Chromogenix S-2238 hydrolysis. In separate experiments, annexin V (10 ng/mL), lactadherin (30 nM), or prothrombin substituted by GLA-domainless prothrombin was added.

4.3.8 *Measurement of phosphatidylserine*

Lipids in AF were dissolved using 1 % peroxide-free Triton X-100 and subsequently extracted with methanol and methyl tert-butyl ether. The phosphatidylserine content within the lipid extract was quantified through fluorometric enzymatic assays following the manufacturer's instructions.

4.3.9 *Flow cytometry analysis*

Washed platelets (2×10^7/mL final concentration) were incubated in recalcified fibrinogen-depleted plasma containing 1:10 AF for 10 min. In selected experiment, rivaroxaban (10 μM), hirudin (25 U/mL), or Annexin V (10 nM) was added. Alternatively, washed platelets (2×10^7/mL) were pre-incubated with 1:10 AF or vehicle (modified HEPES/Tyrode buffer) for 10-min. FITC PAC-1 (1:50) or APC CD62P (1:50) were added to stain for activated integrin αIIbβ3 and P-selectin respectively. In selected experiments, the platelet mixtures were then stimulated with CRP-XL (10μg/mL), ADP (30μM), AYPGKF (250 μM), or U46619 (2 μM) for 20 min. The reactions were stopped by adding

2% paraformaldehyde. Platelet activation was measured using BD FACS Canto II flow cytometer (BD Biosciences, NJ), and analyses were performed on FlowJo software (version 10.8.1). Platelets were identified by logarithmic signal amplification for forward and side scatter characteristics and were collected for 1 min at medium flow rate.

4.3.10 *Weighted gene correlation network analysis (WGCNA)*

To investigate co-expression of proteins in AF we used the WGCNA package in R version 4.2.2. We performed a consensus network analysis using both the human and rhesus log protein intensities filtered for 1,090 unique orthologs. We used the pickSoftThreshold function to test soft thresholds from 4 to 20, and power=6 was selected to obtain an adjacency matrix with approximately scale-free topology (correlation=0.90). We used the blockwise Consensus Modules function with minModule Size=30, deep Split=2, and merge Cut Height=0.25 to generate consensus modules. Each module is then summarized by a value which corresponds to the first principal component of a given module, named the Module Eigenvalue (ME). We used the MEs for correlation with biological traits of interest, in this study clotting time and gestational age, to select modules for further investigation. We also used WGCNA to perform correlation between each protein and clotting time. We used the R package ggplot2 to visualize the distribution of correlation values within each module and species.

4.3.11 *Functional enrichment analysis of modules*

We used the STRINGdb v11.5 package in R to test for enrichment of Biological Processes, KEGG pathways, and Protein Families (Pfam) within each WGCNA module, with species=9544 (Macaca mulatta) and a score threshold = 400 to first plot each module of proteins as a protein-protein interaction network (PPI). We then used the get enrichment function, which returns enrichment for various annotation categories for each module of proteins, considering an FDR (false discovery rate)

adjusted p-value<0.05 as significant enrichment and selecting the top 2 to 3 unique terms per category to summarize the biological relevance of each module.

4.3.12 *Association with clotting time for individual proteins*

For each species, we fit separate linear models for each protein using limma with average clotting time as the predictor variable followed by eBayes moderation of standard errors. For rhesus, we also added a blocking argument and correlation value to account for within-subject variance. The resulting coefficients from the linear models therefore describe the change in protein abundance for each second of clotting time.

4.3.13 *A priori analysis of candidate proteins*

A list of the 75 candidate proteins related to coagulation and hemostatic regulation was generated. We then used this list to filter the untargeted proteomic datasets for each species using GeneName annotation overlap. Pearson correlation analysis between candidate proteins was performed separately in each species in R. The correlation matrix was re-shaped into a table with each pairwise combination of proteins and correlation value. The correlation values were filtered (cor>0.7) and visualized using a chordDiagram with the R package circlize. Positive correlation values were colored red, and negative values were shown in blue. We use the circos.track function to annotate categories of candidate proteins and color by group.

4.3.14 *Gestational age dynamics of candidate proteins*

To determine whether proteins involved in coagulation and hemostatic regulation are variable across gestation, we first visualized the overall longitudinal pattern of expression in each category of candidate proteins. For each species, we normalized expression of each protein by subtracting the mean and dividing by the standard deviation calculated from the reference group (~G85 non-human

primate equivalent). The mean across proteins was used to obtain category-specific Z-scores and plot longitudinally relative to non-human primate gestational age equivalent.

4.3.15 *Gene Set Enrichment Analysis (GSEA)*

To determine whether regulators of coagulation and hemostasis were enriched among proteins associated with gestational age we used the fgsea R package. Proteins in each dataset (human, rhesus) were ranked according to log fold change for association with gestational age. We defined 7 sets of proteins based on the priori candidate list described above. Enrichment scores for each set were calculated by walking down the ranked list of proteins associated with gestational age and using a running-sum statistic, which increases when a protein in the candidate set is encountered and decreases when a protein is not in the set of interest. The enrichment score was defined as the maximum deviation from zero encountered in the random walk. The significance level of enrichment scores was determined by a random permutation test, which generates a null distribution for the enrichment score, and therefore the nominal p-value was derived by comparing the observed enrichment score to the null distribution. Finally, the enrichment score for each protein set was normalized to account for the size of the set to generate a normalized enrichment score, and p-value was adjusted for multiple hypothesis testing. We summarized the normalized enrichment scores using the ComplexHeatmap package in R and consider FDR-adjusted $p<0.05$ as significant.

4.3.16 *Lipidomics*

Lipids were extracted using a MPLEx extraction.[205] Briefly, lipids were extracted by adding -20˚C, chloroform:methanol (2:1, v/v) to sample for a final ratio of chloroform:methanol:water of 8:4:3, v/v/v. The lower chloroform layer was removed and dried. Total lipid extracts (TLEs) were analyzed using liquid chromatography electrospray ionization tandem mass spectrometry (LC-ESI-MS/MS) comprised of a Thermo Vanquish Flex UHPLC system interfaced with a Thermo Velos-ETD Orbitrap

or Thermo Lumos mass spectrometer. Prior to analysis, TLEs were reconstituted in 10% chloroform and 90% methanol, 10µl of which was injected onto a reversed phase Waters CSH column (3.0 mm×150 mm×1.7 µm particle size), and separated over a 34-min gradient (mobile phase A (MPA): ACN/H2O (40:60) containing 10mM ammonium acetate; mobile phase B (MPB):ACN/IPA (10:90) containing 10mM ammonium acetate) at a flow rate of 250µl/min. Eluting lipids were analyzed in both positive and negative ionization modes using HCD (higher-energy collision dissociation) and CID (collision-induced dissociation) using a full scan analysis between 200-2000 m/z at a 120000 resolution. Lipids were analyzed using LIQUID and identified features were aligned to reference database based on identification, m/z, and retention time.[206] All features were manually verified. Peak intensities were log2 transformed and normalized via global median centering.

4.4 Results

4.4.1 *The procoagulant effect of AF at different gestational time points*

We first evaluated the coagulability of AF in human plasma. AF accelerated clotting time and fibrin generation in both species. Clotting time in recalcified human plasma at baseline was ~570 sec. The addition of human AF significantly reduced clotting time: G140 = 326.4 ± 43.1 sec, G175 = 262.1 ± 43.8 sec, G210 = 294.2 ± 34.9 sec (Figure 4.2A). Concurrently, human AF decreased the lag time for fibrin generation as well as the time to reach half-maximal in a dose-dependent manner (Figure 4.2A). The addition of rhesus AF also significantly decreased clotting time with less prominent effect observed in AF collected at later gestational time points: G85 = 156.9 ± 43.1 sec, G110 = 224.6 ± 43.8 sec, G135 = 294.9 ± 34.9 sec. Rhesus AF also shortened the lag time and the time to reach half-maximal for fibrin generation in a similar manner to human AF (Figure 4.3).

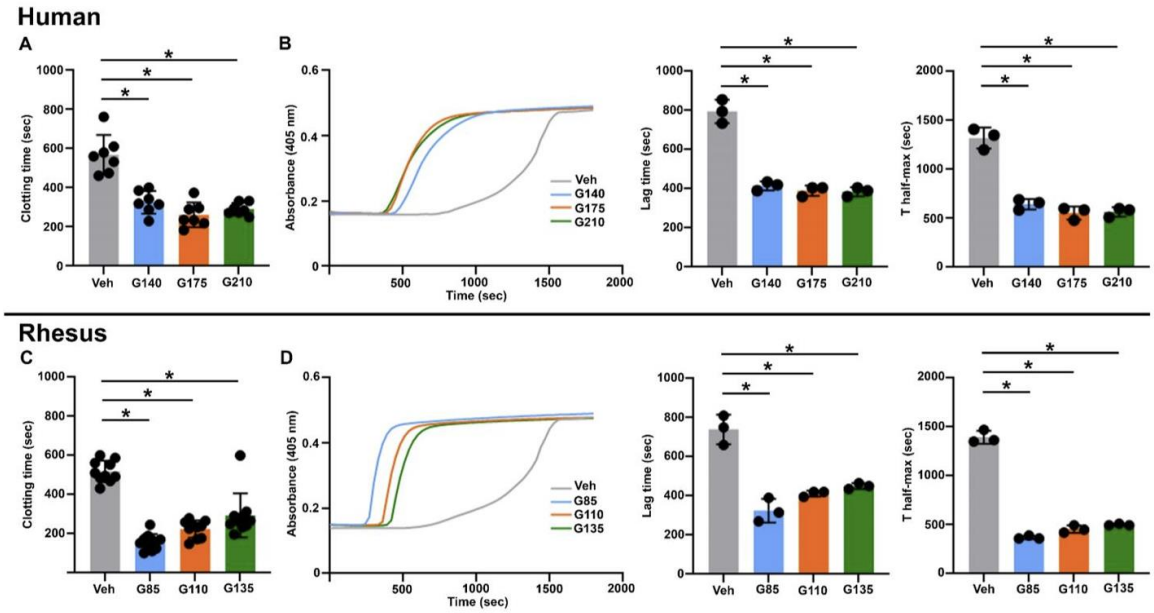

Figure 4.2 The procoagulant effect of AF at different gestational time points.
(A, C) Clotting assay was performed following the addition of human or rhesus AF at various gestational time points in a ratio of 1:10 to recalcified plasma. (B, D) Fibrin generation assay was measured in recalcified plasma preincubated with 10% v/v human or rhesus AF at different gestational time points. Time for fibrin generation initiation (lag time) and reaching half-maximum (Thalf-max) were quantified. Data are mean ± standard deviation (n=7 in clotting time assay and 3 in fibrin generation assay). Mann-Whitney U test was used for statistical comparisons.

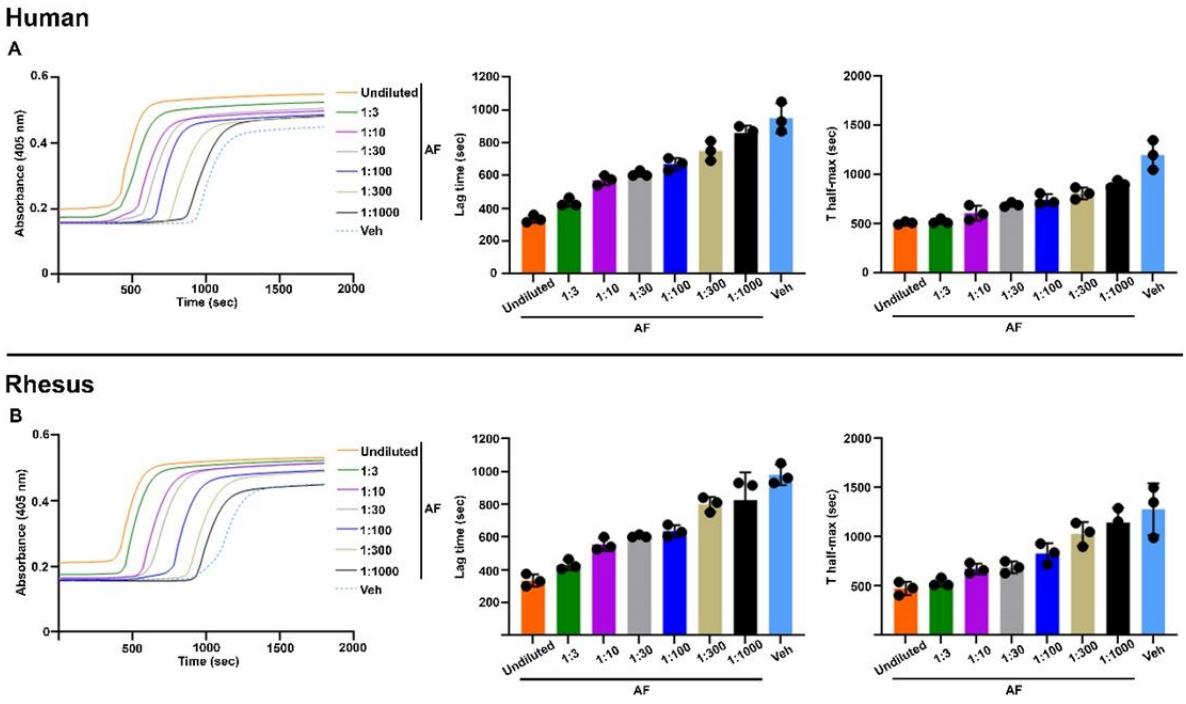

Figure 4.3 Dose-dependent effect of AF on fibrin generation.
(A,B) Fibrin generation assay was measured in recalcified plasma preincubated with 10% v/v human or rhesus AF at different dilutions. Time for fibrin generation initiation (lag time) and reaching half-maximum (Thalf-max) were quantified

4.4.2 *Human and rhesus AF consensus co-expression networks*

We previously compared the human and rhesus AF proteomes using quantitative LC-MS/MS and found 95.5% overlap between species with high correlation of mean protein intensities. In this study, we used a correlation network approach (WGCNA) to identify protein consensus modules using as input 1,090 unique orthologs which were identified in AF from both species. Protein intensities were log normalized within each dataset (species) prior to performing consensus network analysis. We identified seven consensus modules that were subsequently correlated with biological traits and analyzed at the pathway level to characterize the associated biology (Figure 4.4A). The modules were enriched for a variety of biological processes, KEGG pathways, and protein families but were most frequently associated with terms related to extracellular matrix, adhesion, neutrophil mediated immunity, and complement or coagulation cascades.

4.4.3 *Protein modules associated with clotting time*

Focusing on the coagulation-related pathways, the MEred3 module contained 59 proteins and was enriched for proteins involved in endopeptidase activity, proteolysis, and blood coagulation biological processes. Additionally, the MEred3 module had the highest correlation between the module eigenvalue and clotting time for individual human AF samples (Figure 4.4). The majority of module eigenvalues in rhesus AF samples were correlated with clotting time, due to the strong association between gestational age of rhesus AF and clotting time (Figure 4.4) in these longitudinally collected samples. While the MEgrey module eigenvalue was also correlated with clotting time, this module by default contains proteins which were not highly co-expressed and therefore were unassigned to other modules. Analysis of the distributions of individual protein correlation with clotting times within each module confirms that the MEred3 module proteins were individually negatively correlated with clotting time (left skewed distribution), while the MEgrey module proteins were not (Figure 4.4). A STRINGdb protein-protein interaction network of the MEred proteins highlights proteins involved in

complement activation (red), negative regulation of endopeptidase activity (yellow), blood coagulation (green), response to stress (pink), and phosphatidylcholine metabolic process (blue) (Figure 4.5).

4.4.4 *Individual proteins associated with clotting time are enriched for complement and coagulation cascades*

In addition to performing WGCNA-based consensus network analysis to identify clusters of proteins correlated with AF effects on clotting time, we also performed proteome-wide association analysis to identify individual proteins associated with clotting time in each species. In human AF, we detected and analyzed 1,381 proteins of which 1 protein (HEG1) was associated with clotting time at FDR $p<0.05$ and 131 at nominal significance. In rhesus AF, out of 1,381 proteins measured a total of 415 were associated with clotting time at FDR significance (205 up; 210 down). In both species the top significant proteins were highly enriched for the KEGG pathway “complement and coagulation cascades” (Figure 4.5).

A

Name	Color	Size	Biological Process	KEGG	Pfam	Rhesus clotting	Human clotting
MEblack		98	Cell adhesion, neutrophil degranulation	Galactose metabolism, Metabolic pathways	-	-0.32 (0.2)	-0.18 (0.4)
MEturquoise		458	Regulation of peptidase activity, neutrophil mediated immunity	Lysosome, Complement and coagulation cascades	Calcium-binding EGF domain, Serpin (serine protease inhibitor)	0.65 (0.001)	-0.15 (0.5)
MEgreen4		61	-	-	-	0.69 (4e-04)	0.25 (0.3)
MEred3		**59**	**Regulation of endopeptidase activity, Regulation of proteolysis, blood coagulation**	**Complement and coagulation cascades**	**Serpin (serine protease inhibitor)**	**-0.36 (0.1)**	**-0.53 (0.01)**
MEdodgerblue		232	ECM organization, Biological Adhesion	ECM-receptor interaction, Focal adhesion	Calcium-binding EGF domain, Collagen triple helix repeat	-0.56 (0.007)	0.42 (0.05)
MEcoral		74	Cell adhesion, Cell differentiation	Axon guidance, Cell adhesion molecules	Ephrin receptor ligand binding domain, Fibronectin type III domain	-0.65 (0.001)	0.21 (0.4)
MEgrey		108	Cell adhesion, Regulation of response to stimulus	Biosynthesis of amino acids, Complement and coagulation cascades	Fibrinogen alpha/beta chain family, Fibrinogen beta and gamma chains	-0.33 (0.1)	-0.31 (0.2)

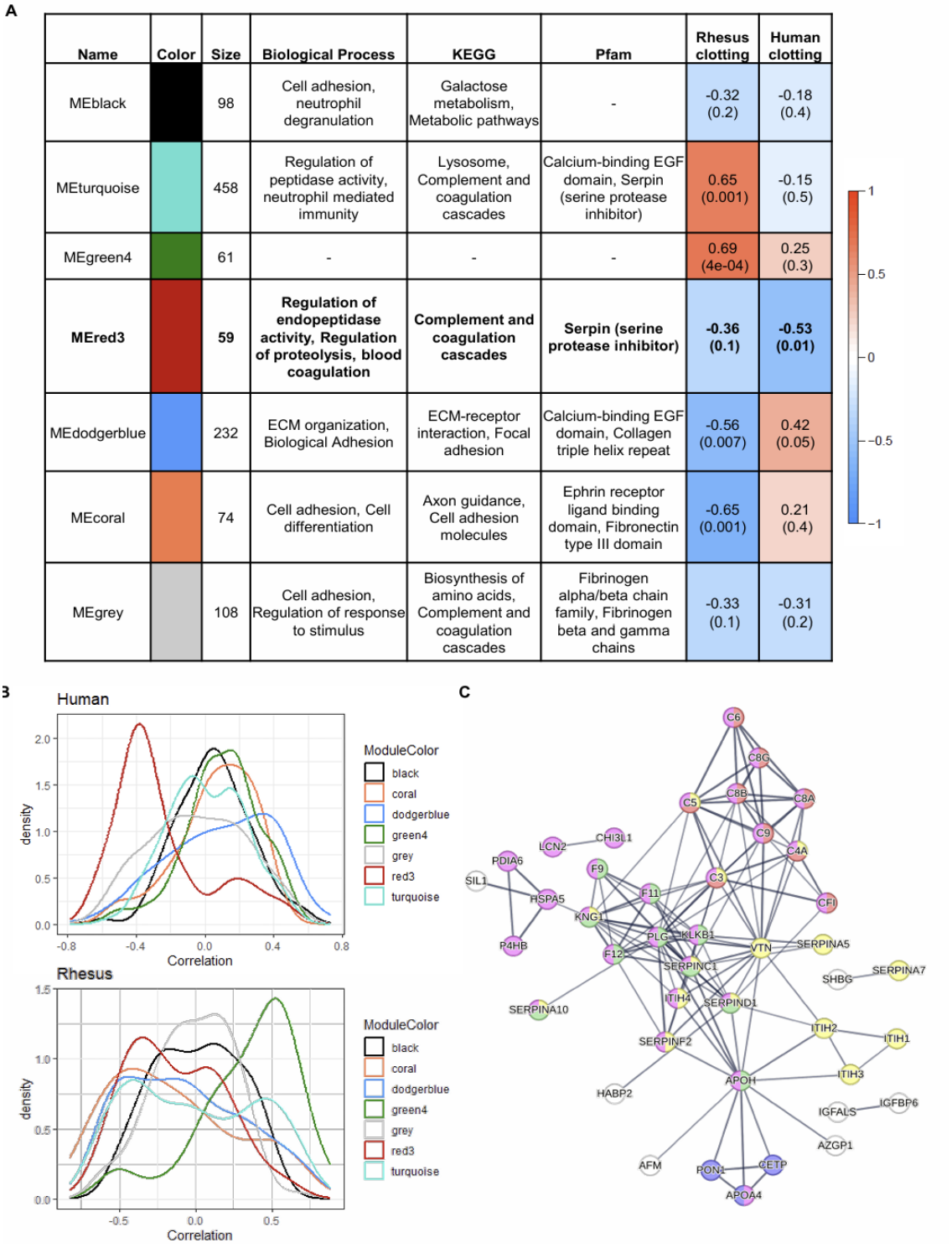

Figure 4.4 Untargeted proteomics identified modules associated with clotting time and enriched for pathways related to coagulation.

We used consensus weighted gene correlation network analysis to cluster all ortholog proteins into modules of correlated proteins. The size of modules, biological enrichment summary, and association with clotting time is presented in (A). We summarize the distribution of correlation values with clotting time for individual proteins in each module separately for each species (B). Proteins identified in the MEred module are presented in a protein-protein interaction network and colored based on STRING enrichment categories: complement activation (red), negative regulation of endopeptidase activity (yellow), blood coagulation (green), response to stress (pink), and phosphatidylcholine metabolic process (blue) (C). Data generated by Lyndsey E. Shorey-Kendrick (OHSU).

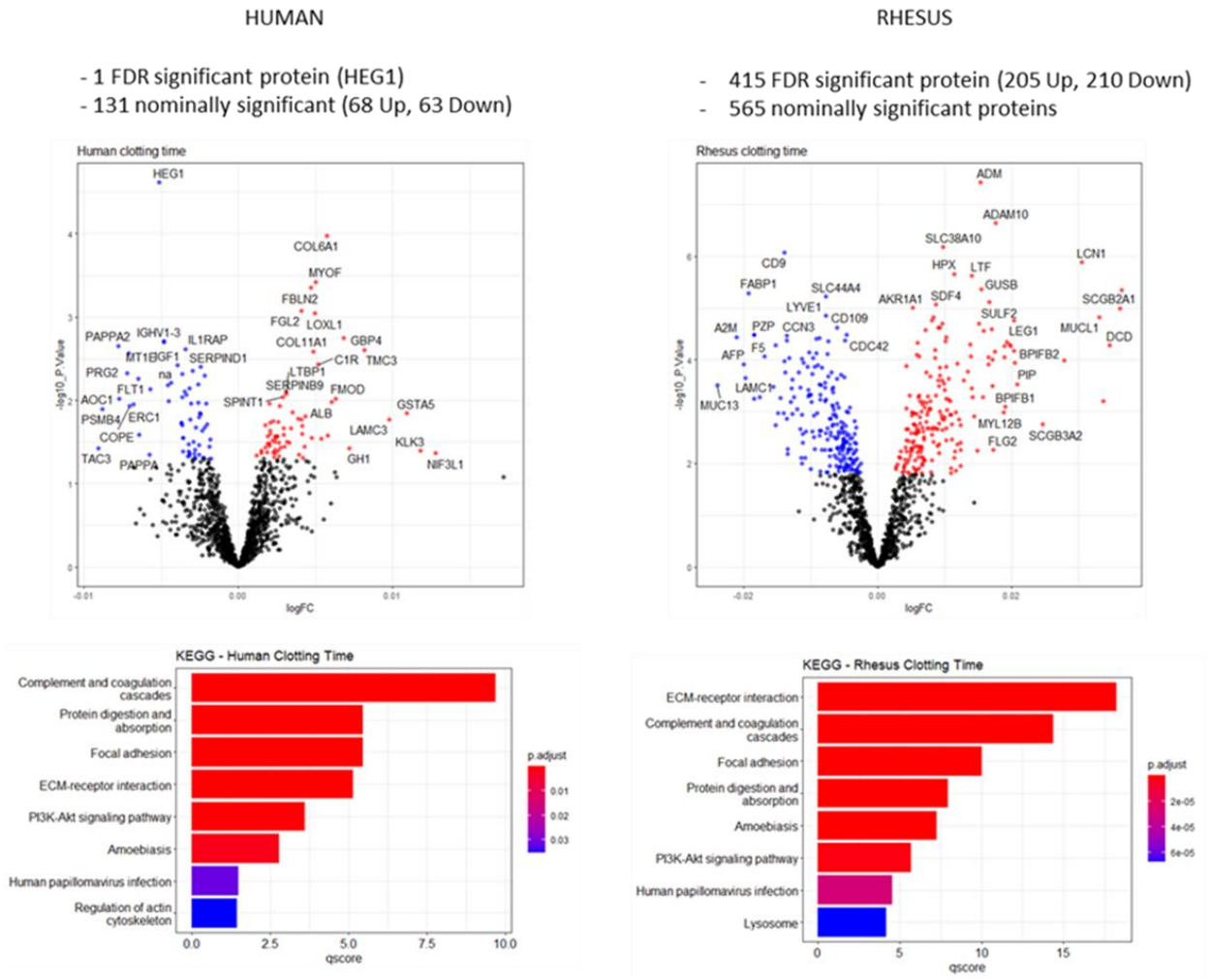

Figure 4.5 Proteome-wide association analysis identified individual proteins associated with clotting time in each species. Volcano plots on top display the logFC on the x-axes and -log10Pvalues on the y-axes. Individual points represent each protein tested and a subset are annotated with gene symbols. Red points indicate increased abundance with increasing clotting time and blue indicates decreased abundance with nominal p<0.05. Human results are displayed on the left and rhesus on the right. Among the candidate differentially expressed proteins in each species we performed KEGG enrichment analysis. Barplots on the bottom show the top 8 terms identified for each species, with the -log10(adjusted P-value) on the x-axis and KEGG terms labeled on the y-axis. Data generated by Lyndsey E. Shorey-Kendrick (OHSU).

4.4.5 *AF coagulation proteins are highly correlated with each other*

We next performed an a priori analysis of candidate proteins known to be involved in hemostatic regulation. Our lookup table consisted of 7 categories: “Complement” (n =37 proteins), “Contact Pathway” (n=2), “Fibrinolysis” (n=7), “Regulators of Coagulation” (n=4), “Primary Hemostasis” (n=5), “Secondary Hemostasis” (n=14), and “Iron Metabolism” (n=6). Out of 75 proteins in the lookup table, 51 were identified in rhesus AF and 55 in human AF. We next examined the correlation between

individual proteins within each species and visualized proteins with correlations above 0.7 in Figure 4.4A for human and rhesus separately. Out of the 55 candidate proteins identified in human AF, 35 were significantly correlated (cor>0.7) with one or more candidate proteins. In human AF, complement component C6 had the largest number of significant correlations (n=11), followed by antithrombin (SERPINC1; n=10) and plasminogen (PLG; n=8). In rhesus AF, there were 35 unique proteins with one or more correlation among candidate proteins: transferrin had the highest number of significant correlations (n=12), followed by complement factor I (CFI), PLG, and SERPINC1 (n=11). Most correlations between candidate proteins were positive apart from tissue factor pathway inhibitor (TFPI), which was negatively correlated with SERPINC1, FV (F5), and transferrin, and a negative correlation between glycoprotein IV (CD36) and FXII (F12) in rhesus. In human AF the only negative correlation was observed between FXIII (F13A) and protein homologous restriction factor (CD59).

4.4.6 *AF coagulation proteins are dynamic across gestation*

We previously determined that gestational age at AF collection was a large source of variability in AF protein composition, with 31.9% of human proteins differentially expressed with gestational age and over 50% of rhesus AF proteins changing with gestational age. As described above, we also observed a strong relationship between clotting time and gestational age in rhesus AF. Therefore, we next examined whether the priori defined hemostatic protein candidates were associated with gestational age. We first visually inspected the relative mean abundance of proteins in each category normalized to G85 rhesus equivalent AF (Figure 4.4B). In human AF, proteins involved in fibrinolysis increased while regulators of primary hemostasis categories either decreased gradually with increasing gestational age or remained stable. In rhesus AF, the trajectory of mean protein expression within each category exhibited two main patterns, with regulators of coagulation, secondary hemostasis, and iron metabolism decreasing slightly compared to G85, while proteins in the contact and complement pathways, fibrinolysis, and primary hemostasis categories decreasing more dramatically between G85

and G110 before plateauing or gradually increasing between G110 and G135. We next used gene set enrichment analysis (GSEA) to determine whether the a priori defined protein categories described above are randomly distributed among ranked lists of proteins according to association with gestational age (GA) from our previous study,[15,202] or whether they are enriched among top up or downregulated proteins with GA.[15] We found no significant enrichment scores for candidate pathways among the proteins associated with gestational age in human AF. However, we did observe significant enrichment of the "Complement" candidate proteins among proteins associated with GA in rhesus AF (ES = -0.55, NES = -1.72, adjusted p-value = 0.03; Figure 4.6).

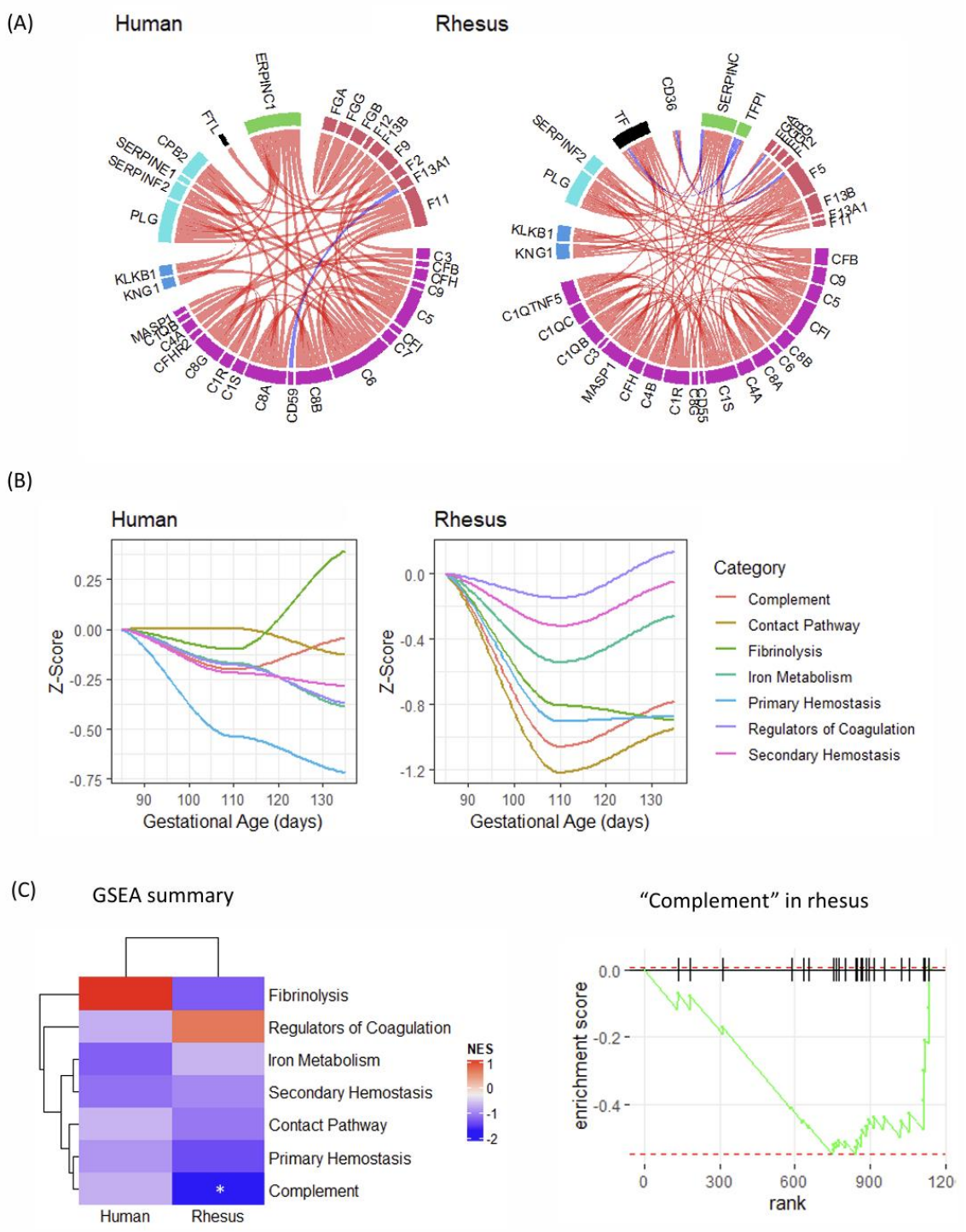

Figure 4.6 Proteins related to coagulation and hemostatic regulation change across gestation.
Untargeted proteomic data filtered for candidate proteins where we summarize significant correlations (absolute value of correlation >0.7) between individual proteins within each species with positive correlations shown in red and negative in blue. Individual candidate proteins are annotated to human ortholog name and colored according to functional categories (A). For each species, we normalized expression of each candidate protein to the reference group (~G85 non-human primate equivalent) and summarize within each category using Z-scores in order to visualize the longitudinal profile across gestation (B). Gene set enrichment analysis was performed to determine whether a priori categories are enriched among proteins associated with gestational age (C). Data generated by Lyndsey E. Shorey-Kendrick (OHSU).

4.4.7 *The procoagulant effect of AF is independent of contact pathway of coagulation*

To assess whether the procoagulant effect of the AF involves the activation of the contact pathway of coagulation, we performed experiments using human plasma deficient in FXII, XI, IX, or prekallikrein. We found that both human and rhesus AF effectively shortened the clotting time of plasma depleted in FXII, FXI, FIX, and prekallikrein (Figure 4.7). To differentiate whether AF itself contained abundant coagulation factors or its procoagulant effect was not associated with contact pathway, we employed pharmacological inhibition of contact pathway with corn trypsin inhibitor. Corn trypsin inhibitor was unable to preclude the ability of AF to reduce clotting time of normal plasma (Figure 4.7). These results separated the procoagulant effects of AF from contact pathway of coagulation. The incubation of normal pooled plasma with AF did not result in significant FXII or PK activation (Figure 4.7). In contrast, the incubation of ellagic acid with AF, which contained a certain amount of FXII and PK zymogen, could generated FXIIa or kallikrein (Figure 4.7).

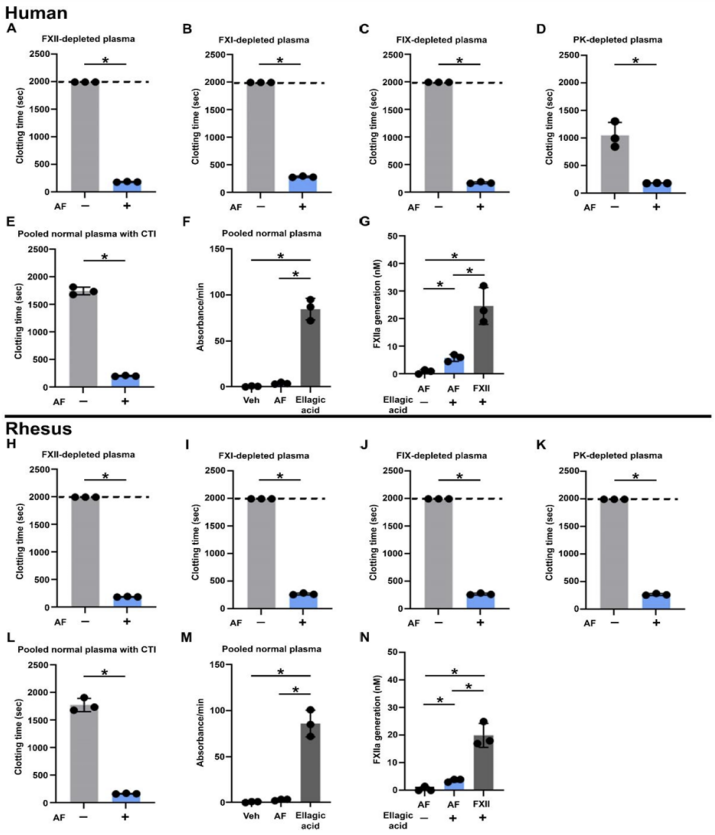

Figure 4.7 Contact pathway of coagulation and procoagulant effect of AF. Clotting assay was performed following the addition of human or rhesus AF in a ratio of 1:10 to recalcified plasma deficient in (A, H) FXII, (B, I) XI, (C, J) IX, (D, K) prekallikrein, or (E, L) pretreated with 50 µg/mL of corn trypsin inhibitor. (F, M) FXIIa generation assay of plasma was performed in the presence human or rhesus AF. Ellagic acid served as a positive control. (G, N) FXIIa generation assay of human or rhesus AF was performed with or without ellagic acid. FXII and ellagic acid served as a positive control. Data are mean ± standard deviation (n=3). Mann-Whitney U test was used for statistical comparisons

4.4.8 *FXa generation is regulated by TFPI in AF*

We next assessed whether AF affected FXa generation initiated by TF-FVIIa complex in a purified system. Surprisingly, the addition of human and rhesus AF led to a moderate reduction in FXa generation (Figure 4.8). Previous research had reported that AF contains TFPI, an anticoagulant protein that inhibits the TF-FVIIa complex.[207] Therefore, we use blocking anti-TFPI K1 and K2 domain antibodies to determine whether TFPI present in AF was responsible for impeding FXa generation. We observed that the blocking anti-TFPI antibodies restored FXa generation in the presence of AF (Figure 4.8). These results suggest that the procoagulant effect of AF was modulated by TFPI. Proteomics of AF confirmed the existence and expression level of TFPI at different gestational time points (Figure 4.8). The amount of TFPI present in the rhesus AF was significantly higher at later gestational time points (Figure 4.8) and correlated with clotting time of plasma with the addition of rhesus AF (Figure 4.8).

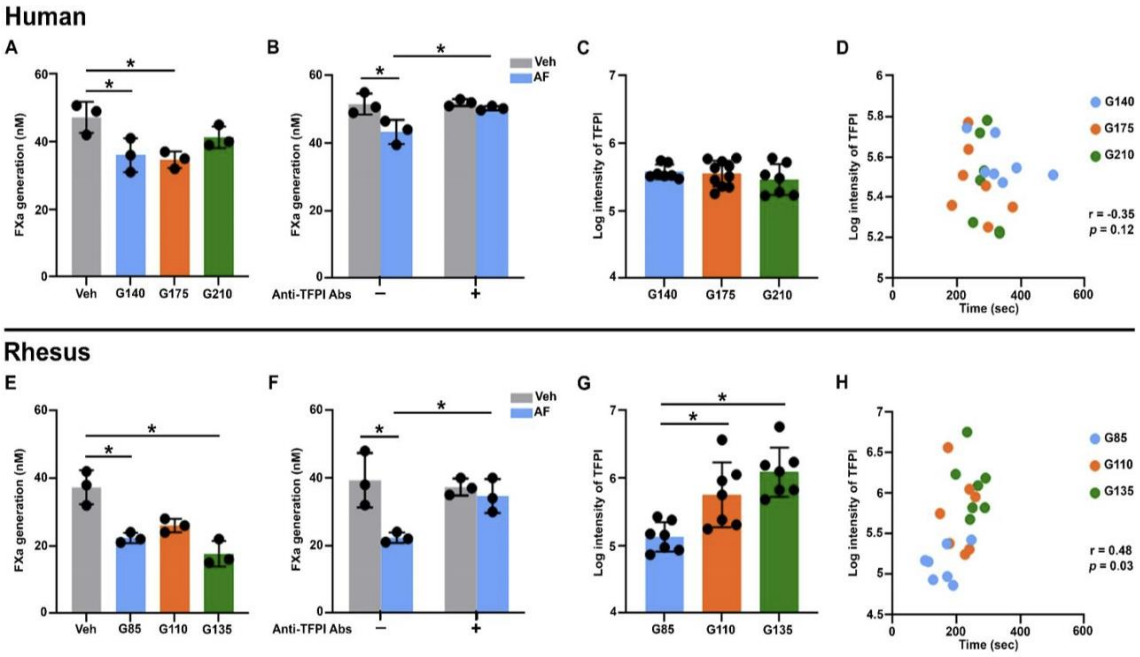

Figure 4.8 FXa generation and TFPI in AF. (A,E) FXa generation after initiation with TF was assessed in the presence of pooled human or rhesus AF at various gestational time points. (B,F) Anti-TFPI K1 and K2 antibodies (10 µg/mL) were added into the assay in the presence of human or rhesus AF. (C,G) Logarithmically normalized expression of TFPI was determined by human or rhesus AF proteomics. (D,H) The correlation between logarithmically normalized expression of TFPI in proteomics and recalcified clotting time of plasma with the addition of human or rhesus AF. Data are mean ± standard deviation (n=3 in FXa generation assay and 7 in proteomics). Mann-Whitney U test was used for statistical comparisons.

4.4.9 *Phospholipids in AF contribute to activation of prothrombin by prothrombinase complex*

The final and most critical step in the convergence of contact and extrinsic pathway of coagulation is the common pathway. In the common pathway, FXa, activated FV, and calcium form the prothrombinase complex, which, along with phospholipids catalyze the proteolytic conversion of prothrombin to thrombin. As shown in Figure 4.9, we found that human and rhesus AF substantially enhanced thrombin generation in the absence of additional phospholipids. To assess the role of phospholipids in AF in thrombin generation, we employed two phospholipid-targeting inhibitors, lactadherin or annexin V. Both of these phospholipid inhibitors significantly blocked prothrombinase-activating action of AF by more than 80% (Figure 4.9) in agreement with previous work.[208] We repeated these thrombin generation experiments using a recombinant prothrombin that lacked the gamma-carboxyglutamic (GLA) domain. The GLA domain is essential for high affinity binding of coagulation factors to phospholipids, and the absence of GLA domain ablates binding to phospholipids, greatly reducing their activities. We found that the ability of AF to potentiate thrombin was significantly reduced when the GLA-domainless prothrombin was used in this system (Figure 4.9), validating a role for phospholipids in AF in thrombin generation. Furthermore, we quantified the level of phosphatidylserine in AF using fluorometric enzymatic assay. The level of phosphatidylserine level in human and rhesus AF was approximately 25 times more than that in plasma, measuring 730.4±139.8 μM and 842±307.8 μM in human and rhesus AF as compared to 31.3±14.0 μM and 26.5±11.3 μM in human and rhesus plasma, respectively (Figure 4.9). Notably, the levels of phosphatidylserine (34:2) in AF lipidomics was inversely correlated with clotting time (Figure 4.9) for both human and rhesus plasma ($R=-0.52$ and -0.91; $p=0.018$ and $1.6E-8$, respectively. This result suggests the indispensable role of phospholipids in the procoagulant effect of AF.

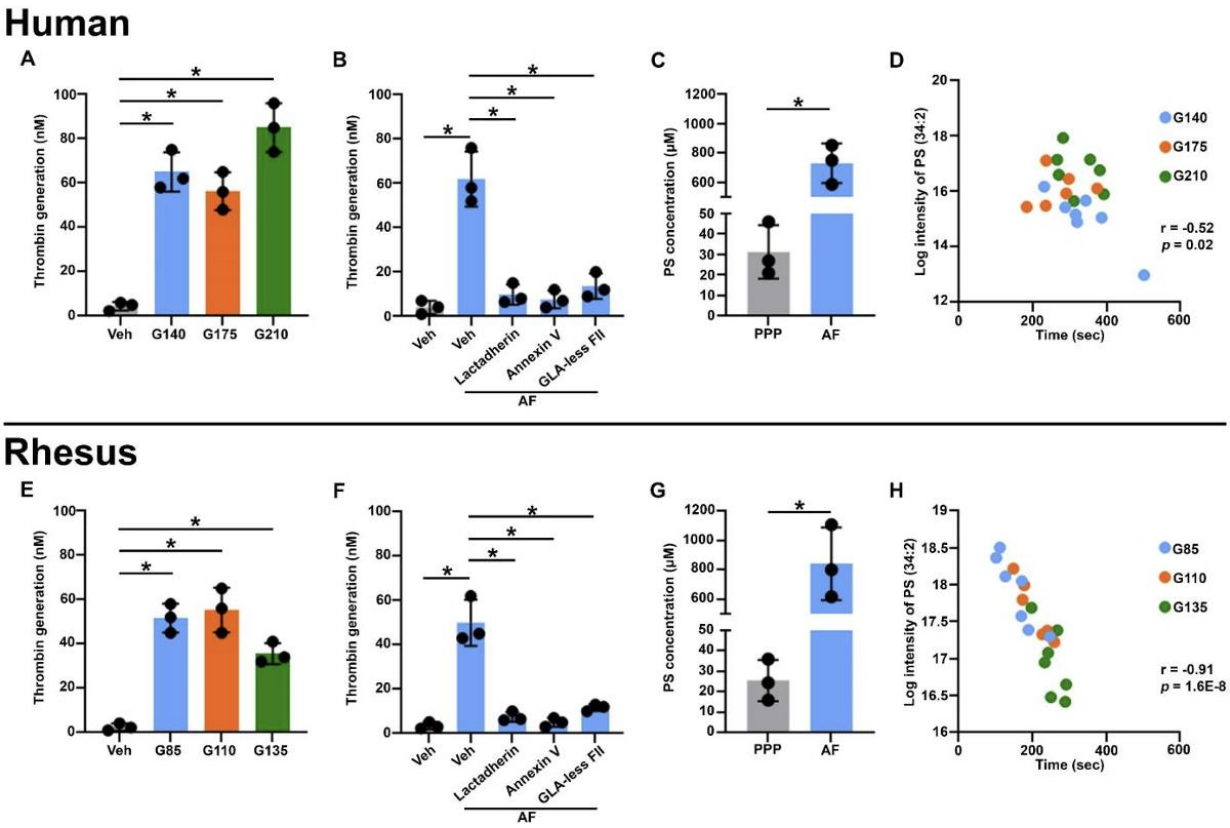

Figure 4.9 Thrombin generation and phosphatidylserine in AF.
(A, E) Thrombin generation assay was evaluated in the presence of pooled human or rhesus AF at various gestational time points. (B, F) Lactadherin (30 nM) or Annexin V (10 nM) was added. In selected experiment, Gla-domainless prothrombin was used. (C, G) Phosphatidylserine level was quantified as L-serine generation following enzymatic cleavage of phosphatidylserine in lipid extracts of human or rhesus AF. (D, H) The correlation between logarithmically normalized expression of phosphatidylserine (34:2) in lipidomics and recalcified clotting time of plasma with the addition of human or rhesus AF. Data are mean ± standard deviation (n=3 in thrombin generation assay and 7 in lipidomics). Mann-Whitney U test was used for statistical comparisons.

4.4.10 *AF triggers platelet activation through thrombin generation in plasma*

To assess the effect of AF-mediated thrombin generation on platelet activation, we used flow cytometry to analyze platelet α-granule secretion and integrin αIIbβ3 activation in plasma settings. Platelets were incubated in recalcified fibrinogen depleted plasma for 10 min followed by staining with APC-CD62P and FITC-PAC1. The surface levels of platelet P-selectin and PAC1 on platelets significantly increased in the presence of human and rhesus AF (Figure 4.10). In separate experiments, the addition of FXa inhibitor rivaroxaban, thrombin inhibitor hirudin, or phospholipid inhibitor annexin V suppressed the effect of AF on platelet activation, indicating that the effect of AF on platelet activation resulted from thrombin generation (Figure 4.10). We next examined the direct effect of AF

on platelets. There was no significant change in α-granule secretion and integrin αIIbβ3 activation in resting or agonist-stimulated platelets in the presence of either human or rhesus AF (Figure 4.10).

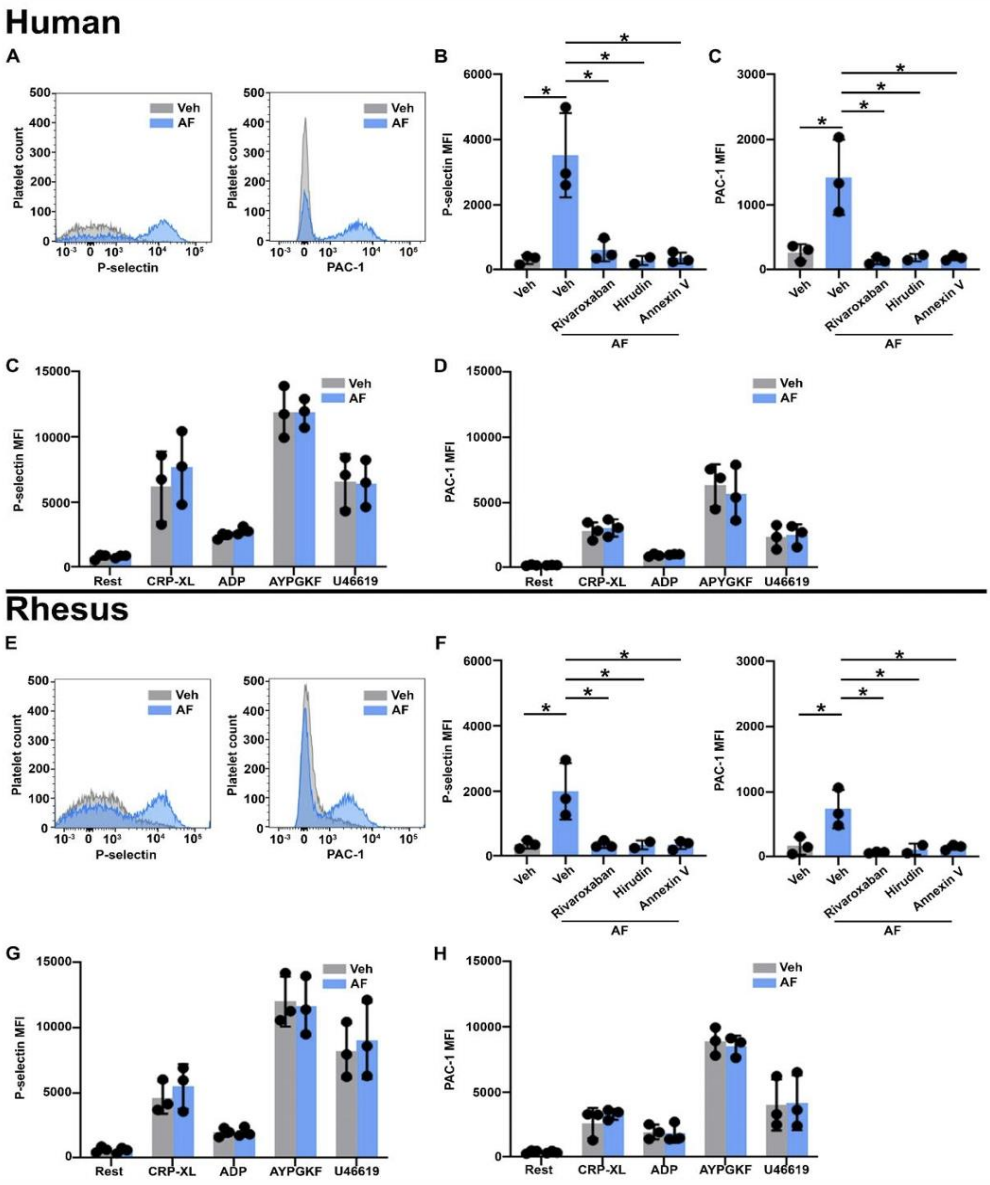

Figure 4.10 Platelet activation and AF.
Platelet activation was assessed by flow cytometry analysis of platelet degranulation and integrin activation. Washed platelets (2×107/mL) in recalcified (20 mM of $CaCl_2$) fibrinogen-depleted plasma were treated with human AF, rhesus AF, or vehicle (modified HEPES/Tyrode buffer), staining with (A, E) APC-CD62P and FITC-PAC1 to monitor platelet α-granule secretion and integrin activation. (B, F) In selected experiment, rivaroxaban, hirudin, or annexin V was added. Alternatively, washed platelets (2×10^7/mL) were pretreated with human AF, rhesus AF, or vehicle (modified HEPES/Tyrode buffer), followed by CRP-XL (10 µg/mL), ADP (30 µM), AYPGKF (250 µM), or U46619 (2 µM) stimulation and staining with (C, G) APC-CD62P and (D, H) FITC-PAC1. Data are mean ± standard deviation (n=3). Mann-Whitney U test was used for statistical comparisons.

4.5 Discussion

This study is the first comprehensive evaluation regarding the effects of AF on coagulation throughout gestation, integrating proteomic and lipidomic data with *in vitro* studies, and utilizing both human and non-human primate samples. We found that FXa generation was moderately reduced by AF, which we hypothesize is due to the presence of TFPI in AF. Yet the abundance of phospholipids in AF was found to promote thrombin generation, which overwhelmed the anticoagulant effects of TFPI to promote global thrombin generation and subsequent platelet activation. This integrative approach offers a detailed understanding of the potential role of AF in both normal and pathological hemostatic processes. This study also offers insights into when in the rare scenario that AF comes into contact with maternal blood - a recognized mechanism for AF embolism, an uncommon but nonetheless obstetric emergency.

AF is initially derived from maternal plasma.[209] Given that embryonic skin contains only simple epithelium, AF could diffuse through the non-keratinizing skin under hydrostatic and osmotic forces in early gestation.[210] The composition of AF at this early stage is reasonably comparable to maternal plasma.[211] By the second half of pregnancy, full keratinization of the fetal skin no longer allows fluid to transfer as easily as before.[212,213] As gestation progresses, fetal urination and lung secretion prevail and significantly contribute to the composition of AF.[209] Yet, AF does not mix in the fetal circulation under physiological conditions. Concurrently, as fetal lung tissue begins developing and producing phospholipids, one of the phospholipids that possesses procoagulability, phosphatidylserine, is synthesized by fetal lung cells as well as from cellular turnover and apoptosis during fetal development.[214] These observations may explain why we observed higher concentrations of phospholipids,[215] and in particular phosphatidylserine, in AF than in plasma. Given our observation that the procoagulant properties of AF are dynamic, with AF being the most procoagulant in the first

trimester, it is possible that this effect supports fetal hemostasis and barrier function in the earliest period of gestation and may be necessary to achieve successful growth and development.

The amnion, a single layer of epithelium lining the amniotic sac, functions as a crucial barrier that separates AF from the vascularized chorion.[216] The intricate interactions between AF and the amniotic epithelium likely contribute to a healthy intrauterine environment for optimal fetal growth and development during pregnancy, which includes regulation of AF composition, immune modulation, as well as secretion of growth factors and cytokines.[217] Recent work revealed that TF-FVIIa within the AF is capable of activating protease-activated receptor 2 on the fetal epithelium, likely contributing to fetal homeostasis during the early phases of development.[197] Herein, we identified a key regulator of TF-FVIIa interaction, TFPI, as a critical regulator of AF's procoagulant activity. TFPI plays a key role in inhibiting coagulation by blocking the extrinsic pathway-mediated generation of FXa.[46,218] We observed that AF-derived TFPI was able to suppress FXa generation. When an anti-TFPI antibody was introduced, this inhibition was reversed, restoring FXa generation and enhancing AF-mediated coagulation *in vitro*. These findings suggest that AF's procoagulant properties are, at least in part, modulated by TFPI. This observation underscores AF's dual role in regulating hemostasis, as it contains both procoagulant and anticoagulant factors, reflecting the tightly regulated mechanisms that control blood coagulation. This balance may be particularly crucial during pregnancy, where a finely tuned hemostatic environment is essential to prevent both hemorrhage and thrombosis. Along these lines, one such study demonstrated that depletion of TFPI in a rabbit model increased susceptibility for development of disseminated intravascular coagulopathy after injection of TF or endotoxin, a condition similar to the aftermath of AF embolism.[219] Consequently, understanding the role of TFPI and other hemostatic regulators in modulating AF's coagulation effects may provide valuable insights into the mechanisms underlying pregnancy-related hemostasis.

This work also identified the pivotal role of phosphatidylserine, a phospholipid present in high concentrations in AF, in driving its procoagulant properties.[208,220] The presence of phosphatidylserine is inversely correlated with clotting time, emphasizing its role in enhancing thrombin generation and accelerating clot formation upon exposure to blood. This phospholipid-dependent mechanism may play a critical role in maintaining hemostatic balance during pregnancy, particularly in early gestation when AF's procoagulant effects peak. While this observation is speculative, it generates intriguing hypotheses and invites comparisons to the mechanisms of obstetric antiphospholipid syndrome (APS). Obstetric APS is characterized by prothrombotic antibodies targeting phospholipids and phospholipid-binding proteins, leading to severe complications such as recurrent miscarriage, preeclampsia, and placental insufficiency, as well as inhibiting phospholipid-dependent thrombin generation.[221] Although the mechanisms driving pregnancy loss in obstetric APS have been theorized to be prothrombotic, our findings suggest that phospholipid-dependent clotting may be a normal physiological process in healthy pregnancy, supporting hemostasis at the maternal-fetal interface and preparing the body for the heightened hemostatic demands of delivery. In obstetric APS, disruption of this phospholipid-driven coagulation may contribute to the increased risk of pregnancy complications. Further studies are needed to better define the potential role of AF in this obstetric pathology. Understanding how antiphospholipid antibodies interfere with normal phospholipid function in AF could offer valuable insights into the pathophysiology of obstetric APS and inform the development of targeted therapies.

An increasing trend in TFPI expression across gestation was observed, which was associated with longer clotting times, was more pronounced and consistent in rhesus AF compared to human AF. While biological differences between species may account for this, the observation could also be attributed to lower inter-individual variability in rhesus AF in the context of a longitudinal versus cross-sectional sampling design. In support of this overall trend, we also observed the strong and

inverse correlation between expression of phosphatidylserine (34:2) and clotting time in rhesus AF over gestation.

Platelet activation has been considered a significant factor in the development of AF embolism, as it manifests several thromboembolic characteristics.[222,223] Therefore, we examined whether AF activates platelets, which may also contribute to maternal thrombosis when AF encounters maternal blood. We demonstrated that although AF itself does not directly affect platelet activation, AF activates platelets through thrombin generated in the plasma.

In conclusion, AF demonstrates a significant procoagulant effect, accelerating clotting and fibrin production, which is dynamic through gestation and largely dependent on phospholipids, as indicated by the counteraction of this effect through phospholipid inhibition. Importantly, the consistent correlation between clotting time, expression of coagulation proteins, and phosphatidylserine levels observed in both rhesus and human AF further underscores the translational strength of the non-human primate model. This supports its use in future investigations into the procoagulant properties of AF and their implications in pregnancy-related hemostasis and pathologies, an understudied but biologically significant topic.

Our study had several strengths, particularly in leveraging unique AF samples from both a translational rhesus model and human pregnancies to address critical knowledge gaps in understanding the procoagulant properties of AF. Rhesus macaques and humans share similar physiological, genetic, reproductive, and developmental traits, making the rhesus model ideal for pregnancy studies and longitudinal AF sampling, which would be neither feasible nor ethical in humans. Furthermore, all rhesus samples were collected by a single board-certified Maternal-Fetal Medicine specialist (J.O.L) under ultrasound guidance, ensuring rigor and reproducibility in the collection process. The rhesus

subjects were also controlled for age, size, and housing conditions, minimizing the confounding variables often present in human cross-sectional study designs. Additionally, our ability to deeply phenotype the prothrombotic contents of AF and corroborate these observations with direct mechanistic *in vitro* experiments further strengthens the findings of our study.

There are some limitations in this study. First of all, the limited size of the human plasma pool (n=4) may introduce potential bias into the results. Secondly, our study was not able to specify the subtypes of TFPI present in AF. When referring to TFPI, we generally mean TFPI-1. However, TFPI-2, a placenta-derived protein that is structurally homologous to TFPI-1, exhibits distinct biological functions.[224] Unlike TFPI-1, TFPI-2 may possess procoagulant characteristics and has been associated with an elevated risk of venous thromboembolism.[225] Since TFPI-2 levels in AF have not yet been established, further studies are needed to comprehensively understand the roles of different TFPI subtypes in the amniotic environment. Additionally, the relatively high concentrations of annexin-V and lactadherin used in our study could block the prothrombinase-activating effects not only of phospholipids but also of other procoagulant anionic molecules such as skeletal muscle myosin,[226] potentially masking their contribution to prothrombin activation. Lastly, although previous studies found no *in vitro* evidence for an effect of AF on fibrinolysis,[227-229] we did not specifically assess the potential impact of AF on fibrinolysis in this current study. Therefore, more research is required to better characterize the full spectrum of procoagulant properties in AF.

Chapter 5. Characterization of the Binding of Skeletal Muscle Myosin to Fibrin in Trauma

Chih Jen Yang, Amelia A. Rodolf, Joseph P. Garay, Ethan C. Kelmser, André L. Lira, Jiaqing Pang, Helen H. Vu, Hiroshi Deguchi, Danielle F. Peterson, Natasha S. McKibben, Catherine E. Hutchison, Talia Trapalis, Joseph J. Shatzel, Cristina Puy, Joseph E. Aslan, Zachary M. Working, Martin A. Schreiber, Michael P. Hutchens, John H. Griffin, Owen J. T. McCarty.

This work is accepted by Journal of Trauma and Acute Care Surgery. January 2026

Permission is not required by the publisher for this type of use.

5.1 Abstract

Background: The procoagulant phenotype of skeletal muscle myosin (SkM) includes the promotion of thrombin generation to form fibrin, and subsequent increased resistance of fibrin clots to fibrinolysis. The release of SkM into circulation following localized tissue injury is hypothesized to promote systemic hypercoagulation. Yet, in trauma patients and in animal models of tissue injury, an unexplained decrease in SkM levels has been observed.

Methods: Plasma samples were collected from orthopedic trauma patients at admission and 6-weeks later and from pigs subjected to experimentally extensive muscle injury. Plasma SkM and myoglobin levels were measured. Binding of SkM to fibrin was quantified *in vitro* using fluorescence imaging assays. Fibrinolysis was measured using turbidimetric assays and thromboelastography.

Results: SkM plasma levels in trauma patients were lower at admission compared to 6-weeks later, while plasma myoglobin levels were higher at admission than at 6 weeks. In the pig injury model, plasma SkM levels at 24 hours after injury were decreased while myoglobin levels were increased. *In vitro*, SkM bound to fibrin, but not fibrinogen, with apparent K_d of 0.18 μM and was associated with a

decrease in the level of SkM in solution. Fluorescence imaging of the fibrin clots confirmed the presence of SkM within fibrin clots, which increased the resistance of the fibrin clot to fibrinolysis.

Conclusions: Direct binding of SkM to fibrin may explain the reduced circulating SkM levels observed after trauma and may help identify potential roles for SkM in trauma-associated coagulopathy.

5.2 Introduction

While physiological fluids such as amniotic fluid illustrate how coagulation operates under homeostatic conditions, pathological states can significantly reshape the coagulation phenotype. Trauma represents a striking example in which tissue injury, cellular disruption, and release of intracellular components rapidly alter the balance between hemostasis and thrombosis. Trauma is a leading cause of mortality in individuals under 50, causing 4.4 million deaths globally each year.[10] Trauma-induced coagulopathy (TIC) contributes to preventable mortality following trauma, through bleeding, thrombotic, and mixed phenotypes.[230-232] TIC is a dynamic condition, with early TIC (within the first 6 hours) marked by hypocoagulability and impaired hemostasis, leading to uncontrolled bleeding and shock. In contrast, late TIC (after 24 hours) reflects a transition to hypercoagulability, predisposing patients to thromboembolic complications. The mechanism of TIC remains unclear, but it involves both hemorrhagic shock and tissue injury. Shock is associated with a hypocoagulable phenotype, whereas tissue injury promotes a hypercoagulable state with suppressed fibrinolysis.[233] Hypoperfusion and tissue hypoxia during shock lead to metabolic acidosis that impairs clot formation and promotes hyperfibrinolysis. In parallel, tissue injury triggers the release of tissue factor, histones, and damage associated molecular patterns, promoting coagulation.[234] Shock and tissue injury frequently coexist, creating a complex hemostatic environment.

Myosins are motor proteins that hydrolyze ATP, bind actin, and generate force. They include skeletal, cardiac, and smooth muscle isoforms, each adapted to its tissue. Skeletal muscle myosin (SkM), the principal contractile component of sarcomeres in skeletal muscle, appears throughout the body and in plasma.[235,236] The procoagulant role of SkM was first suggested by a genetic variant in the MYH gene cluster at chr17p13.1 (clustered SkM heavy chain genes[237]), which was linked to unprovoked venous thromboembolism.[238,239] Subsequent studies demonstrated that SkM promotes thrombin generation through interaction with coagulation factors Xa, Va, and XI.[226,240,241] Cardiac muscle myosin is similarly procoagulant and exacerbates myocardial damage caused by ischemia/reperfusion in mice.[242] These findings raise the possibility that SkM released from damaged muscle during trauma contribute to TIC. A recent study observed an association between SkM deficiency and coagulopathy in trauma patient.[243] To investigate this link, we assessed SkM release after trauma in patients and animals. We found that while plasma myoglobin levels increased after injury, plasma SkM levels decreased. Given the strong binding affinity of SkM for fibrin,[244] we hypothesized that SkM may be incorporated into fibrin clots following injury, explaining the observed decrease in plasma SkM.

5.3 Materials and methods

5.3.1 *Patient with orthopedic trauma*

Ten patient serum samples were collected in an ongoing double blinded randomized controlled trial at a level one academic trauma center (Institutional Review Board approval number #00022441). This single center, pilot, double blind randomized controlled trial was designed to evaluate the feasibility of intravenous iron therapy following orthopedic trauma.[245] Patients aged 18-89 who sustained a lower extremity or pelvis fracture and demonstrated hemoglobin between 7-11 g/dL during their inpatient stay were included. Exclusion criteria included active haemorrhage requiring ongoing blood product resuscitation in excess of two units of packed red cells, multiple planned procedures, pre-existing haematologic disorders or chronic inflammatory states, and vulnerable populations. We used

biobanked samples from this on[10]going study for analysis of SkM levels. Demographic and injury characteristics including age, sex, body mass index (BMI), and Injury Severity Score (ISS) were recorded.

5.3.2 *Pig model of extensive muscle injury*

The ARRIVE guideline was used to ensure proper reporting of methods, results, and discussion of animal studies. Twelve female Yorkshire-Landrace crossbred pigs weighing between 40-50 kg were fasted for 18 hours prior to surgery. Water was available ad libitum. On the day of the experiment, animals were sedated, intubated, and mechanically ventilated with maintenance isoflurane at 1-3% throughout surgery. Surgery involved placing arterial and venous catheters and a small midline laparotomy to place a catheter in the bladder for urine sampling. Following the placement of the catheters, baseline arterial blood samples were collected. Animals received ketamine via continuous infusion for sedation at a minimum dose of 5 mg/kg/hr. A captive bolt gun (Schermer Stunner Model MKL, Paderborn, Germany) was used to administer a traumatic crush injury via a 21-gauge charge. The bolt gun was placed on the rear hindquarters of the animal targeting the muscle mass midline to the femur. Two blasts were applied to each hindquarter. Swine received maintenance IV fluid with 5% dextrose-lactated Ringer's solution at a rate of 10 mL/kg/hour for the first 3 hours after intervention, 5 mL/kg/hour for the following 3 hours, and 2.5 mL/kg/hour for the remainder of the experiment. Blood was collected again 24 hours after the injury.

5.3.3 *Coagulation profiles*

Human and pig plasma were prepared via centrifugation of citrated blood (in 0.32%w/v sodium citrate; BD, Franklin Lakes, NJ) at 2000×g for 10-min twice. To measure prothrombin time (PT), 50 µL plasma was incubated with 100 µL Innovin (Thermo Fisher, Waltham, MA) and the time to clot formation was determined using a KC4 Coagulation Analyzer (Trinity Biotech, Ireland). For activated

partial thromboplastin time (aPTT), 50 µL plasma was incubated with 50 µL aPTT reagent (Thermo Fisher, Waltham, MA) for 3 min. Clotting was initiated with $CaCl_2$ (50 µL, 8.3 mM final) and the time to clot formation was measured. For recalcified clotting time, 50 µL plasma was incubated with 50 µL of HBS buffer (25mM HEPES, 150 mM NaCl, pH 7.4). Clot formation was initiated with $CaCl_2$ (50 µL, 8.3 mM final) and the time to clot formation was recorded.

5.3.4 *Myoglobin and SkM measurement*

Human and pig plasma myoglobin levels were measured using Human Myoglobin ELISA kits (Abcam, Waltham, MA) and Pig Myoglobin MYO-9 ELISA kits (Life Diagnostics, West Chester, PA) per the manufacturer's instructions. For SkM, Immunoblotting was performed to evaluate SkM levels. Plasma samples were size fractioned by sodium dodecyl sulfate polyacrylamide gel electrophoresis (SDS-PAGE) under reducing conditions. Proteins were then transferred to polyvinylidene fluoride (PVDF) membranes, and the blots were probed with either anti-MYH antibody (for human plasma; #sc-53095, Santa Cruz Biotechnology, Dallas, TX) or an in-house anti-SkM chain antibody (for pig plasma; clone 22D4) followed by an HRP-conjugated secondary antibody. Blots were imaged on a ProteinSimple FluorChem and Jess Imaging system. The SkM band at 250 kDa corresponds to intact SkM heavy chain, while the 160 kDa band represents the heavy meromyosin fragment of SkM heavy chain. SkM band intensities were quantified using ImageJ and reported as fold change, with a value of 1 defined at admission (for human plasma) or pre-trauma (for pig plasma).

5.3.5 *SkM preparation*

SkM from rabbit muscle (Sigma-Aldrich, St. Louis, MO) was dialyzed against a buffer containing 600 mM NaCl and 50 mM Tris (pH 7.4), followed by centrifugation at 21,000×g for 1 min.

5.3.6 *Coomassie blue staining and western blot*

An aliquot containing 6 μM fibrinogen and 100 nM SkM was incubated for 10 min prior to the addition of 10 U/mL thrombin (Sigma-Aldrich, St. Louis, MO) and 6 mM $CaCl_2$. After a 30-min incubation to allow fibrin clot formation, the fibrin clot was removed, and the remaining supernatant was collected. Samples were either separated by SDS-PAGE under reducing conditions and stained with Coomassie blue or transferred to PVDF membrane for immunoblotting with an anti-MYH antibody (#sc-376157, Santa Cruz, Dallas, TX) followed by an HRP-conjugated secondary antibody. In parallel, 100 nM human serum albumin (Thermo Fisher, Waltham, MA)) was used as a control. For plasma-based experiments, citrated pooled normal plasma was incubated with 100 nM SkM, and coagulation was initiated either by 10 U/mL thrombin or tissue factor (1 nM Innovin) in the presence of 6mM $CaCl_2$. After a 30-min incubation, the fibrin clot was removed, and the supernatant was collected for immunoblotting analysis

5.3.7 *Characterization of fibrin and fibrinogen binding to SkM*

SkM was prepared at 10 μg/mL by diluting concentrated SkM stock (4.4 mg/mL) into 0.1 M Na_2CO_3 buffer (pH 9.6). For plate coating, 50 μL of this SkM solution was mixed with 50 μL of 0.1 M Na_2CO_3 buffer (pH 9.6) and added to each well of a 96-well microtiter plate, resulting in a final concentration of 5 μg/mL SkM per well. Plates were incubated overnight at 4°C, then blocked with 1% bovine serum albumin (BSA) for 1 hour at 37°C, washed three times with buffer, and incubated with increasing concentrations of either fibrin-FITC (0-1 μM; Innovative Research, Novi, MI) or fibrinogen-FITC (0-10 μM; Innovative Research, Novi, MI). Incubations were performed in HEPES-$NaHCO_3$ buffer (150 mM NaCl, 10 mM $NaHCO_3$, 10 mM HEPES, 5.5 mM dextrose, 0.1% BSA, pH 7.1) supplemented with 2 mM $CaCl_2$ for 1 hour at 37°C. Following three washes with HEPES buffer, bound fluorescence was measured at 485 nm excitation (bandwidth 9 nm) and 520 nm emission (bandwidth 20 nm). Apparent dissociation constants (Kdapp) were determined by fitting specific binding data to a one-site

binding isotherm. All fluorescence signals were corrected for nonspecific binding by subtracting the signal from BSA-coated control wells. The specific bound fluorescence, B, was then modeled as a function of total ligand concentration, C, using the following nonlinear least-squares regression model:

$$B(C) = \frac{B_{max} \cdot C}{K_d^{app} + C}$$

This analysis assumes that the total ligand concentration approximates the free ligand concentration. The reported Kdapp values represent the best-fit parameter, expressed with a ± 95% confidence interval. For experiments where saturation was not observed within the tested concentration range, an apparent Kdapp could not be determined; in these cases, the affinity was reported as >Cmax, where Cmax is the highest ligand concentration tested.

5.3.8 *Fluorescence imaging for fibrin clot*

SkM was fluorescently labeled using an Atto 647N Protein labeling Kit (Sigma-Aldrich, St. Louis, MO). Fibrinogen (6 μM), containing 1% of FITC-labeled fibrinogen (Invitrogen, Waltham, MA), was incubated with varying concentrations of Atto 647-labeled SkM for 10 min. Coagulation was then initiated by the addition 10 U/mL thrombin and 6 mM $CaCl_2$ for 30 min. The fibrin clot was then collected and imaged using a BZ-X810 fluorescence microscope (Keyence, Itasca, IL) at 4× magnification.

5.3.9 *Fibrin generation and fibrinolysis assay*

For fibrin generation assay, citrated pooled normal plasma (50 μL) was incubated with varying concentrations of SkM followed by incubation with 50 μL of HBS for 3 min. $CaCl_2$ (50μL, 8.3 mM final) was added to each plasma mixture. Fibrin formation was monitored by measuring turbidity at an absorbance of 405 nm for 30 min using an Infinite M200 spectrophotometer (Tecan, CH). The lag time required to initiate fibrin formation and time to reach half maximum turbidity (T1/2 max) were

obtained. For fibrinolysis assay, In the purified system, fibrin clot was generated in a 96-well plate using a 100 μL reaction mixture containing 3 μM fibrinogen, 0.25 U/mL thrombin, varying concentrations of SkM, with the addition of 11 nM plasmin. Turbidity was monitored overtime at 340 nm to assess clot formation and subsequent fibrinolysis. For plasma, clot lysis was assessed in which tissue plasminogen activator (tPA)-mediated fibrinolysis of a thrombin-induced clot through turbidity change, as described.[242] Briefly, 100 μL of a reaction mixture containing thrombin (0.5 U/mL final), $CaCl_2$ (2.3 mM final), and tPA (100 ng/mL final) in HBS buffer was added to 100 μL of citrated pooled normal plasma pretreated with varying concentrations of SkM. Following mixing, 100 μL of the mixture was transferred to a 96-well plate, and turbidity was measured over time at 405 nm. Complete clot lysis time (T fibrinolysis) was defined as the interval from maximum turbidity to complete clot dissolution, and half clot lysis time ($T_{1/2}$ fibrinolysis) was defined as the time from the maximum turbidity to the midpoint of the decrease in turbidity.

5.3.10 *Thromboelastrography*

Viscoelastic properties of fibrin clot were evaluated using citrated whole blood obtained from healthy volunteers. Blood samples were treated with tPA 150 ng/mL in the presence or absence of SkM (100 nM) and analyzed using a TEG® 5000 hemostasis analyzer system (Haemonetics, Boston, MA). The initiation phase of clot formation was measured as R time, defined as the time from test until clot formation begins. The degree of fibrinolysis was quantified as LY30 (%), defined as the percentage reduction in clot amplitude 30 min after reaching maximum clot strength.

5.3.11 *Data analysis*

Statistical analyses were performed using GraphPad Prism 10.0 (GraphPad Software Inc., La Jolla, CA). Data are presented as mean ± SD. Comparisons between two different time points within the same individuals were performed using the Wilcoxon signed-rank test. Comparisons between two

groups were conducted using Mann-Whitney U test as appropriate. For comparisons involving three or more groups, one-way ANOVA was applied. A p-value < 0.05 was considered statistically significant. Based on the observed data in plasma SkM levels, post hoc power calculations indicated that detecting the observed differences with 90% power at α of 0.05 would require approximately 29 patients per group and 7 animals per group.

5.4 Results

5.4.1 *Reduced plasma SkM levels are observed following injuries compared to recovery in orthopedic trauma patients*

Serum from ten patients who sustained a lower extremity or pelvis fracture was analyzed to evaluate coagulation profiles and muscle injury markers after tissue trauma. The cohort had a mean age of 61±14.4 years, was 30% male, with a mean BMI of 29.9±6.9, and an ISS 10.9±5.4 (Table 5.1). Blood samples were collected during the primary inpatient admission and again at the 6-week follow-up. Coagulation parameters including PT, aPTT, and recalcified clotting time did not differ significantly between admission and 6-week follow-up (Figure 5.1A). Plasma myoglobin levels were significantly elevated at admission compared to the 6-week follow-up (18.3±14.3 ng/mL vs 5.5±5.1 ng/mL), reflecting muscle injury associated with musculoskeletal trauma (Figure 5.1B). In contrast, plasma SkM levels were lower at admission than at the 6-week follow-up (Figure 5.1C). We detected a 2.2-fold increase in the 250 kDa and 160 kDa SkM bands between admission and follow-up.

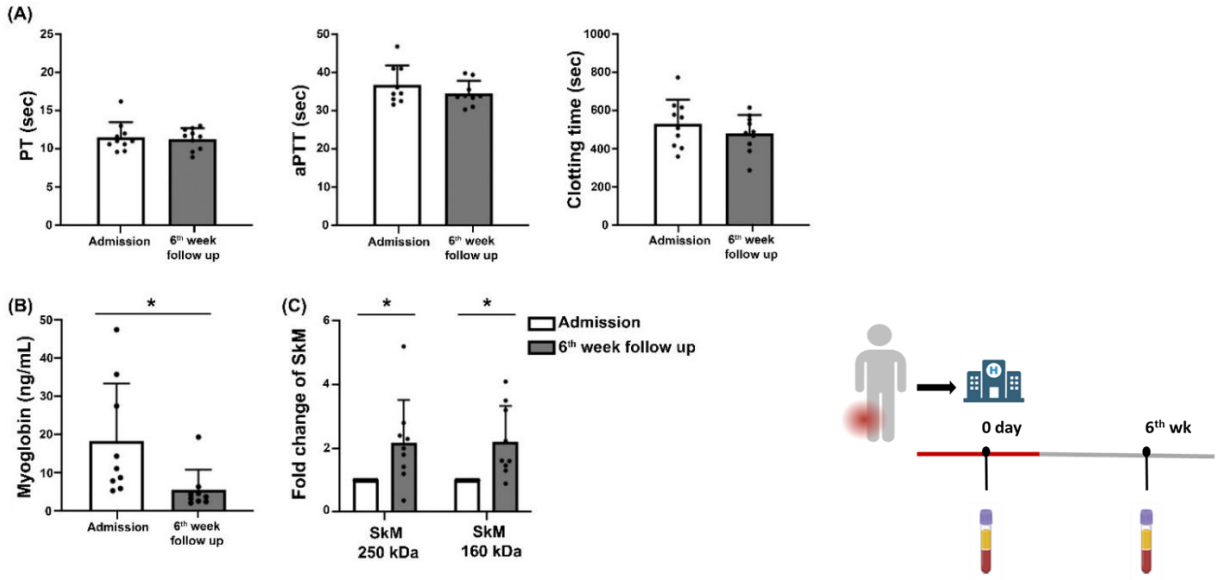

Figure 5.1. Reduced SkM levels following injuries compared to recovery in orthopedic trauma patients.
Coagulation profiles of orthopedic trauma patients at admission and at 6-week follow-up, including (A) prothrombin time (PT), activated partial thromboplastin time (aPTT), and recalcified clotting time. (B,C) Plasma markers of muscle injury, myoglobin and skeletal muscle myosin (SkM), at admission and 6-week follow-up. Data are mean ± standard deviation (n=10). Wilcoxon signed-rank test was used for statistical comparisons. Schematic illustration created with Biorender.com.

Table 5.1. Demographics of enrolled patients.

No.	Age	Sex	BMI	ISS
1	45	F	40.9	4
2	39	M	30	17
3	70	F	37.5	22
4	44	F	22.5	4
5	81	F	24.1	9
6	64	F	21.2	9
7	82	F	29.8	10
8	64	M	33.6	16
9	53	M	21.9	9
10	68	F	37.7	9

5.4.2 *Reduced SkM levels after extensive muscle trauma compared to baseline in a swine model*

Based on our observations in patients with bone fractures, we next used a pig model of extensive muscle injury to investigate changes in coagulation phenotype and muscle markers during muscle injury. Twelve pigs were anesthetized and subjected to bilateral hindlimb muscle contusion using a bolt gun. Blood samples were collected at baseline and 24 hours post-injury. The aPTT and recalcified clotting time did not differ at 24 hours compared with baseline, but the PT was significantly prolonged (14.4±0.6 sec vs 17.5±0.6 sec), indicating coagulopathy after extensive muscle injury (Figure 5.2A).

Plasma myoglobin levels were elevated at 24 hours compared with baseline (0.09±0.04 µg/mL vs. 3.8±4.2 µg/mL, Figure 5.2B). In line with a previous study,[233] plasma SkM levels were lower 24 hours post-trauma compared with baseline (Figure 5.2C). We detected a over an 80% reduction in the 250 kDa and 160 kDa SkM bands, respectively, prior to and following injury.

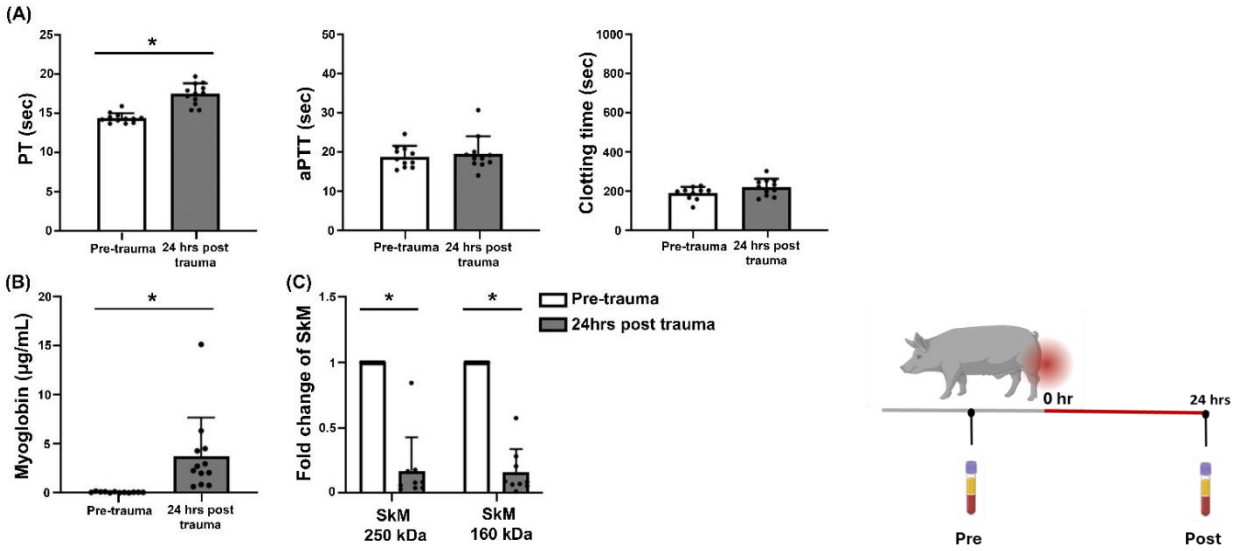

Figure 5.2. Reduced SkM levels after extensive muscle trauma compared to baseline in a swine model.
Coagulation profiles of pigs before and 24 hours after muscle injury including (A) prothrombin time (PT), activated partial thromboplastin time (aPTT), and recalcified clotting time. (B,C) Plasma levels of myoglobin and skeletal muscle myosin (SkM) were obtained before and 24 hours after muscle injury. Data are mean ± standard deviation (n=12). Wilcoxon signed-rank test was used for statistical comparisons. Schematic illustration created with Biorender.com.

5.4.3 *Consumption of SkM during fibrin clot formation*

We next examined the dynamics of SkM levels during fibrin formation *in vitro*. We hypothesized that SkM binding to fibrin depletes circulating SkM levels. In a purified system, SkM was incubated with excess molar fibrinogen, with both proteins being detectable by Coomassie blue staining or Western blotting with an anti-SkM antibody following electrophoresis. Thrombin and $CaCl_2$ were added to initiate coagulation and convert soluble fibrinogen into an insoluble fibrin clot. We first confirmed that the generation of an insoluble fibrin clot resulted in the clearance of soluble fibrinogen. Under these conditions, SkM was also cleared from the solution, as observed by Coomassie blue staining or by Western blotting using an anti-SkM antibody (Figure 5.3A &B). The addition of hirudin to prevent

fibrin generation preserved fibrinogen and SkM levels. We confirmed that SkM levels were unaffected by the enzymatic activity of thrombin alone (Figure 5.3A-B). In contrast, the concentration of albumin remained constant over time (Figure 5.3C), excluding nonspecific binding or physical entrapment of proteins during fibrin formation as a mechanism of non-specific clearance. Finally, we translated our studies from a purified system to a plasma-based system. In plasma, the concentration of SkM significantly decreased following fibrin formation induced by either thrombin or tissue factor (Figure 5.3D). The loss of SkM was reversed by the addition of the thrombin-specific inhibitor, hirudin.

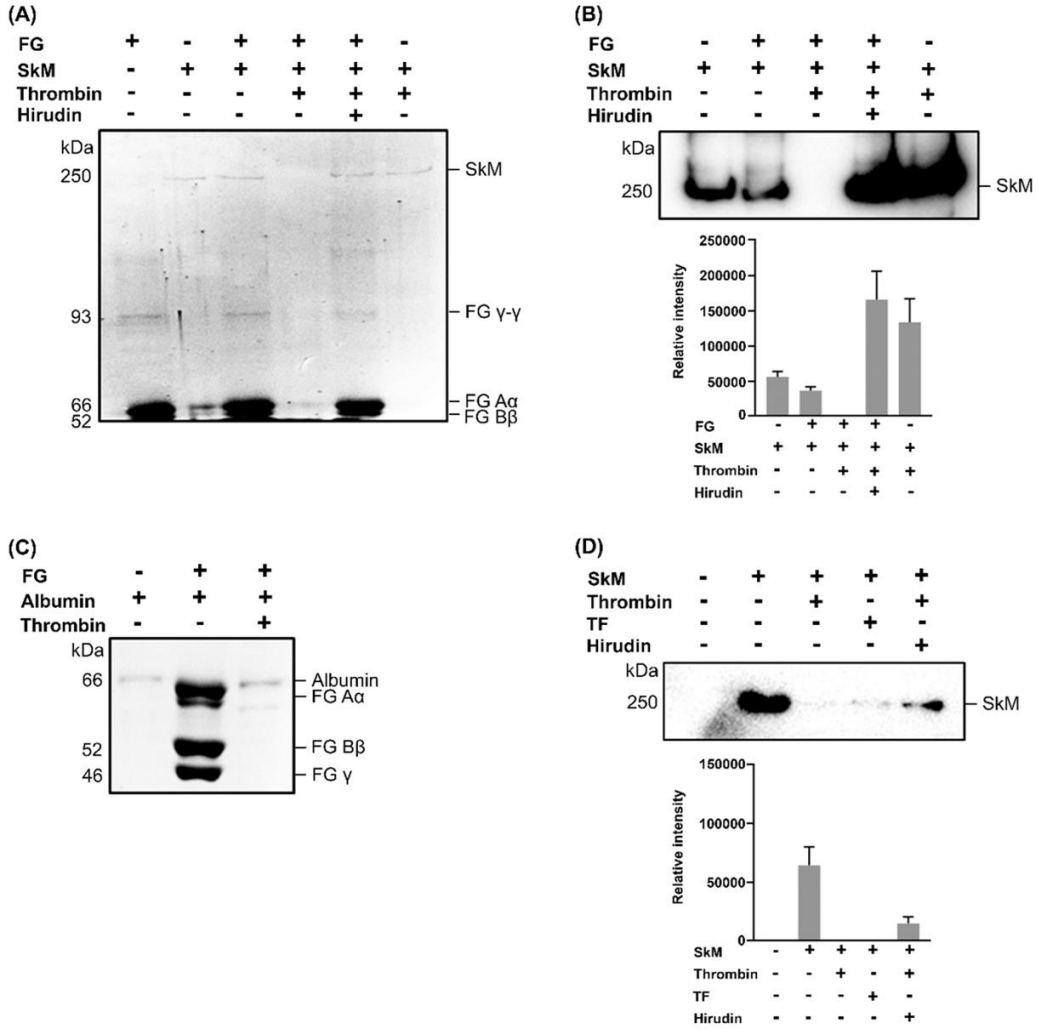

Figure 5.3 Consumption of SkM during fibrin clot formation.
Skeletal muscle myosin (SkM) was incubated with fibrinogen, and coagulation was initiated by adding thrombin and $CaCl_2$. After 30 min, the fibrin clot was removed, and the supernatant was analyzed by (A) Coomassie blue staining and (B) Western blotting using anti-SkM antibodies. (C) Human albumin was used in parallel as a control and analyzed by Coomassie blue staining. (D) Plasma was incubated with SkM, and coagulation was initiated with either thrombin or tissue factor. In select studies, the thrombin-specific inhibitor hirudin was added. Following clot formation and removal, the supernatant was blotted with anti-SkM antibodies. FG, fibrinogen; TF, tissue factor.

5.4.4 *Binding of fibrin to SkM*

Saturation binding assays were performed to quantify the affinity of SkM for fibrin(ogen). SkM was placed on 96-well plates, and the binding of fibrin-FITC or fibrinogen-FITC was evaluated. Total fluorescence increased in a concentration-dependent manner for both ligands (Figure 5.4). Fibrin-FITC displayed a rapid increase in fluorescence at sub-micromolar concentrations, reaching a plateau at approximately 1 μM (Figure 5.4A). Nonlinear regression analysis of the specific binding component indicated a Kdapp of 0.18 μM and a maximal binding (Bmax) of 20.8 RFU (n=3), reflective of a strong interaction between fibrin and SkM. In contrast, fibrinogen-FITC exhibited a nearly linear increase in fluorescence up to 10 μM without reaching saturation, indicating substantially weaker binding (Figure 5.4B). Because no plateau was observed, a reliable Kdapp could not be determined. As a negative control, BSA immobilized on the plates showed only weak interactions with both fibrin-FITC and fibrinogen-FITC, confirming the specificity of the observed binding.

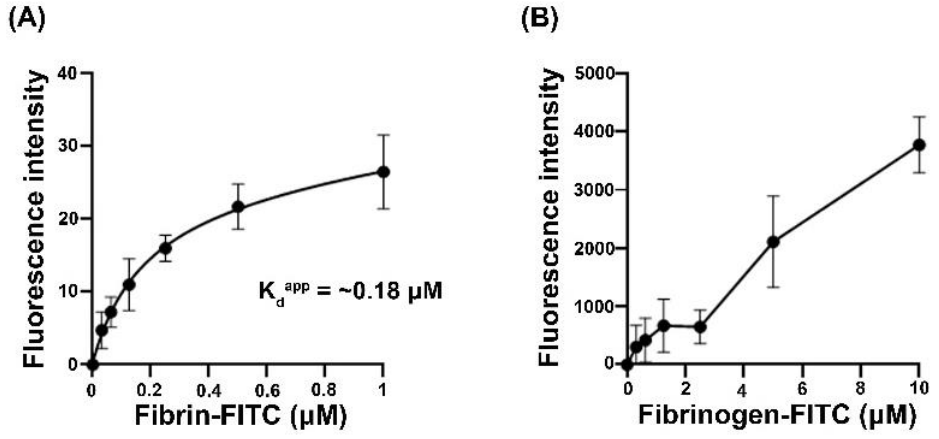

Figure 5.1 Binding of SkM to fibrin and fibrinogen.
Specific binding of (A) fibrin-FITC and (B) fibrinogen-FITC to skeletal muscle myosin (SkM) immobilized on 96-well plates is shown. Plates were incubated for 1 hour at 37°C in 20 mM HEPES–$NaHCO_3$ buffer, pH 7.1, with 2 mM $CaCl_2$; 1% bovine serum albumin was used as a control for nonspecific binding. (A) Fibrin-FITC binding reached saturation at sub-micromolar concentrations. The curve represents nonlinear least-squares regression to a one-site binding isotherm. The apparent dissociation constant (Kd^{app}) was 0.18 μM, and maximal binding (B_{max}) was 20.8 RFU. (B) Fibrinogen-FITC binding increased nearly linearly over the tested concentration range (0–10 μM) without reaching saturation, indicating substantially weaker interaction with SkM. Because no plateau was observed, an accurate Kd^{app} could not be determined. Error bars represent the standard deviation from 3 independent replicates.

5.4.5 *Incorporation of SkM into fibrin clot*

We investigated whether SkM was incorporated into fibrin clots. Clots were formed by adding thrombin and $CaCl_2$ to a fibrinogen solution or plasma containing 1% of FITC-labeled fibrinogen and SkM labeled with Atto 647N. In both systems, we observed colocalization of fluorescently-labeled SkM with fibrin within the fibrin network (Figure 5.5A-B).

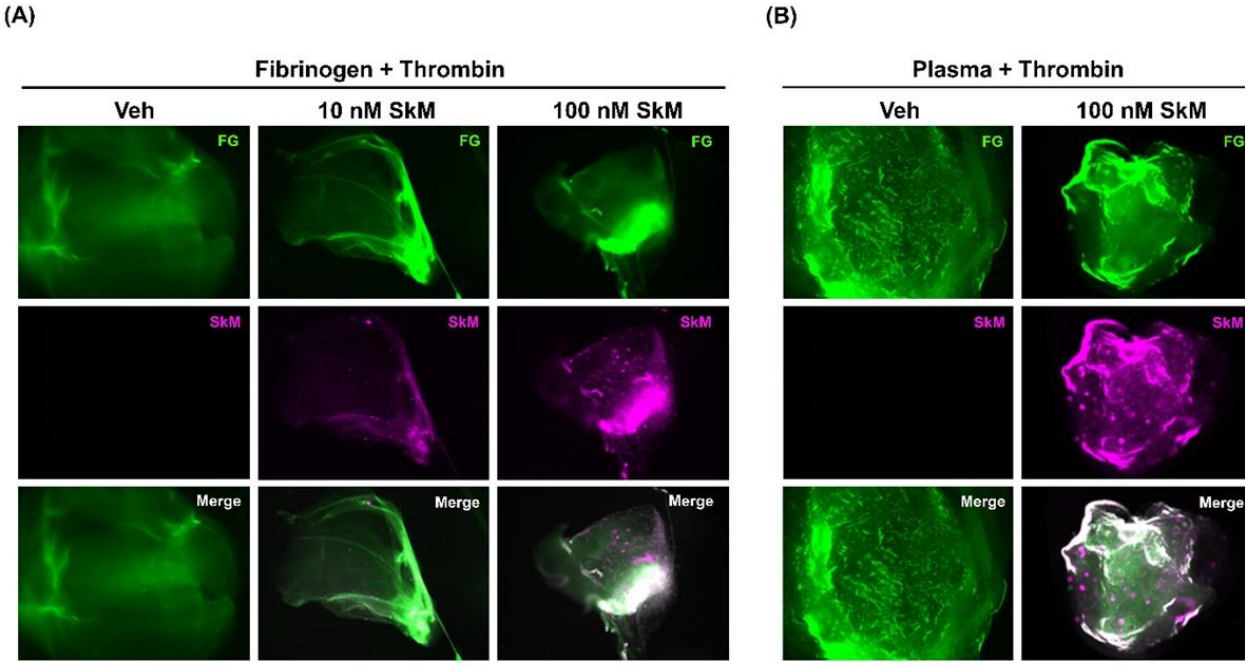

Figure 5.5 SkM is incorporated into fibrin clot.

(A) Fibrinogen containing 1% of FITC-labeled fibrinogen was incubated with varying concentrations of Atto 647-labeled skeletal muscle myosin (SkM) for 10 min. Coagulation was then initiated by adding thrombin and $CaCl_2$ for 30 min before the fibrin clot was imaged. (B) Plasma containing 1% of FITC-labeled fibrinogen was incubated with 100 nM Atto 647-labeled SkM for 10 min and coagulation was initiated with thrombin and $CaCl_2$, and the fibrin. clot was imaged after 30 min. FG, fibrinogen; Veh, vehicle.

5.4.6 *Incorporation of SkM enhances clot resistance to fibrinolysis*

We next examined whether SkM affected clot formation and stability. Consistent with previous reports,[240] SkM exhibited procoagulant activity in a fibrin generation assay, as evidenced by the shortened lag time (6.0±0.7 min in control vs. 4.3±0.2 min and 4.1±0.5 min with 30 nM and 100 nM SkM) and reduced $T_{1/2}$ max (15.7±0.8 min vs. 9.2±0.2 min and 8.0±0.4 min; Figure 5.6A) in the presence of SkM. Turbidity assays were used to study the effect of SkM on fibrinolysis. While SkM did not significantly alter the complete lysis time or $T_{1/2}$ fibrinolysis in the purified system (Figure

5.6B), it markedly prolonged both parameters in plasma. The complete lysis time increased from 83.3±5.0 min to 119.7±10.9 min and 119.2±5.4 min, while the $T_{1/2}$ fibrinolysis increased from 36.4±1.8 min to 58.5±14.4 min and 65.5±6.4 min in the presence of 30 nM and 100 nM SkM, respectively (Figure 5.6C). In whole blood, SkM shortened the R-time as measured by thromboelastography in the presence of tPA (Figure 5.6D)[246]. However, SkM did not affect LY30 (51.5% vs. 47.0%, p=0.7; Figure 5.6D), the angle, or the maximal amplitude for lysis.

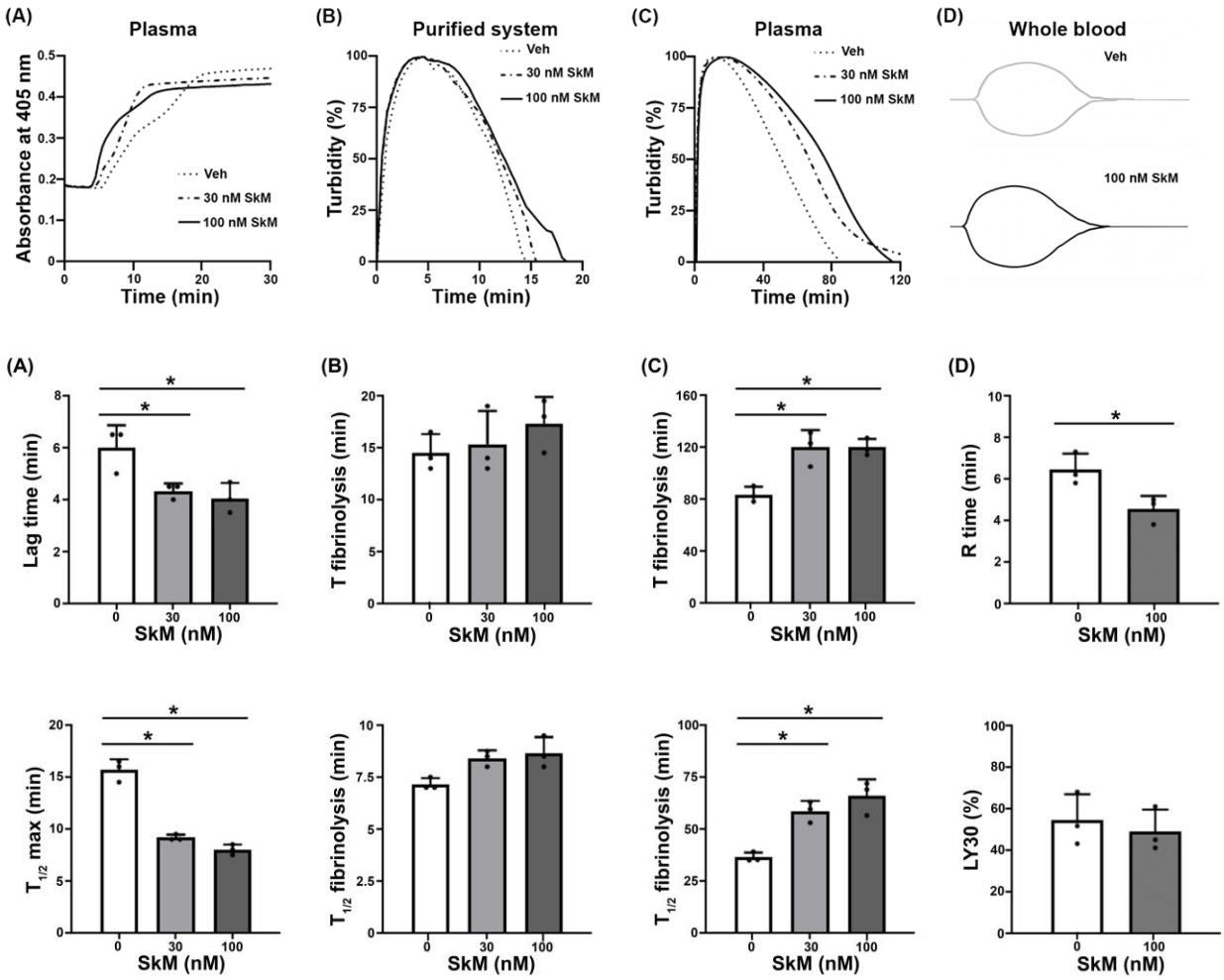

Figure 5.6 Effect of SkM on fibrin generation and fibrinolysis.

(A) Fibrin generation assay in recalcified plasma pretreated with varying concentrations of skeletal muscle myosin (SkM) for 10 min and coagulation was initiated by adding 25 mM $CaCl_2$. Lag time and time to reach half-maximum ($T_{1/2\ max}$) were quantified. (B) Fibrinolysis assay using a 100-µL aliquot containing fibrinogen, thrombin, $CaCl_2$, plasmin, and different concentrations of SkM. Turbidity at 340 nm was monitored at 37°C for 20 min during which a clot was rapidly formed (turbidity increase) and subsequently resolved (turbidity decrease). Complete and half clot lysis time were measured. (C) Fibrinolysis assay using a 100-µL aliquot containing plasma, thrombin, $CaCl_2$, tissue plasminogen activator (tPA), and different concentrations of SkM, Turbidity at 405 nm was monitored at 37°C for 120 min. Complete and half clot lysis time were measured. (D) Thromboelastography in the presence of tPA with or without SkM. The initiation phase of clot formation was assessed by measuring R time, fibrinolysis by measuring LY30 (%). Data are mean ± standard deviation (n=3). One-way ANOVA and Mann-Whitney U test were used for statistical comparisons.

5.5 Discussion

Elucidating the mechanistic pathways underlying TIC could inform treatment for patients at risk of hematologic complications. We report decreased plasma SkM after muscle injury and propose that incorporation of SkM into fibrin clots may explain this phenomenon. Orthopedic trauma patients and experimentally injured pigs exhibited increased plasma myoglobin levels after trauma compared to

recovery or baseline. Conversely, plasma SkM levels decreased after injury. SkM was previously shown to promote thrombin activation,[238] while diminished plasma SkM levels are associated with coagulopathy in trauma patients.[243] We hypothesized that SkM binds fibrinogen and is incorporated into fibrin clots after injury, explaining the decrease in plasma SkM. Our *in vitro* results showed that, during clot formation, SkM disappeared from the supernatant and colocalized with the fibrin network.

Our fluorescence binding assays demonstrated distinct interaction profiles for fibrin-FITC and fibrinogen-FITC with SkM. Fibrin-FITC exhibited a strong and saturable interaction with SkM, with an apparent dissociation constant Kdapp of 0.18 μM, consistent with previous surface plasmon resonance measurements reporting a Kd of 0.9 μM.[244] Despite these methodological differences, both approaches indicate sub-micromolar affinity, confirming a robust interaction between fibrin and SkM. In contrast, fibrinogen-FITC displayed a nearly linear increase in fluorescence over the concentrations tested, without reaching a clear saturation, indicating weaker binding to SkM. Although fibrinogen produced higher absolute fluorescence signals, this does not necessarily reflect a greater number of binding sites, but may be due to differences in fluorophore properties, extent of labeling fibrinogen versus fibrin, or ligand behavior.[247-249] The lack of a plateau suggests a higher Kd for fibrinogen relative to fibrin-FITC and a less specific interaction with SkM. These findings emphasize that fibrin and fibrinogen engage SkM through distinct binding behaviors. The potential mechanisms for binding of SkM to fibrin remain under debate. While one study suggested noncovalent binding,[244] others proposed non-disulfide covalent cross-linking regulated by transglutaminase activity.[250] In the present study, experiments in a purified system demonstrated that SkM can interact with fibrin independently of transglutaminase activity.(Table 5.2)

Possible binding sites between myosin and fibrin identified by HPLC-MS/MS.

Peptide (complex)	Peptide (myosin)	Position within myosin	Protein(myosin) ID	Peptide (fibrinogen)	Position within fibrinogen	Protein(fibrinogen) ID
EFVEGTFTFHADLCTLPEDEKQIK	LAHDSIMDLENDKQQLDEK	K1085	Myosin, heavy chain 1G (NP_001382912.1)	QIKEIE	Q195	Fibrinogen C-terminal domain-containing protein (A0A4X1T6V5)
LATALQKLEEAEKAADESER	KLEGDLK	K1060	Myosin, heavy chain 1G (NP_001382912.1)	ALQTH	Q695	Fibrinogen α-chain (F1RX36)
	KLEDECSELKK	K948				
	KLESDISQIQSEMEDTIQEAR	K1733	Myosin, heavy chain (BAA89233.1)			
MTLKQLK	NAYEESLDHLETLK	K1505	Myosin, heavy chain 1G (NP_001382912.1)	QLQD	Q115	Fibrinogen β-chain (F1RX37)
				QLYID	Q184	
				QLTRM	Q335	
				QLVGE	Q393	
				QLEAK	Q157	Fibrinogen γ-chain (I3LJW2)
				QLEDW	Q276	
				QLDQV	Q204	Fibrinogen α-chain (A0A4X1SSQ4)
				QLIEM	Q163	
LKQELPELK	AITDAAMMAEELK	K1776	Myosin, heavy chain 1G (NP_001382912.1)	QELLD	Q134	Fibrinogen C-domain containing 1 (F1S0X3)
	LEGDLK	K1066				
	LEDECSELK	K957				
	LDEAEQLALK	K1812				
	TQEDLK	K1674				
	IAEKDEEIDQLK	K1593				
	QAFTQQIEELK	K1322				

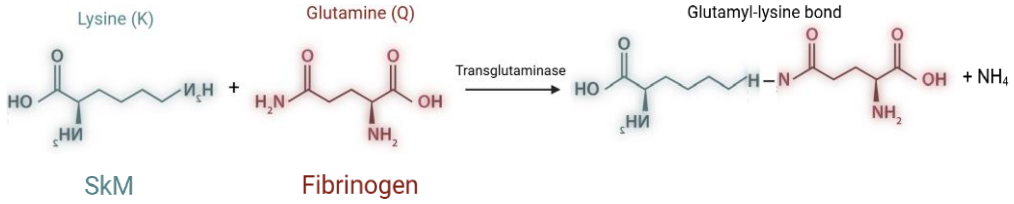

Table 5.2. Potential binding site of SkM to fibrin and fibrinogen. Adapted from Du et al, Insight into the mechanism of myosin-fibrin gelation induced by non-disulfide covalent cross-linking Food Res Int. (2022). Reprinted with permission.

Previous studies demonstrated consumption of other plasma proteins in fibrin clots. Clots in human plasma can passively trap hemoglobin, immunoglobulins, and β-lipoproteins.[251] The cytoskeletal protein actin is incorporated in a manner dependent on actin filament length, affecting the viscoelastic properties of fibrin clots and inhibiting fibrinolysis.[252] Our results showed similar inhibition of fibrinolysis by SkM, suggesting an avenue for future research characterizing the mechanical properties of SkM-fibrin clots. While our *in vitro* results demonstrated that fibrin clots can consume SkM, other pathways, such as enzymatic degradation or clearance by organs, may decrease SkM levels *in vivo*.[253] Moreover, trauma patients often receive fluids or blood transfusions, raising the possibility that a dilution effect could decrease SkM levels. However, in this case, we would expect a similar reduction in myoglobin levels. Instead, we observed an increase in myoglobin levels, suggesting that dilution is unlikely to explain the decrease in SkM.

TIC is a clinical diagnosis encompassing hemostatic disturbances ranging from hypocoagulability to hypercoagulability and is associated with uncontrolled hemorrhage and thrombotic events.[254] Historically, TIC was attributed to dilution of clotting factors by fluids administered during critical care, but it is now known to involve coagulation factor consumption, protein C activation, and tPA release.[255-258] Severe trauma often involves tissue injury and hemorrhagic shock, and both factors are thought to act synergistically in driving severe TIC. These factors contribute to TIC through distinct mechanisms: tissue injury promotes coagulation activation, whereas hemorrhagic shock impairs clot formation and stability. Tissue injury disrupts the endothelium, leading to tissue factor exposure and inflammatory responses, including release of histones and damage-associated molecular patterns. SkM released from damaged muscle may contribute to tissue injury-mediated coagulopathy. A prior study reported that cardiac muscle myosin aggravates myocardial injury in a murine ischemia/reperfusion injury model. SkM drives thrombin generation by providing a surface for the prothrombinase complex of factor Xa and factor Va and stabilizes fibrin clots against degradation by plasmin. Our results demonstrated accelerated clotting and resistance to fibrinolysis in the presence of SkM, consistent with previous findings that tissue injury promotes hypercoagulability and impairs fibrinolytic activity. Given these findings, consumption of SkM in tissue injury-induced coagulation may reflect the extent of TIC. Indeed, unlike tissue injury, rhabdomyolysis alone is rarely associated with thromboembolic complications, except in cases where disseminated intravascular coagulation develops due to dysregulated coagulation activation.[259,260] This implies that the procoagulant and antifibrinolytic effects of SkM depend on concurrent coagulation activation. By itself, SkM does not initiate coagulation; rather, it acts as a modulator that amplifies the process once it begins.

Further research is needed to connect our *in vitro* results to clinical outcomes, including blood loss, thromboembolic events, and mortality. This study was limited by small sample sizes and few time points in the clinical study and animal model. A larger study would be required to compare the range

and time-dependent variability of SkM in the plasma in a healthy patient population. Measuring SkM in an animal model immediately after tissue injury would provide insight on the initial release of SkM from damaged muscle. The patient cohort represented relatively low-severity, non-shock trauma, which may not fully capture the spectrum of TIC. Furthermore, since we did not evaluate fibrinolysis activity in plasma samples from patients and animals, we are unable to relate this activity to SkM levels in individuals. Future studies are needed to characterize the stoichiometric relationship between SkM and fibrin and to assess how varying SkM-to-fibrinogen ratios affects clot formation and stability. Research on the textural properties of meat products has explored the rheological properties of myosin-fibrin gels,[250] and similar investigations could characterize the effect of SkM on the rheological properties of human fibrin clots. In summary, our current findings document the decrease in SkM following traumatic injury and suggest an explanation for this phenomenon by demonstrating that SkM disappears from solution as it becomes incorporated in fibrin clots.

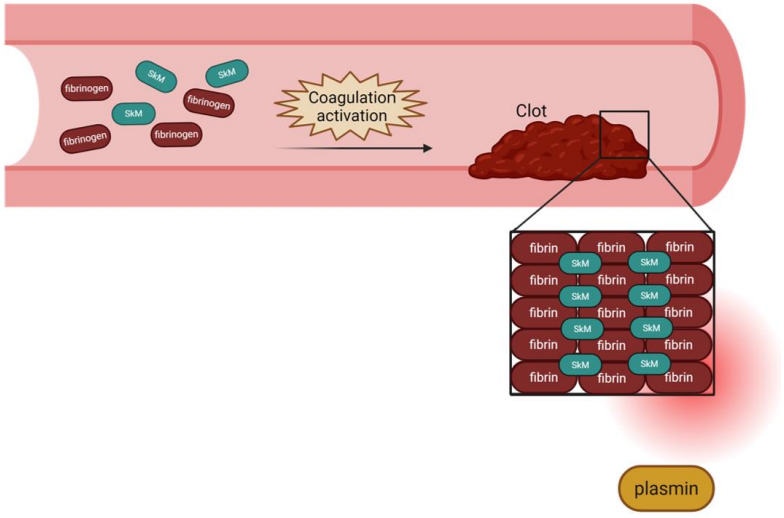

Figure 5.7 Schematic of conclusion. Created with BioRender.com.

Chapter 6. Conclusions and Future Directions

6.1 Conclusions

This dissertation investigated mechanisms regulating coagulation and thromboinflammatory responses in conditions of injury and disease. The overall goal was to identify pathways that contribute to pathological coagulation without compromising hemostasis. The studies first examined intrinsic pathway activation and its intersection with inflammation, highlighting FXI-mediated HK cleavage as a mechanistic link between coagulation and innate immune signaling. Subsequent work explored procoagulant properties of amniotic fluid and the role of skeletal muscle myosin in coagulation following tissue injury. These findings underscore that coagulation dynamics are highly context-dependent, revealing additional layers of regulation beyond the classical coagulation cascade.

Future work will build on these insights by targeting coagulation pathways in clinically relevant conditions. One direction will focus on heatstroke, aiming to define how thermal injury and systemic inflammation alter coagulation, and to evaluate whether selective signaling pathway modulation of thrombin on endothelial cells can reduce thermal injury.

6.2 Limitations

With the mechanistic insights gained from these studies, several limitations should be acknowledged, particularly the need for future work to translate these findings into more clinically relevant models. First, the investigation of FXIa-mediated HK cleavage was largely conducted in purified systems, which did not fully capture the complexity of plasma, where competing substrates, inhibitors, and cofactors can modulate FXIa activity. Moreover, we did not examine the role of another kinin, low-molecular-weight-kininogen in contact pathway coagulation. Second, while the amniotic fluid studies demonstrate significant procoagulant phenotype, variability in sample composition and clinical context may influence coagulation responses, limiting direct extrapolation across physiological or pathological

states. In addition, although these experiments establish functional coagulation potential, they do not fully resolve the relative contributions of individual factors within this complex biological fluid. Third, the incorporation of skeletal muscle myosin into fibrin clots highlights a novel mechanism linking tissue injury to altered clot structure, however, these findings are primarily derived from *vitro* and *ex vivo* models. Future studies are needed to link these *in vitro* and *ex vivo* findings to clinically meaningful trauma outcomes, including blood loss, thromboembolic events, and mortality. Larger, longitudinal studies with increased sampling frequency will be required to define the range and time-dependent variability of circulating myosin levels.

The studies presented in this dissertation highlight how dysregulated coagulation contributes to inflammatory and injury-associated disease states such as sepsis, obstetric complications, and trauma. Similar thromboinflammatory mechanisms are also central to other forms of systemic injury, including heatstroke. Heatstroke is increasingly recognized not only as a direct thermal injury, but also as a condition characterized by endothelial dysfunction, dysregulated inflammation and coagulation activation. These shared pathophysiological features suggest that pathways explored in this dissertation.

6.3 Future direction: Targeting thrombin in heatstroke

Building on the mechanistic insights from this dissertation, several future research directions emerge that extend these findings into thromboinflammatory disease contexts. In particular, understanding how coagulation signaling contributes to systemic injury responses may provide opportunities for therapeutic intervention. On the other hand, despite dysregulated coagulation is implicated in a broad range of clinical conditions, therapeutic strategies targeting the coagulation system remain suboptimal because of the inherent risk of bleeding. Decades of clinical use of direct oral anticoagulants do not fully address this limitation, underscoring a persistent unmet need for antithrombotic therapies that

effectively prevent thrombosis while preserving hemostasis. Advances in our understanding of coagulation biology and the development of more selective pharmacologic agents now provide an opportunity to overcome this long-standing clinical dilemma.

In heatstroke, systemic activation of coagulation frequently contributes to microvascular thrombosis and organ injury, and anticoagulant therapies have been explored to mitigate these complications. However, clinical application remains challenging because patients with severe heatstroke often simultaneously exhibit coagulopathy and bleeding risk, highlighting the need for targeted strategies that attenuate thrombin-driven pathology while preserving essential hemostatic function. Therefore, ongoing efforts aim to develop and apply novel anticoagulant approaches capable of mitigating thromboinflammatory responses in heatstroke without compromising physiological hemostasis.

6.3.1 *Thrombin as a central mediator in the pathophysiology of heatstroke*

Heat injury has emerged as a growing global health concern due to climate change, with approximately 500,000 heat-related deaths worldwide each year.[261] Heatstroke represents the most severe form of heat injury and is a life-threatening medical emergency characterized by failure of thermoregulation, leading to a core body temperature typically ≥104°F accompanied by central nervous system dysfunction.[262] Beyond direct thermal tissue damage, inflammation and coagulation are central drivers of organ dysfunction in heatstroke.[263,264] Thermal injury leads to the release of damage-associated molecular patterns, which stimulate macrophages to produce proinflammatory cytokines, including TNF-α, interleukin-1β, and IL-6. Concurrently, activated macrophages/monocytes upregulate tissue factor expression and release procoagulant microvesicles, thereby initiating coagulation. Inflammatory cytokines further activate neutrophils to undergo NETosis, releasing NET that injure the endothelium and trigger contact pathway activation. Together, extrinsic and intrinsic pathways converge to amplify coagulation and generate thrombin, a critical mediator that further propagates both inflammatory and procoagulant signaling, ultimately culminating in the formation of inflammatory thrombi (Figure 6.1).[264]

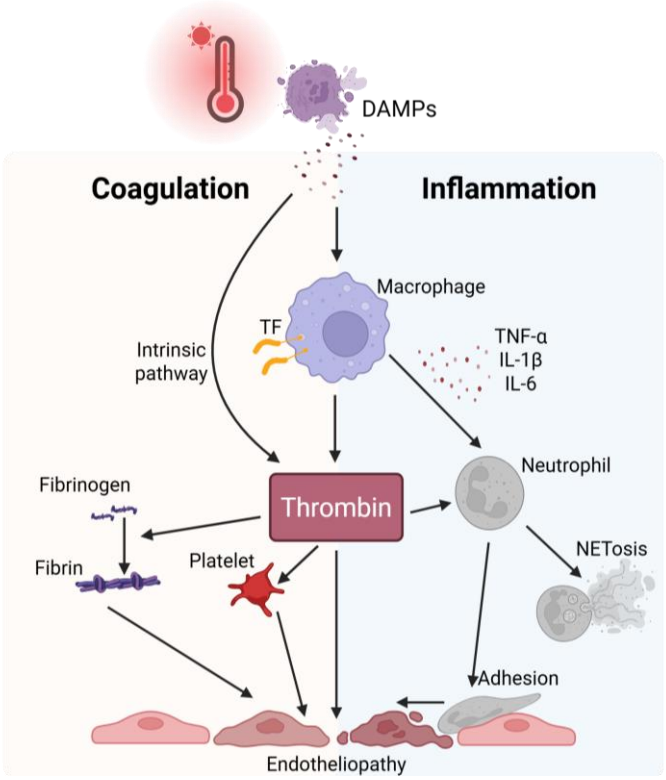

Figure 6.1 Pathophysiology of heatstroke.
Created with BioRender.com.

6.3.2 *PAR1 as a central thrombin receptor*

Protease-activated receptor 1 (PAR1) is a G protein-coupled, trans-membrane receptor identified as the first high-affinity thrombin receptor. PAR1 is broadly expressed on cells of the vascular wall,

including endothelial cells, vascular smooth muscle cells, platelets, neutrophils, and macrophages.[265] Activation of PAR1 through proteolytic cleavage of its extracellular N-terminus by thrombin initiates intracellular signaling that regulates platelet activation, cellular proliferation, vascular development, and angiogenesis.[266] In endothelial cells, thrombin-mediated PAR1 activation increases vascular permeability and promotes a shift toward proinflammatory and procoagulant phenotypes.[267] Notably, PAR1 expression is upregulated in heatstroke and studies have shown that PAR1 mediates heat stress-induced endothelial barrier disruption and apoptosis.[268]

6.3.3 *Ligand-biased signaling of PAR1*

While thrombin-PAR1 signaling predominantly elicits stress-associated and detrimental responses in endothelial cells, activated protein C (aPC), an anticoagulant protease generated downstream of thrombin, exerts fundamentally distinct effects through the same receptor.[269] The generation and signaling of aPC require thrombin binding to endothelial thrombomodulin and subsequent association of aPC with the endothelial protein C receptor (EPCR), which localizes aPC to the cell surface and facilitates PAR1 cleavage.[22,270] Unlike thrombin, which cleaves PAR1 at the canonical Arg41 site, aPC cleaves PAR1 at an alternative site, resulting in exposure of a different tethered ligand and induction of biased receptor signaling.[271] This mode of PAR1 activation preferentially engages cytoprotective signaling pathways rather than proinflammatory responses.[272] As a result, aPC-PAR1 signaling promotes endothelial barrier stabilization, suppresses inflammatory activation, and enhances cell survival (Figure 6.2).[273,274] The ligand-biased signaling of PAR1 underscores the highly fine-tuned nature of the coagulation system and the pleiotropic role of PAR1 as a context-dependent molecular switch regulating endothelial function.[271]

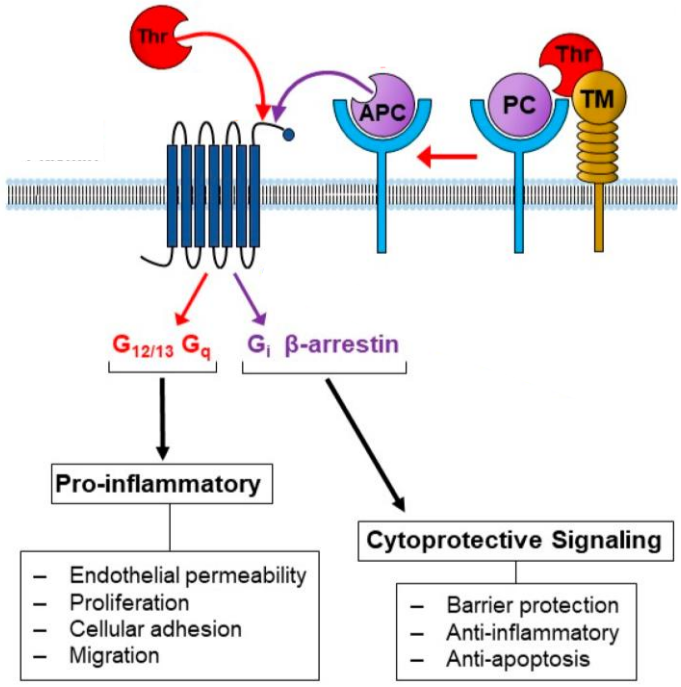

Figure 6.2 Distinct mechanisms of PAR1 activation by thrombin- and aPC/EPCR complex resulting in different biological effects. from Pontarollo et al. Comment on "Endothelial Protein C Receptor (EPCR), Protease Activated Receptor-1 (PAR1) and Their Interplay in Cancer Growth and Metastatic Dissemination**.** Cancers (2019). Reprinted with permission.

6.3.4 *Rationale for targeting PAR1 in heatstroke*

Previous studies provide strong evidence that modulating thrombin-PAR1 signaling improves outcomes in experimental heatstroke. In rodent models, administration of antithrombin III, an endogenous thrombin inhibitor, attenuated heat stress-induced systemic inflammation, improved organ injury, and significantly increased survival.[275,276] On the other hand, complementary studies targeting the protein C pathway further support this concept. Systemic delivery of aPC in a heatstroke setting markedly improved survival, reduced DIC, dampened inflammatory cytokine production, and limited multiorgan injury in rat models.[277] Similarly, treatment with recombinant soluble thrombomodulin, which promotes endogenous protein C activation, suppressed inflammatory mediator release, corrected coagulopathy, improved liver injury, and reduced mortality.[278] Together, these studies demonstrate that therapeutic strategies which either inhibit thrombin signaling or enhance aPC generation confer

protection in heatstroke, providing the rationale of thrombin-PAR1 axis as target in heatstroke settings (Figure 6.3).

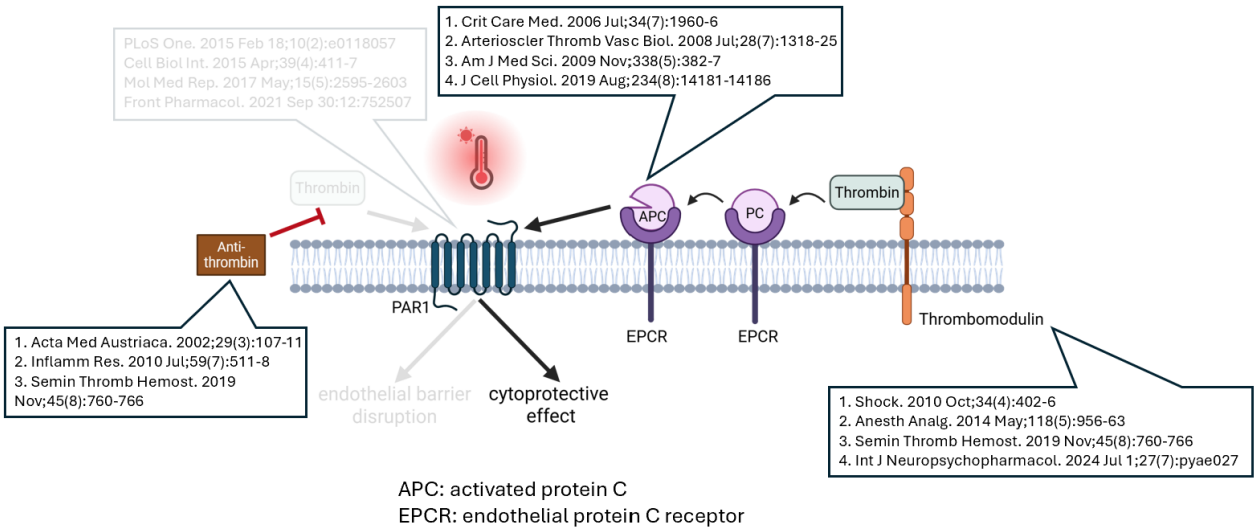

Figure 6.3 Targeting the thrombin–aPC–PAR1 signaling axis in heatstroke. Created with BioRender.com.

6.3.5 *WE thrombin*

W215A/E217A thrombin (WE thrombin) is a recombinant thrombin variant engineered to markedly reduce procoagulant and proinflammatory signaling while preserving the ability to activate the protein C pathway.[3,279] Mutations at residues W215 and E217 diminish thrombin's capacity to cleave fibrinogen and activate platelets and PAR1, yet maintain efficient binding to thrombomodulin, therefore selectively promoting aPC generation.[280,281] As a result, WE thrombin shifts thrombin signaling away from pathogenic thrombin-PAR1 activation and toward aPC-mediated cytoprotective pathways, including endothelial barrier stabilization, anti-inflammatory signaling, and enhanced cell survival (Figure 6.4).[282-284] WE thrombin has demonstrated therapeutic efficacy in multiple thromboinflammatory conditions, including ischemic stroke and relapsing-remitting multiple sclerosis, where it reduced tissue injury and inflammation without increasing hemorrhagic risk.[283,284] During heatstroke, where excessive thrombin generation drives endothelial dysfunction, inflammation, and

microvascular thrombosis, WE thrombin offers a rational therapeutic strategy of cytoprotective aPC-PAR1 signaling without exacerbating thrombin-mediated inflammation or coagulopathy.

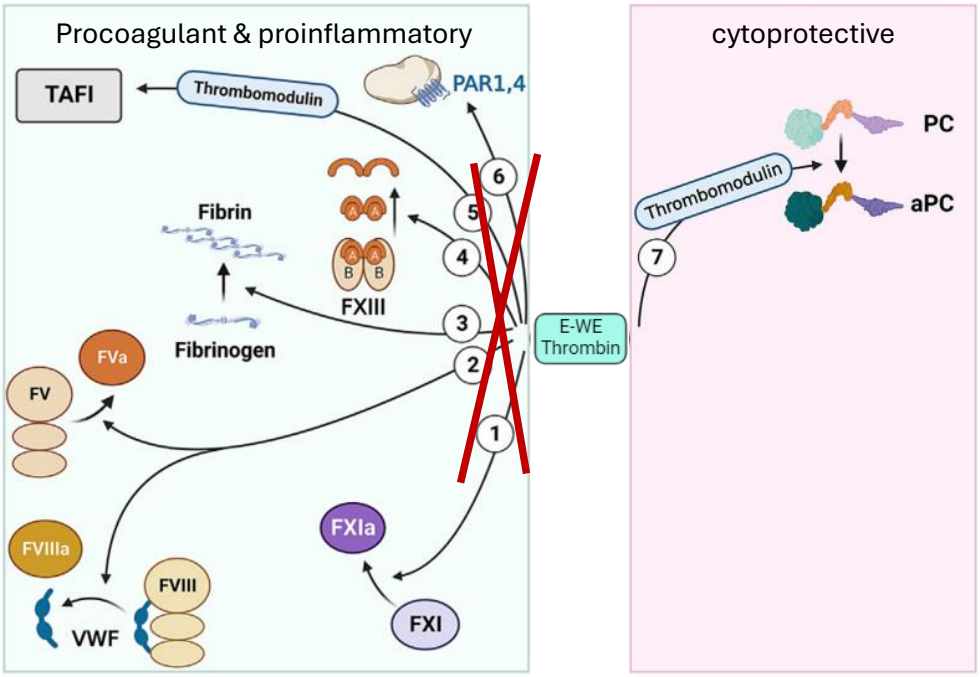

Figure 6.4 Cytoprotective role of E –WE thrombin. Adapted from Guzzetta et al. Hemostasis Management of the Pediatric Surgical Patient chapter 1 (2024). Reprinted with permission.

6.3.6 *WE thrombin on heatstroke*

To evaluate whether WE thrombin mitigates heat-induced endothelial injury, we will apply parallel *in vitro* and *in vivo* experimental designs.[285] *In vitro*, endothelial cells will be treated with vehicle or WE thrombin and exposed to normothermic (37°C) or hyperthermic (42°C) conditions for 2 hours to model acute heat stress (Figure 6.5). Cellular injury and stress responses will be assessed by measuring intracellular reactive oxygen species generation, cell viability, and apoptotic cell death. Activation of inflammatory and oxidative stress signaling pathways will be analyzed to determine whether WE thrombin attenuates heat-induced

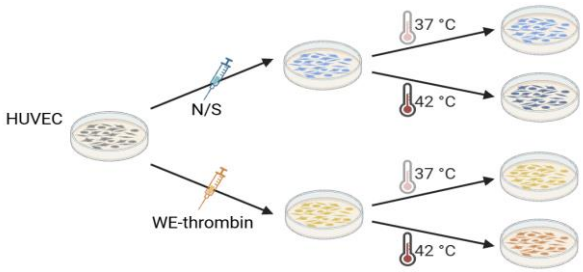

Figure 6.5 *In vitro* Experimental framework for assessing WE thrombin in heatstroke. Create with Biorender.com.

endothelial activation and pro-injury signaling. Endothelial barrier function will be evaluated by measuring transendothelial electrical resistance to quantify changes in endothelial resistance and permeability under heat stress.

In vivo, animals will be assigned to four experimental groups: normal saline at room temperature, normal saline with heat stress at 42°C, WE thrombin at room temperature, and WE thrombin with heat stress at 42°C (Figure 6.6). Outcomes will include survival and lung injury severity assessed by histological analysis and lung wet/dry ratio, as well as endothelial permeability measured by bronchoalveolar lavage fluid protein content. In addition to pulmonary injury, systemic organ dysfunction will be evaluated by assessing kidney injury (serum creatinine and renal histology), liver injury (serum aminotransferases and hepatic histology), intestinal barrier disruption (gut permeability assays and circulating markers of epithelial injury), and brain injury (blood-brain barrier permeability and neuroinflammatory markers). Inflammatory and oxidative stress responses across organs will be assessed by ROS measurements and immunoblotting of stress and apoptotic signaling markers.

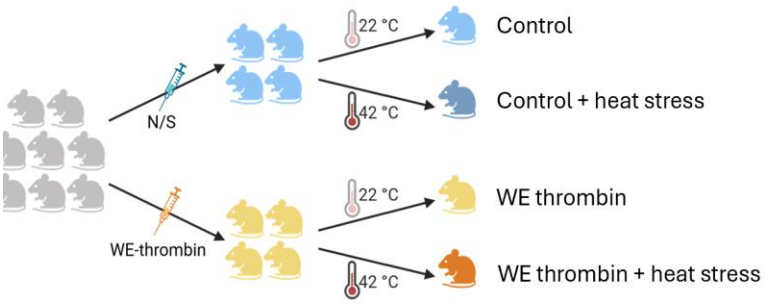

Figure 6.6 *In vivo* experimental framework for assessing WE thrombin in heatstroke. Create with Biorender.com.

References

1 Davie, E. W., Fujikawa, K. & Kisiel, W. The coagulation cascade: initiation, maintenance, and regulation. *Biochemistry* **30**, 10363-10370 (1991). https://doi.org/10.1021/bi00107a001

2 Hoffman, M. & Monroe, D. M., 3rd. A cell-based model of hemostasis. *Thromb Haemost* **85**, 958-965 (2001).

3 Di Cera, E. Thrombin. *Mol Aspects Med* **29**, 203-254 (2008). https://doi.org/10.1016/j.mam.2008.01.001

4 Lira, A. L. *et al.* The physicochemical properties of lipopolysaccharide chemotypes regulate activation of the contact pathway of blood coagulation. *J Biol Chem* **301**, 108110 (2025). https://doi.org/10.1016/j.jbc.2024.108110

5 Esmon, C. T. The interactions between inflammation and coagulation. *Br J Haematol* **131**, 417-430 (2005). https://doi.org/10.1111/j.1365-2141.2005.05753.x

6 Coughlin, S. R. Protease-activated receptors in hemostasis, thrombosis and vascular biology. *J Thromb Haemost* **3**, 1800-1814 (2005). https://doi.org/10.1111/j.1538-7836.2005.01377.x

7 Levi, M. & van der Poll, T. Inflammation and coagulation. *Crit Care Med* **38**, S26-34 (2010). https://doi.org/10.1097/CCM.0b013e3181c98d21

8 Engelmann, B. & Massberg, S. Thrombosis as an intravascular effector of innate immunity. *Nat Rev Immunol* **13**, 34-45 (2013). https://doi.org/10.1038/nri3345

9 Thrombosis: a major contributor to the global disease burden. *J Thromb Haemost* **12**, 1580-1590 (2014). https://doi.org/10.1111/jth.12698

10 Global Health Estimates 2021: Deaths by Cause, Age, Sex, by Country and by Region, 2000-2021. (World Health Organization 2024).

11 Weitz, J. I., Eikelboom, J. W. & Samama, M. M. New antithrombotic drugs: Antithrombotic Therapy and Prevention of Thrombosis, 9th ed: American College of Chest Physicians Evidence-Based Clinical Practice Guidelines. *Chest* **141**, e120S-e151S (2012). https://doi.org/10.1378/chest.11-2294

12 Eikelboom, J. W. *et al.* Risk of bleeding with 2 doses of dabigatran compared with warfarin in older and younger patients with atrial fibrillation: an analysis of the randomized evaluation of long-term anticoagulant therapy (RE-LY) trial. *Circulation* **123**, 2363-2372 (2011). https://doi.org/10.1161/circulationaha.110.004747

13 Gailani, D. & Renné, T. Intrinsic pathway of coagulation and arterial thrombosis. *Arterioscler Thromb Vasc Biol* **27**, 2507-2513 (2007). https://doi.org/10.1161/atvbaha.107.155952

14 Mackman, N. Role of tissue factor in hemostasis, thrombosis, and vascular development. *Arterioscler Thromb Vasc Biol* **24**, 1015-1022 (2004). https://doi.org/10.1161/01.Atv.0000130465.23430.74

15 Bogdanov, V. Y. *et al.* Alternatively spliced human tissue factor: a circulating, soluble, thrombogenic protein. *Nat Med* **9**, 458-462 (2003). https://doi.org/10.1038/nm841

16 Mann, K. G., Butenas, S. & Brummel, K. The dynamics of thrombin formation. *Arterioscler Thromb Vasc Biol* **23**, 17-25 (2003). https://doi.org/10.1161/01.atv.0000046238.23903.fc

17 Berkner, K. L. The vitamin K-dependent carboxylase. *Annu Rev Nutr* **25**, 127-149 (2005). https://doi.org/10.1146/annurev.nutr.25.050304.092713

18 Zwaal, R. F. & Schroit, A. J. Pathophysiologic implications of membrane phospholipid asymmetry in blood cells. *Blood* **89**, 1121-1132 (1997).

19 Gailani, D. & Broze, G. J., Jr. Factor XI activation in a revised model of blood coagulation. *Science* **253**, 909-912 (1991). https://doi.org/10.1126/science.1652157

20 White, G. C., 2nd *et al.* Definitions in hemophilia. Recommendation of the scientific subcommittee on factor VIII and factor IX of the scientific and standardization committee of the International Society on Thrombosis and Haemostasis. *Thromb Haemost* **85**, 560 (2001).

21 Broze, G. J., Jr. & Girard, T. J. Tissue factor pathway inhibitor: structure-function. *Front Biosci (Landmark Ed)* **17**, 262-280 (2012). https://doi.org/10.2741/3926

22 Esmon, C. T. The protein C pathway. *Chest* **124**, 26s-32s (2003). https://doi.org/10.1378/chest.124.3_suppl.26s

23 Mosesson, M. W. Fibrinogen and fibrin structure and functions. *J Thromb Haemost* **3**, 1894-1904 (2005). https://doi.org/10.1111/j.1538-7836.2005.01365.x

24 Muszbek, L., Bereczky, Z., Bagoly, Z., Komáromi, I. & Katona, É. Factor XIII: a coagulation factor with multiple plasmatic and cellular functions. *Physiol Rev* **91**, 931-972 (2011). https://doi.org/10.1152/physrev.00016.2010

25 Renné, T., Schmaier, A. H., Nickel, K. F., Blombäck, M. & Maas, C. *In vivo* roles of factor XII. *Blood* **120**, 4296-4303 (2012). https://doi.org/10.1182/blood-2012-07-292094

26 Renné, T. *et al.* Defective thrombus formation in mice lacking coagulation factor XII. *J Exp Med* **202**, 271-281 (2005). https://doi.org/10.1084/jem.20050664

27 Tucker, E. I. *et al.* Inhibition of factor XI activation attenuates inflammation and coagulopathy while improving the survival of mouse polymicrobial sepsis. *Blood* **119**, 4762-4768 (2012). https://doi.org/10.1182/blood-2011-10-386185

28 Long, A. T., Kenne, E., Jung, R., Fuchs, T. A. & Renné, T. Contact system revisited: an interface between inflammation, coagulation, and innate immunity. *J Thromb Haemost* **14**, 427-437 (2016). https://doi.org/10.1111/jth.13235

29 Schmaier, A. H. The contact activation and kallikrein/kinin systems: pathophysiologic and physiologic activities. *J Thromb Haemost* **14**, 28-39 (2016). https://doi.org/10.1111/jth.13194

30 Raghunathan, V. *et al.* The contact pathway and sepsis. *Res Pract Thromb Haemost* **3**, 331-339 (2019). https://doi.org/10.1002/rth2.12217

31 Colman, R. W. & Schmaier, A. H. Contact system: a vascular biology modulator with anticoagulant, profibrinolytic, antiadhesive, and proinflammatory attributes. *Blood* **90**, 3819-3843 (1997).

32 Maas, C. & Renné, T. Coagulation factor XII in thrombosis and inflammation. *Blood* **131**, 1903-1909 (2018). https://doi.org/10.1182/blood-2017-04-569111

33 Silverberg, M., Dunn, J. T., Garen, L. & Kaplan, A. P. Autoactivation of human Hageman factor. Demonstration utilizing a synthetic substrate. *J Biol Chem* **255**, 7281-7286 (1980).

34 Pixley, R. A., Schapira, M. & Colman, R. W. The regulation of human factor XIIa by plasma proteinase inhibitors. *J Biol Chem* **260**, 1723-1729 (1985).

35 Cichon, S. *et al.* Increased activity of coagulation factor XII (Hageman factor) causes hereditary angioedema type III. *Am J Hum Genet* **79**, 1098-1104 (2006). https://doi.org/10.1086/509899

36 Müller, F. *et al.* Platelet polyphosphates are proinflammatory and procoagulant mediators *in vivo*. *Cell* **139**, 1143-1156 (2009). https://doi.org/10.1016/j.cell.2009.11.001

37 Xu, J. *et al.* Extracellular histones are major mediators of death in sepsis. *Nat Med* **15**, 1318-1321 (2009). https://doi.org/10.1038/nm.2053

38 Fujikawa, K., Chung, D. W., Hendrickson, L. E. & Davie, E. W. Amino acid sequence of human factor XI, a blood coagulation factor with four tandem repeats that are highly homologous with plasma prekallikrein. *Biochemistry* **25**, 2417-2424 (1986). https://doi.org/10.1021/bi00357a018

39 Ponczek, M. B. *et al.* The evolution of factor XI and the kallikrein-kinin system. *Blood Adv* **4**, 6135-6147 (2020). https://doi.org/10.1182/bloodadvances.2020002456

40 Papagrigoriou, E., McEwan, P. A., Walsh, P. N. & Emsley, J. Crystal structure of the factor XI zymogen reveals a pathway for transactivation. *Nat Struct Mol Biol* **13**, 557-558 (2006). https://doi.org/10.1038/nsmb1095

41 Shearin, S. & Venkateswarlu, D. Structural insights into the activation of blood coagulation factor XI zymogen by thrombin: A computational molecular dynamics study. *Biophys Chem* **281**, 106737 (2022). https://doi.org/10.1016/j.bpc.2021.106737

42 Emsley, J., McEwan, P. A. & Gailani, D. Structure and function of factor XI. *Blood* **115**, 2569-2577 (2010). https://doi.org/10.1182/blood-2009-09-199182

43 Vogler, E. A. & Siedlecki, C. A. Contact activation of blood-plasma coagulation. *Biomaterials* **30**, 1857-1869 (2009). https://doi.org/10.1016/j.biomaterials.2008.12.041

44 Wielders, S. J., Béguin, S., Hemker, H. C. & Lindhout, T. Factor XI-dependent reciprocal thrombin generation consolidates blood coagulation when tissue factor is not available. *Arterioscler Thromb Vasc Biol* **24**, 1138-1142 (2004). https://doi.org/10.1161/01.ATV.0000128125.80559.9c

45 von dem Borne, P. A., Meijers, J. C. & Bouma, B. N. Feedback activation of factor XI by thrombin in plasma results in additional formation of thrombin that protects fibrin clots from fibrinolysis. *Blood* **86**, 3035-3042 (1995).

46 Puy, C. *et al.* Activated factor XI increases the procoagulant activity of the extrinsic pathway by inactivating tissue factor pathway inhibitor. *Blood* **125**, 1488-1496 (2015). https://doi.org/10.1182/blood-2014-10-604587

47 Whelihan, M. F., Orfeo, T., Gissel, M. T. & Mann, K. G. Coagulation procofactor activation by factor XIa. *J Thromb Haemost* **8**, 1532-1539 (2010). https://doi.org/10.1111/j.1538-7836.2010.03899.x

48 Matafonov, A. *et al.* Evidence for factor IX-independent roles for factor XIa in blood coagulation. *J Thromb Haemost* **11**, 2118-2127 (2013). https://doi.org/10.1111/jth.12435

49 Rosenthal, R. L., Dreskin, O. H. & Rosenthal, N. New hemophilia-like disease caused by deficiency of a third plasma thromboplastin factor. *Proc Soc Exp Biol Med* **82**, 171-174 (1953). https://doi.org/10.3181/00379727-82-20057

50 Seligsohn, U. Factor XI deficiency in humans. *J Thromb Haemost* **7 Suppl 1**, 84-87 (2009). https://doi.org/10.1111/j.1538-7836.2009.03395.x

51 Bolton-Maggs, P. H., Patterson, D. A., Wensley, R. T. & Tuddenham, E. G. Definition of the bleeding tendency in factor XI-deficient kindreds--a clinical and laboratory study. *Thromb Haemost* **73**, 194-202 (1995).

52 Asakai, R., Chung, D. W., Davie, E. W. & Seligsohn, U. Factor XI deficiency in Ashkenazi Jews in Israel. *N Engl J Med* **325**, 153-158 (1991). https://doi.org/10.1056/nejm199107183250303

53 Gailani, D. & Gruber, A. Targeting factor XI and factor XIa to prevent thrombosis. *Blood* **143**, 1465-1475 (2024). https://doi.org/10.1182/blood.2023020722

54 Büller, H. R. *et al.* Factor XI antisense oligonucleotide for prevention of venous thrombosis. *N Engl J Med* **372**, 232-240 (2015). https://doi.org/10.1056/NEJMoa1405760

55 Cao, Y. *et al.* Liver-heart cross-talk mediated by coagulation factor XI protects against heart failure. *Science* **377**, 1399-1406 (2022). https://doi.org/10.1126/science.abn0910

56 Ji, Y. *et al.* Association of Coagulation Factor XI Level With Cardiovascular Events and Cardiac Function in Community-Dwelling Adults: From ARIC and CHS. *Circulation* **151**, 356-367 (2025). https://doi.org/10.1161/circulationaha.124.070278

57 Daghlas, I. & Gill, D. Human Genetic Evidence Does Not Support a Causal Role for Reduced FXI Levels in Heart Failure Pathogenesis-Brief Report. *Arterioscler Thromb Vasc Biol* **45**, 1664-1669 (2025). https://doi.org/10.1161/atvbaha.125.322971

58 Kaplan, A. P. & Joseph, K. The bradykinin-forming cascade and its role in hereditary angioedema. *Ann Allergy Asthma Immunol* **104**, 193-204 (2010). https://doi.org/10.1016/j.anai.2010.01.007

59 Hasan, A. A., Cines, D. B., Herwald, H., Schmaier, A. H. & Müller-Esterl, W. Mapping the cell binding site on high molecular weight kininogen domain 5. *J Biol Chem* **270**, 19256-19261 (1995). https://doi.org/10.1074/jbc.270.33.19256

60 Couture, R., Blaes, N. & Girolami, J. P. Kinin receptors in vascular biology and pathology. *Curr Vasc Pharmacol* **12**, 223-248 (2014). https://doi.org/10.2174/15701611126661402261216 27

61 Zuraw, B. L. Clinical practice. Hereditary angioedema. *N Engl J Med* **359**, 1027-1036 (2008). https://doi.org/10.1056/NEJMcp0803977

62 Betschel, S. D., Banerji, A., Busse, P. J., Cohn, D. M. & Magerl, M. Hereditary Angioedema: A Review of the Current and Evolving Treatment Landscape. *J Allergy Clin Immunol Pract* **11**, 2315-2325 (2023). https://doi.org/10.1016/j.jaip.2023.04.017

63 Scott, C. F., Silver, L. D., Purdon, A. D. & Colman, R. W. Cleavage of human high molecular weight kininogen by factor XIa *in vitro*. Effect on structure and function. *J Biol Chem* **260**, 10856-10863 (1985).

64 Ewald, G. A. & Eisenberg, P. R. Plasmin-mediated activation of contact system in response to pharmacological thrombolysis. *Circulation* **91**, 28-36 (1995). https://doi.org/10.1161/01.cir.91.1.28

65 Dobó, J. *et al.* Cleavage of kininogen and subsequent bradykinin release by the complement component: mannose-binding lectin-associated serine protease (MASP)-1. *PLoS One* **6**, e20036 (2011). https://doi.org/10.1371/journal.pone.0020036

66 Furie, B. & Furie, B. C. Mechanisms of thrombus formation. *N Engl J Med* **359**, 938-949 (2008). https://doi.org/10.1056/NEJMra0801082

67 Mackman, N. Triggers, targets and treatments for thrombosis. *Nature* **451**, 914-918 (2008). https://doi.org/10.1038/nature06797

68 Collen, D. The plasminogen (fibrinolytic) system. *Thromb Haemost* **82**, 259-270 (1999).

69 Cesarman-Maus, G. & Hajjar, K. A. Molecular mechanisms of fibrinolysis. *Br J Haematol* **129**, 307-321 (2005). https://doi.org/10.1111/j.1365-2141.2005.05444.x

70 Rijken, D. C. & Lijnen, H. R. New insights into the molecular mechanisms of the fibrinolytic system. *J Thromb Haemost* **7**, 4-13 (2009). https://doi.org/10.1111/j.1538-7836.2008.03220.x

71 Weisel, J. W. & Litvinov, R. I. Mechanisms of fibrin polymerization and clinical implications. *Blood* **121**, 1712-1719 (2013). https://doi.org/10.1182/blood-2012-09-306639

72 Longstaff, C. & Kolev, K. Basic mechanisms and regulation of fibrinolysis. *J Thromb Haemost* **13 Suppl 1**, S98-105 (2015). https://doi.org/10.1111/jth.12935

73 Lijnen, H. R. Elements of the fibrinolytic system. *Ann N Y Acad Sci* **936**, 226-236 (2001). https://doi.org/10.1111/j.1749-6632.2001.tb03511.x

74 Mignatti, P. & Rifkin, D. B. Biology and biochemistry of proteinases in tumor invasion. *Physiol Rev* **73**, 161-195 (1993). https://doi.org/10.1152/physrev.1993.73.1.161

75 Wiman, B. & Collen, D. On the mechanism of the reaction between human alpha 2-antiplasmin and plasmin. *J Biol Chem* **254**, 9291-9297 (1979).

76 Hall, S. W., Humphries, J. E. & Gonias, S. L. Inhibition of cell surface receptor-bound plasmin by alpha 2-antiplasmin and alpha 2-macroglobulin. *J Biol Chem* **266**, 12329-12336 (1991).

77 Wiman, B. Plasminogen activator inhibitor 1 (PAI-1) in plasma: its role in thrombotic disease. *Thromb Haemost* **74**, 71-76 (1995).

78 Hunt, B. J. Bleeding and coagulopathies in critical care. *N Engl J Med* **370**, 847-859 (2014). https://doi.org/10.1056/NEJMra1208626

79 Moore, H. B. *et al.* Fibrinolysis Shutdown in Trauma: Historical Review and Clinical Implications. *Anesth Analg* **129**, 762-773 (2019). https://doi.org/10.1213/ane.0000000000004234

80 Gawaz, M., Langer, H. & May, A. E. Platelets in inflammation and atherogenesis. *J Clin Invest* **115**, 3378-3384 (2005). https://doi.org/10.1172/jci27196

81 Wagner, D. D. & Burger, P. C. Platelets in inflammation and thrombosis. *Arterioscler Thromb Vasc Biol* **23**, 2131-2137 (2003). https://doi.org/10.1161/01.Atv.0000095974.95122.Ec

82 Machlus, K. R. & Italiano, J. E., Jr. The incredible journey: From megakaryocyte development to platelet formation. *J Cell Biol* **201**, 785-796 (2013). https://doi.org/10.1083/jcb.201304054

83 Versteeg, H. H., Heemskerk, J. W., Levi, M. & Reitsma, P. H. New fundamentals in hemostasis. *Physiol Rev* **93**, 327-358 (2013). https://doi.org/10.1152/physrev.00016.2011

84 Ruggeri, Z. M. Platelets in atherothrombosis. *Nat Med* **8**, 1227-1234 (2002). https://doi.org/10.1038/nm1102-1227

85 Kapur, R. & Semple, J. W. Platelets as immune-sensing cells. *Blood Adv* **1**, 10-14 (2016). https://doi.org/10.1182/bloodadvances.2016000067

86 Semple, J. W., Italiano, J. E., Jr. & Freedman, J. Platelets and the immune continuum. *Nat Rev Immunol* **11**, 264-274 (2011). https://doi.org/10.1038/nri2956

87 Clemetson, K. J. Platelets and primary haemostasis. *Thromb Res* **129**, 220-224 (2012). https://doi.org/10.1016/j.thromres.2011.11.036

88 Shattil, S. J., Kim, C. & Ginsberg, M. H. The final steps of integrin activation: the end game. *Nat Rev Mol Cell Biol* **11**, 288-300 (2010). https://doi.org/10.1038/nrm2871

89 Li, Z., Delaney, M. K., O'Brien, K. A. & Du, X. Signaling during platelet adhesion and activation. *Arterioscler Thromb Vasc Biol* **30**, 2341-2349 (2010). https://doi.org/10.1161/atvbaha.110.207522

90 Bevers, E. M. & Williamson, P. L. Phospholipid scramblase: an update. *FEBS Lett* **584**, 2724-2730 (2010). https://doi.org/10.1016/j.febslet.2010.03.020

91 Bevers, E. M., Comfurius, P. & Zwaal, R. F. Platelet procoagulant activity: physiological significance and mechanisms of exposure. *Blood Rev* **5**, 146-154 (1991). https://doi.org/10.1016/0268-960x(91)90031-7

92 Semple, J. W. & Freedman, J. Platelets and innate immunity. *Cell Mol Life Sci* **67**, 499-511 (2010). https://doi.org/10.1007/s00018-009-0205-1

93 Italiano, J. E., Jr. & Battinelli, E. M. Selective sorting of alpha-granule proteins. *J Thromb Haemost* **7 Suppl 1**, 173-176 (2009). https://doi.org/10.1111/j.1538-7836.2009.03387.x

94 Rondina, M. T., Weyrich, A. S. & Zimmerman, G. A. Platelets as cellular effectors of inflammation in vascular diseases. *Circ Res* **112**, 1506-1519 (2013). https://doi.org/10.1161/circresaha.113.300512

95 Lindemann, S. *et al.* Activated platelets mediate inflammatory signaling by regulated interleukin 1beta synthesis. *J Cell Biol* **154**, 485-490 (2001). https://doi.org/10.1083/jcb.200105058

96 Yeaman, M. R. Platelets: at the nexus of antimicrobial defence. *Nat Rev Microbiol* **12**, 426-437 (2014). https://doi.org/10.1038/nrmicro3269

97 Frenette, P. S., Johnson, R. C., Hynes, R. O. & Wagner, D. D. Platelets roll on stimulated endothelium *in vivo*: an interaction mediated by endothelial P-selectin. *Proc Natl Acad Sci U S A* **92**, 7450-7454 (1995). https://doi.org/10.1073/pnas.92.16.7450

98 Zarbock, A., Polanowska-Grabowska, R. K. & Ley, K. Platelet-neutrophil-interactions: linking hemostasis and inflammation. *Blood Rev* **21**, 99-111 (2007). https://doi.org/10.1016/j.blre.2006.06.001

99 Gaertner, F. & Massberg, S. Blood coagulation in immunothrombosis-At the frontline of intravascular immunity. *Semin Immunol* **28**, 561-569 (2016). https://doi.org/10.1016/j.smim.2016.10.010

100 Delabranche, X., Helms, J. & Meziani, F. Immunohaemostasis: a new view on haemostasis during sepsis. *Ann Intensive Care* **7**, 117 (2017). https://doi.org/10.1186/s13613-017-0339-5

101 Rock, K. L., Latz, E., Ontiveros, F. & Kono, H. The sterile inflammatory response. *Annu Rev Immunol* **28**, 321-342 (2010). https://doi.org/10.1146/annurev-immunol-030409-101311

102 Medzhitov, R. Origin and physiological roles of inflammation. *Nature* **454**, 428-435 (2008). https://doi.org/10.1038/nature07201

103 Serhan, C. N. & Savill, J. Resolution of inflammation: the beginning programs the end. *Nat Immunol* **6**, 1191-1197 (2005). https://doi.org/10.1038/ni1276

104 Angus, D. C. & van der Poll, T. Severe sepsis and septic shock. *N Engl J Med* **369**, 840-851 (2013). https://doi.org/10.1056/NEJMra1208623

105 Aird, W. C. Phenotypic heterogeneity of the endothelium: I. Structure, function, and mechanisms. *Circ Res* **100**, 158-173 (2007). https://doi.org/10.1161/01.RES.0000255691.76142.4a

106 Oehmcke, S. & Herwald, H. Contact system activation in severe infectious diseases. *J Mol Med (Berl)* **88**, 121-126 (2010). https://doi.org/10.1007/s00109-009-0564-y

107 Nawroth, P. P. *et al.* Tumor necrosis factor/cachectin interacts with endothelial cell receptors to induce release of interleukin 1. *J Exp Med* **163**, 1363-1375 (1986). https://doi.org/10.1084/jem.163.6.1363

108 Ruf, W., Dorfleutner, A. & Riewald, M. Specificity of coagulation factor signaling. *J Thromb Haemost* **1**, 1495-1503 (2003). https://doi.org/10.1046/j.1538-7836.2003.00300.x

109 Iba, T., Levi, M. & Levy, J. H. Sepsis-Induced Coagulopathy and Disseminated Intravascular Coagulation. *Semin Thromb Hemost* **46**, 89-95 (2020). https://doi.org/10.1055/s-0039-1694995

110 Aird, W. C. The role of the endothelium in severe sepsis and multiple organ dysfunction syndrome. *Blood* **101**, 3765-3777 (2003). https://doi.org/10.1182/blood-2002-06-1887

111 Andonegui, G. *et al.* Platelets express functional Toll-like receptor-4. *Blood* **106**, 2417-2423 (2005). https://doi.org/10.1182/blood-2005-03-0916

112 Fuchs, T. A. *et al.* Extracellular DNA traps promote thrombosis. *Proc Natl Acad Sci U S A* **107**, 15880-15885 (2010). https://doi.org/10.1073/pnas.1005743107

113 von Brühl, M. L. *et al.* Monocytes, neutrophils, and platelets cooperate to initiate and propagate venous thrombosis in mice *in vivo*. *J Exp Med* **209**, 819-835 (2012). https://doi.org/10.1084/jem.20112322

114 Matafonov, A. *et al.* Factor XII inhibition reduces thrombus formation in a primate thrombosis model. *Blood* **123**, 1739-1746 (2014). https://doi.org/10.1182/blood-2013-04-499111

115 Mannucci, P. M. & Tuddenham, E. G. The hemophilias--from royal genes to gene therapy. *N Engl J Med* **344**, 1773-1779 (2001). https://doi.org/10.1056/nejm200106073442307

116 Blanchette, V. S. *et al.* Definitions in hemophilia: communication from the SSC of the ISTH. *J Thromb Haemost* **12**, 1935-1939 (2014). https://doi.org/10.1111/jth.12672

117 Peyvandi, F., Duga, S., Akhavan, S. & Mannucci, P. M. Rare coagulation deficiencies. *Haemophilia* **8**, 308-321 (2002). https://doi.org/10.1046/j.1365-2516.2002.00633.x

118 Bolton-Maggs, P. H. *et al.* The rare coagulation disorders--review with guidelines for management from the United Kingdom Haemophilia Centre Doctors' Organisation. *Haemophilia* **10**, 593-628 (2004). https://doi.org/10.1111/j.1365-2516.2004.00944.x

119 Casini, A., de Moerloose, P. & Neerman-Arbez, M. Clinical Features and Management of Congenital Fibrinogen Deficiencies. *Semin Thromb Hemost* **42**, 366-374 (2016). https://doi.org/10.1055/s-0036-1571339

120 Lane, D. A. *et al.* Inherited thrombophilia: Part 1. *Thromb Haemost* **76**, 651-662 (1996).

121 Dahlbäck, B. Advances in understanding pathogenic mechanisms of thrombophilic disorders. *Blood* **112**, 19-27 (2008). https://doi.org/10.1182/blood-2008-01-077909

122 Patnaik, M. M. & Moll, S. Inherited antithrombin deficiency: a review. *Haemophilia* **14**, 1229-1239 (2008). https://doi.org/10.1111/j.1365-2516.2008.01830.x

123 Kujovich, J. L. Factor V Leiden thrombophilia. *Genet Med* **13**, 1-16 (2011). https://doi.org/10.1097/GIM.0b013e3181faa0f2

124 Poort, S. R., Rosendaal, F. R., Reitsma, P. H. & Bertina, R. M. A common genetic variation in the 3'-untranslated region of the prothrombin gene is associated with elevated plasma prothrombin levels and an increase in venous thrombosis. *Blood* **88**, 3698-3703 (1996).

125 Iba, T. *et al.* Diagnosis of sepsis-induced disseminated intravascular coagulation and coagulopathy. *Acute Med Surg* **6**, 223-232 (2019). https://doi.org/10.1002/ams2.411

126 Kearon, C. *et al.* Antithrombotic Therapy for VTE Disease: CHEST Guideline and Expert Panel Report. *Chest* **149**, 315-352 (2016). https://doi.org/10.1016/j.chest.2015.11.026

127 Ansell, J. *et al.* The pharmacology and management of the vitamin K antagonists: the Seventh ACCP Conference on Antithrombotic and Thrombolytic Therapy. *Chest* **126**, 204s-233s (2004). https://doi.org/10.1378/chest.126.3_suppl.204S

128 Ruff, C. T. *et al.* Comparison of the efficacy and safety of new oral anticoagulants with warfarin in patients with atrial fibrillation: a meta-analysis of randomised trials. *Lancet* **383**, 955-962 (2014). https://doi.org/10.1016/s0140-6736(13)62343-0

129 Patel, M. R. *et al.* Rivaroxaban versus warfarin in nonvalvular atrial fibrillation. *N Engl J Med* **365**, 883-891 (2011). https://doi.org/10.1056/NEJMoa1009638

130 Van Gelder, I. C. *et al.* 2024 ESC Guidelines for the management of atrial fibrillation developed in collaboration with the European Association for Cardio-Thoracic Surgery (EACTS). *Eur Heart J* **45**, 3314-3414 (2024). https://doi.org/10.1093/eurheartj/ehae176

131 Schulman, S. & Kearon, C. Definition of major bleeding in clinical investigations of antihemostatic medicinal products in non-surgical patients. *J Thromb Haemost* **3**, 692-694 (2005). https://doi.org/10.1111/j.1538-7836.2005.01204.x

132 Linkins, L. A., Choi, P. T. & Douketis, J. D. Clinical impact of bleeding in patients taking oral anticoagulant therapy for venous thromboembolism: a meta-analysis. *Ann Intern Med* **139**, 893-900 (2003). https://doi.org/10.7326/0003-4819-139-11-200312020-00007

133 Gage, B. F. *et al.* Clinical classification schemes for predicting hemorrhage: results from the National Registry of Atrial Fibrillation (NRAF). *Am Heart J* **151**, 713-719 (2006). https://doi.org/10.1016/j.ahj.2005.04.017

134 Gomes, T. *et al.* Rates of hemorrhage during warfarin therapy for atrial fibrillation. *Cmaj* **185**, E121-127 (2013). https://doi.org/10.1503/cmaj.121218

135 Rubboli, A. *et al.* Antithrombotic therapy in patients treated with oral anticoagulation undergoing coronary artery stenting. An expert consensus document with focus on atrial fibrillation. *Ann Med* **40**, 428-436 (2008). https://doi.org/10.1080/07853890802089786

136 Ogilvie, I. M., Newton, N., Welner, S. A., Cowell, W. & Lip, G. Y. Underuse of oral anticoagulants in atrial fibrillation: a systematic review. *Am J Med* **123**, 638-645.e634 (2010). https://doi.org/10.1016/j.amjmed.2009.11.025

137 Preis, M. *et al.* Factor XI deficiency is associated with lower risk for cardiovascular and venous thromboembolism events. *Blood* **129**, 1210-1215 (2017). https://doi.org/10.1182/blood-2016-09-742262

138 Salomon, O., Steinberg, D. M., Koren-Morag, N., Tanne, D. & Seligsohn, U. Reduced incidence of ischemic stroke in patients with severe factor XI deficiency. *Blood* **111**, 4113-4117 (2008). https://doi.org/10.1182/blood-2007-10-120139

139 Weitz, J. I. *et al.* Milvexian for the Prevention of Venous Thromboembolism. *N Engl J Med* **385**, 2161-2172 (2021). https://doi.org/10.1056/NEJMoa2113194

140 Greco, A. *et al.* Pharmacology and Clinical Development of Factor XI Inhibitors. *Circulation* **147**, 897-913 (2023). https://doi.org/10.1161/circulationaha.122.062353

141 Miller, K. M. & Brenner, M. J. Betrixaban for Extended Venous Thromboembolism Prophylaxis in High-Risk Hospitalized Patients: Putting the APEX Results into Practice. *Drugs* **79**, 291-302 (2019). https://doi.org/10.1007/s40265-019-1059-y

142 Verhamme, P. *et al.* Abelacimab for Prevention of Venous Thromboembolism. *N Engl J Med* **385**, 609-617 (2021). https://doi.org/10.1056/NEJMoa2105872

143 Piccini, J. P. *et al.* Asundexian versus Apixaban in Patients with Atrial Fibrillation. *N Engl J Med* **392**, 23-32 (2025). https://doi.org/10.1056/NEJMoa2407105

144 Rudd, K. E. *et al.* Global, regional, and national sepsis incidence and mortality, 1990-2017: analysis for the Global Burden of Disease Study. *Lancet* **395**, 200-211 (2020). https://doi.org/10.1016/s0140-6736(19)32989-7

145 Schouten, M., Wiersinga, W. J., Levi, M. & van der Poll, T. Inflammation, endothelium, and coagulation in sepsis. *J Leukoc Biol* **83**, 536-545 (2008). https://doi.org/10.1189/jlb.0607373

146 Silasi, R. *et al.* Protective effects of factor XI inhibition by abelacimab in a baboon model of live Staphylococcus aureus sepsis. *J Thromb Haemost* **23**, 3370-3385 (2025). https://doi.org/10.1016/j.jtha.2025.06.018

147 Silasi, R. *et al.* Inhibition of contact-mediated activation of factor XI protects baboons against S aureus-induced organ damage and death. *Blood Adv* **3**, 658-669 (2019). https://doi.org/10.1182/bloodadvances.2018029983

148 Bane, C. E., Jr. *et al.* Factor XI Deficiency Alters the Cytokine Response and Activation of Contact Proteases during Polymicrobial Sepsis in Mice. *PLoS One* **11**, e0152968 (2016). https://doi.org/10.1371/journal.pone.0152968

149 Mandle, R. J., Colman, R. W. & Kaplan, A. P. Identification of prekallikrein and high-molecular-weight kininogen as a complex in human plasma. *Proc Natl Acad Sci U S A* **73**, 4179-4183 (1976). https://doi.org/10.1073/pnas.73.11.4179

150 Bouma, B. N., Vlooswijk, R. A. & Griffin, J. H. Immunologic studies of human coagulation factor XI and its complex with high molecular weight kininogen. *Blood* **62**, 1123-1131 (1983).

151 Asmis, L. M., Asmis, R., Sulzer, I., Furlan, M. & Lämmle, B. Contact system activation in human sepsis - 47kD HK, a marker of sepsis severity? *Swiss Med Wkly* **138**, 142-149 (2008). https://doi.org/10.4414/smw.2008.11788

152 Ruiz-Sanmartín, A. *et al.* Characterization of a proteomic profile associated with organ dysfunction and mortality of sepsis and septic shock. *PLoS One* **17**, e0278708 (2022). https://doi.org/10.1371/journal.pone.0278708

153 Pixley, R. A. *et al.* The contact system contributes to hypotension but not disseminated intravascular coagulation in lethal bacteremia. *In vivo* use of a monoclonal anti-factor XII antibody to block contact activation in baboons. *J Clin Invest* **91**, 61-68 (1993). https://doi.org/10.1172/jci116201

154 Martínez-Brotóns, F., Oncins, J. R., Mestres, J., Amargós, V. & Reynaldo, C. Plasma kallikrein-kinin system in patients with uncomplicated sepsis and septic shock--comparison with cardiogenic shock. *Thromb Haemost* **58**, 709-713 (1987).

155 Mauron, T., Lämmle, B. & Wuillemin, W. A. High molecular weight kininogen is cleaved by FXIa at three sites: Arg409-Arg410, Lys502-Thr503 and Lys325-Lys326. *Thromb Haemost* **83**, 709-714 (2000).

156 Khan, M. M. *et al.* High-molecular-weight kininogen fragments stimulate the secretion of cytokines and chemokines through uPAR, Mac-1, and gC1qR in monocytes. *Arterioscler Thromb Vasc Biol* **26**, 2260-2266 (2006). https://doi.org/10.1161/01.ATV.0000240290.70852.c0

157 Yang, A. *et al.* An essential role of high-molecular-weight kininogen in endotoxemia. *J Exp Med* **214**, 2649-2670 (2017). https://doi.org/10.1084/jem.20161900

158 Ponda, M. P. & Breslow, J. L. Serum stimulation of CCR7 chemotaxis due to coagulation factor XIIa-dependent production of high-molecular-weight kininogen domain 5. *Proc Natl Acad Sci U S A* **113**, E7059-e7068 (2016). https://doi.org/10.1073/pnas.1615671113

159 Morrissey, J. H. & Smith, S. A. Polyphosphate as modulator of hemostasis, thrombosis, and inflammation. *J Thromb Haemost* **13 Suppl 1**, S92-97 (2015). https://doi.org/10.1111/jth.12896

160 Choi, S. H., Smith, S. A. & Morrissey, J. H. Polyphosphate is a cofactor for the activation of factor XI by thrombin. *Blood* **118**, 6963-6970 (2011). https://doi.org/10.1182/blood-2011-07-368811

161 Puy, C. *et al.* Cross-Talk between the Complement Pathway and the Contact Activation System of Coagulation: Activated Factor XI Neutralizes Complement Factor H. *J Immunol* **206**, 1784-1792 (2021). https://doi.org/10.4049/jimmunol.2000398

162 Puy, C. *et al.* Platelet-Derived Short-Chain Polyphosphates Enhance the Inactivation of Tissue Factor Pathway Inhibitor by Activated Coagulation Factor XI. *PLoS One* **11**, e0165172 (2016). https://doi.org/10.1371/journal.pone.0165172

163 Kravtsov, D. V. *et al.* Factor XI contributes to thrombin generation in the absence of factor XII. *Blood* **114**, 452-458 (2009). https://doi.org/10.1182/blood-2009-02-203604

164 Geng, Y. *et al.* The dimeric structure of factor XI and zymogen activation. *Blood* **121**, 3962-3969 (2013). https://doi.org/10.1182/blood-2012-12-473629

165 Eng, J. K., Jahan, T. A. & Hoopmann, M. R. Comet: an open-source MS/MS sequence database search tool. *Proteomics* **13**, 22-24 (2013). https://doi.org/10.1002/pmic.201200439

166 Wilmarth, P. A., Riviere, M. A. & David, L. L. Techniques for accurate protein identification in shotgun proteomic studies of human, mouse, bovine, and chicken lenses. *J Ocul Biol Dis Infor* **2**, 223-234 (2009). https://doi.org/10.1007/s12177-009-9042-6

167 Keller, A., Nesvizhskii, A. I., Kolker, E. & Aebersold, R. Empirical statistical model to estimate the accuracy of peptide identifications made by MS/MS and database search. *Anal Chem* **74**, 5383-5392 (2002). https://doi.org/10.1021/ac025747h

168 Geng, Y. *et al.* Factor XI anion-binding sites are required for productive interactions with polyphosphate. *J Thromb Haemost* **11**, 2020-2028 (2013). https://doi.org/10.1111/jth.12414

169 Choi, S. H., Smith, S. A. & Morrissey, J. H. Polyphosphate accelerates factor V activation by factor XIa. *Thromb Haemost* **113**, 599-604 (2015). https://doi.org/10.1160/th14-06-0515

170 Lin, Y., Pixley, R. A. & Colman, R. W. Kinetic analysis of the role of zinc in the interaction of domain 5 of high-molecular weight kininogen (HK) with heparin. *Biochemistry* **39**, 5104-5110 (2000). https://doi.org/10.1021/bi992048z

171 Pixley, R. A., Lin, Y., Isordia-Salas, I. & Colman, R. W. Fine mapping of the sequences in domain 5 of high molecular weight kininogen (HK) interacting with heparin and zinc. *J Thromb Haemost* **1**, 1791-1798 (2003). https://doi.org/10.1046/j.1538-7836.2003.00291.x

172 Khan, M. M. *et al.* Upregulation of tissue factor in monocytes by cleaved high molecular weight kininogen is dependent on TNF-alpha and IL-1beta. *Am J Physiol Heart Circ Physiol* **298**, H652-658 (2010). https://doi.org/10.1152/ajpheart.00825.2009

173 Tait, J. F. & Fujikawa, K. Identification of the binding site for plasma prekallikrein in human high molecular weight kininogen. A region from residues 185 to 224 of the kininogen light chain retains full binding activity. *J Biol Chem* **261**, 15396-15401 (1986).

174 DeLa Cadena, R. A. & Colman, R. W. The sequence HGLGHGHEQQHGLGHGH in the light chain of high molecular weight kininogen serves as a primary structural feature for zinc-dependent binding to an anionic surface. *Protein Sci* **1**, 151-160 (1992). https://doi.org/10.1002/pro.5560010115

175 Imamura, T. *et al.* Release of a new vascular permeability enhancing peptide from kininogens by human neutrophil elastase. *Biochem Biophys Res Commun* **294**, 423-428 (2002). https://doi.org/10.1016/s0006-291x(02)00490-4

176 Kleniewski, J. & Donaldson, V. H. Comparison of human high molecular weight kininogen digestion by plasma kallikrein and by plasmin. A revised method of purification of high molecular weight kininogen. *J Lab Clin Med* **109**, 469-479 (1987).

177 Schmaier, A. H., Wahl, R., Fisher, S. J. & Brenner, D. The pharmacokinetics of the kininogens. *Thromb Res* **92**, 293-297 (1998). https://doi.org/10.1016/s0049-3848(98)00142-x

178 Suffritti, C., Gualtierotti, R., Zanichelli, A., Vidali, M. & Cugno, M. Measurement of cleaved high-molecular-weight kininogen in patients with hereditary angioedema due to C1-inhibitor deficiency: preanalytical and analytical optimization. *J Immunol Methods* **544**, 113981 (2025). https://doi.org/10.1016/j.jim.2025.113981

179 Palarasah, Y. *et al.* Plasma Kallikrein Cleaved H-kininogen: An End-Point Marker for Contact Activation *in vitro* and ex vivo. *Front Cardiovasc Med* **9**, 873975 (2022). https://doi.org/10.3389/fcvm.2022.873975

180 Nordahl, E. A., Rydengård, V., Mörgelin, M. & Schmidtchen, A. Domain 5 of high molecular weight kininogen is antibacterial. *J Biol Chem* **280**, 34832-34839 (2005). https://doi.org/10.1074/jbc.M507249200

181 Zhang, J. C. *et al.* Two-chain high molecular weight kininogen induces endothelial cell apoptosis and inhibits angiogenesis: partial activity within domain 5. *Faseb j* **14**, 2589-2600 (2000). https://doi.org/10.1096/fj.99-1025com

182 Chavakis, T. *et al.* Different mechanisms define the antiadhesive function of high molecular weight kininogen in integrin- and urokinase receptor-dependent interactions. *Blood* **96**, 514-522 (2000).

183 Weisel, J. W. *et al.* The shape of high molecular weight kininogen. Organization into structural domains, changes with activation, and interactions with prekallikrein, as determined by electron microscopy. *J Biol Chem* **269**, 10100-10106 (1994).

184 Emsley, J., Ma, Y. & Meijers, J. C. M. Structure and interactions of the proteins from the contact system. *Blood* **146**, 1422-1430 (2025). https://doi.org/10.1182/blood.2024025322

185 Li, C. *et al.* Structures of factor XI and prekallikrein bound to domain 6 of high-molecular weight kininogen reveal alternate domain 6 conformations and exosites. *J Thromb Haemost* **21**, 2378-2389 (2023). https://doi.org/10.1016/j.jtha.2023.03.042

186 Puy, C. *et al.* Coagulation factor XI regulates endothelial cell permeability and barrier function *in vitro* and *in vivo*. *Blood* **144**, 1821-1833 (2024). https://doi.org/10.1182/blood.2023022257

187 Ding, C. *et al.* Limited role of kininogen in the host response during gram-negative pneumonia-derived sepsis. *Am J Physiol Lung Cell Mol Physiol* **314**, L397-l405 (2018). https://doi.org/10.1152/ajplung.00288.2017

188 Köhler, J. *et al.* The contact system proteases play disparate roles in streptococcal sepsis. *Haematologica* **105**, 1424-1435 (2020). https://doi.org/10.3324/haematol.2019.223545

189 Yang, A. *et al.* High-molecular-weight kininogen is a critical component of host defense against Escherichia coli sepsis. *Innate Immun* **31**, 17534259251405951 (2025). https://doi.org/10.1177/17534259251405951

190 Ben Nasr, A. *et al.* Absorption of kininogen from human plasma by Streptococcus pyogenes is followed by the release of bradykinin. *Biochem J* **326 (Pt 3)**, 657-660 (1997).

191 Weiner, A. E., Reid, D. E. & Roby, C. C. The Hemostatic Activity of Amniotic Fluid. *Science* **110**, 190-191 (1949). https://doi.org/10.1126/science.110.2851.190

192 Yang, R. L., Lang, M. Z., Li, H. & Qiao, X. M. Immune storm and coagulation storm in the pathogenesis of amniotic fluid embolism. *Eur Rev Med Pharmacol Sci* **25**, 1796-1803 (2021). https://doi.org/10.26355/eurrev_202102_25073

193 Gupta, R. & Cabacungan, E. T. Neonatal Birth Trauma: Analysis of Yearly Trends, Risk Factors, and Outcomes. *J Pediatr* **238**, 174-180.e173 (2021). https://doi.org/10.1016/j.jpeds.2021.06.080

194 Oda, T. *et al.* Amniotic fluid as a potent activator of blood coagulation and platelet aggregation: Study with rotational thromboelastometry. *Thromb Res* **172**, 142-149 (2018). https://doi.org/10.1016/j.thromres.2018.11.001

195 Sarig, G., Klil-Drori, A. J., Chap-Marshak, D., Brenner, B. & Drugan, A. Activation of coagulation in amniotic fluid during normal human pregnancy. *Thromb Res* **128**, 490-495 (2011). https://doi.org/10.1016/j.thromres.2011.03.023

196 Lockwood, C. J. *et al.* Amniotic fluid contains tissue factor, a potent initiator of coagulation. *Am J Obstet Gynecol* **165**, 1335-1341 (1991). https://doi.org/10.1016/0002-9378(91)90363-v

197 Hu, Y. *et al.* Coagulation signaling from amniotic fluid to fetal skin. *Blood Adv* **6**, 5538-5541 (2022). https://doi.org/10.1182/bloodadvances.2022007971

198 Hell, L. *et al.* Procoagulant extracellular vesicles in amniotic fluid. *Transl Res* **184**, 12-20.e11 (2017). https://doi.org/10.1016/j.trsl.2017.01.003

199 Benson, M. D., Cheema, N., Kaufman, M. W., Goldschmidt, R. A. & Beaumont, J. L. Uterine intravascular fetal material and coagulopathy at peripartum hysterectomy. *Gynecol Obstet Invest* **73**, 158-161 (2012). https://doi.org/10.1159/000332373

200 Marik, P. E. & Plante, L. A. Venous thromboembolic disease and pregnancy. *N Engl J Med* **359**, 2025-2033 (2008). https://doi.org/10.1056/NEJMra0707993

201 Devis, P. & Knuttinen, M. G. Deep venous thrombosis in pregnancy: incidence, pathogenesis and endovascular management. *Cardiovasc Diagn Ther* **7**, S309-s319 (2017). https://doi.org/10.21037/cdt.2017.10.08

202 Shorey-Kendrick, L. E. *et al.* The amniotic fluid proteome changes across gestation in humans and rhesus macaques. *Sci Rep* **13**, 17039 (2023). https://doi.org/10.1038/s41598-023-44125-3

203 Bhatti, G. *et al.* The amniotic fluid proteome changes with term labor and informs biomarker discovery in maternal plasma. *Sci Rep* **13**, 3136 (2023). https://doi.org/10.1038/s41598-023-28157-3

204 Bhatti, G. *et al.* The amniotic fluid proteome changes with gestational age in normal pregnancy: a cross-sectional study. *Sci Rep* **12**, 601 (2022). https://doi.org/10.1038/s41598-021-04050-9

205 Nakayasu, E. S. *et al.* MPLEx: a Robust and Universal Protocol for Single-Sample Integrative Proteomic, Metabolomic, and Lipidomic Analyses. *mSystems* **1** (2016). https://doi.org/10.1128/mSystems.00043-16

206 Kyle, J. E. *et al.* LIQUID: an-open source software for identifying lipids in LC-MS/MS-based lipidomics data. *Bioinformatics* **33**, 1744-1746 (2017). https://doi.org/10.1093/bioinformatics/btx046

207 Uszyński, W., Żekanowska, E., Uszyński, M. & Kieszkowski, P. Activation contact system (ACS) and tissue factor (TF) in human amniotic fluid: measurements of ACS components and TF, and some implications on the pathophysiology of amniotic fluid embolism. *Thromb Res* **135**, 699-702 (2015). https://doi.org/10.1016/j.thromres.2014.10.014

208 Zhou, J. *et al.* Procoagulant activity and phosphatidylserine of amniotic fluid cells. *Thromb Haemost* **101**, 845-851 (2009).

209 Cunningham, F. G. *et al.* in *Williams Obstetrics, 25e* 83-87 (McGraw-Hill Education, 2018).

210 Beall, M. H., van den Wijngaard, J. P., van Gemert, M. J. & Ross, M. G. Amniotic fluid water dynamics. *Placenta* **28**, 816-823 (2007). https://doi.org/10.1016/j.placenta.2006.11.009

211 Brace, R. A. Physiology of amniotic fluid volume regulation. *Clin Obstet Gynecol* **40**, 280-289 (1997). https://doi.org/10.1097/00003081-199706000-00005

212 Suliburska, J. *et al.* Concentrations of Mineral in Amniotic Fluid and Their Relations to Selected Maternal and Fetal Parameters. *Biol Trace Elem Res* **172**, 37-45 (2016). https://doi.org/10.1007/s12011-015-0557-3

213 Dale, B. A., Holbrook, K. A., Kimball, J. R., Hoff, M. & Sun, T. T. Expression of epidermal keratins and filaggrin during human fetal skin development. *J Cell Biol* **101**, 1257-1269 (1985). https://doi.org/10.1083/jcb.101.4.1257

214 Schlegel, R. A. & Williamson, P. Phosphatidylserine, a death knell. *Cell Death Differ* **8**, 551-563 (2001). https://doi.org/10.1038/sj.cdd.4400817

215 Gluck, L. *et al.* Diagnosis of the respiratory distress syndrome by amniocentesis. *Am J Obstet Gynecol* **109**, 440-445 (1971). https://doi.org/10.1016/0002-9378(71)90342-5

216 Miki, T., Lehmann, T., Cai, H., Stolz, D. B. & Strom, S. C. Stem Cell Characteristics of Amniotic Epithelial Cells. *Stem Cells* **23**, 1549-1559 (2005). https://doi.org/10.1634/stemcells.2004-0357

217 Underwood, M. A., Gilbert, W. M. & Sherman, M. P. Amniotic fluid: not just fetal urine anymore. *J Perinatol* **25**, 341-348 (2005). https://doi.org/10.1038/sj.jp.7211290

218 Baugh, R. J., Broze, G. J., Jr. & Krishnaswamy, S. Regulation of extrinsic pathway factor Xa formation by tissue factor pathway inhibitor. *J Biol Chem* **273**, 4378-4386 (1998). https://doi.org/10.1074/jbc.273.8.4378

219 Warr, T. A., Rao, L. V. & Rapaport, S. I. Disseminated intravascular coagulation in rabbits induced by administration of endotoxin or tissue factor: effect of anti-tissue factor antibodies and measurement of plasma extrinsic pathway inhibitor activity. *Blood* **75**, 1481-1489 (1990).

220 Bishop, A. J., Israels, L. G., Chernick, V. & Israels, E. D. Placental Transfer of Intravascular Coagulation between Mother and Fetus. *Pediatric Research* **5**, 113-125 (1971). https://doi.org/10.1203/00006450-197103000-00003

221 Knight, J. S., Branch, D. W. & Ortel, T. L. Antiphospholipid syndrome: advances in diagnosis, pathogenesis, and management. *Bmj* **380**, e069717 (2023). https://doi.org/10.1136/bmj-2021-069717

222 Furukawa, S. *et al.* A rare case of amniotic fluid embolism with massive platelet aggregations in pulmonary capillaries. *J Obstet Gynaecol Res* **36**, 397-400 (2010). https://doi.org/10.1111/j.1447-0756.2009.01151.x

223 Salem, H. H., Walters, W. A., Perkin, J. L., Handley, C. J. & Firkin, B. G. Aggregation of human platelets by amniotic fluid. *Br J Obstet Gynaecol* **89**, 733-737 (1982). https://doi.org/10.1111/j.1471-0528.1982.tb05100.x

224 Kobayashi, H., Matsubara, S., Yoshimoto, C., Shigetomi, H. & Imanaka, S. Tissue Factor Pathway Inhibitors as Potential Targets for Understanding the Pathophysiology of Preeclampsia. *Biomedicines* **11** (2023). https://doi.org/10.3390/biomedicines11051237

225 Miyagi, E. *et al.* Validation of tissue factor pathway inhibitor 2 as a specific biomarker for preoperative prediction of clear cell carcinoma of the ovary. *Int J Clin Oncol* **26**, 1336-1344 (2021). https://doi.org/10.1007/s10147-021-01914-y

226 Morla, S. *et al.* Procoagulant activities of skeletal muscle and cardiac myosins require both myosin protein and myosin-associated anionic phospholipids. *Blood* **137**, 1839-1842 (2021). https://doi.org/10.1182/blood.2020008580

227 Liu, E. H., Shailaja, S., Koh, S. C. & Lee, T. L. An assessment of the effects on coagulation of midtrimester and final-trimester amniotic fluid on whole blood by Thrombelastograph analysis. *Anesth Analg* **90**, 333-336 (2000). https://doi.org/10.1097/00000539-200002000-00018

228 Harnett, M. J., Hepner, D. L., Datta, S. & Kodali, B. S. Effect of amniotic fluid on coagulation and platelet function in pregnancy: an evaluation using thromboelastography. *Anaesthesia* **60**, 1068-1072 (2005). https://doi.org/10.1111/j.1365-2044.2005.04373.x

229 Perez-Riverol, Y. *et al.* The PRIDE database resources in 2022: a hub for mass spectrometry-based proteomics evidences. *Nucleic Acids Res* **50**, D543-d552 (2022). https://doi.org/10.1093/nar/gkab1038

230 Moore, E. E. *et al.* Trauma-induced coagulopathy. *Nat Rev Dis Primers* **7**, 30 (2021). https://doi.org/10.1038/s41572-021-00264-3

231 Tisherman, S. A. *et al.* Detailed description of all deaths in both the shock and traumatic brain injury hypertonic saline trials of the Resuscitation Outcomes Consortium. *Ann Surg* **261**, 586-590 (2015). https://doi.org/10.1097/sla.0000000000000837

232 Moore, H. B. *et al.* Fibrinolysis shutdown phenotype masks changes in rodent coagulation in tissue injury versus hemorrhagic shock. *Surgery* **158**, 386-392 (2015). https://doi.org/10.1016/j.surg.2015.04.008

233 Cralley, A. L. *et al.* Hemorrhagic shock and tissue injury provoke distinct components of trauma-induced coagulopathy in a swine model. *Eur J Trauma Emerg Surg* **49**, 1079-1089 (2023). https://doi.org/10.1007/s00068-022-02148-x

234 Johansson, P. I., Windeløv, N. A., Rasmussen, L. S., Sørensen, A. M. & Ostrowski, S. R. Blood levels of histone-complexed DNA fragments are associated with coagulopathy, inflammation and endothelial damage early after trauma. *J Emerg Trauma Shock* **6**, 171-175 (2013). https://doi.org/10.4103/0974-2700.115327

235 Liu, T. *et al.* High dynamic range characterization of the trauma patient plasma proteome. *Mol Cell Proteomics* **5**, 1899-1913 (2006). https://doi.org/10.1074/mcp.M600068-MCP200

236 Deguchi, T. K., Deguchi, H., Guo, Z., Elias, D. J. & Griffin, J. H. Plasma skeletal muscle myosin phenotypes identified by immunoblotting are associated with pulmonary embolism occurrence in young adults. *Thromb Res* **189**, 88-92 (2020). https://doi.org/10.1016/j.thromres.2020.02.020

237 Yoon, S. J., Seiler, S. H., Kucherlapati, R. & Leinwand, L. Organization of the human skeletal myosin heavy chain gene cluster. *Proc Natl Acad Sci U S A* **89**, 12078-12082 (1992). https://doi.org/10.1073/pnas.89.24.12078

238 Deguchi, H., Morla, S. & Griffin, J. H. Novel blood coagulation molecules: Skeletal muscle myosin and cardiac myosin. *J Thromb Haemost* **19**, 7-19 (2021). https://doi.org/10.1111/jth.15097

239 Deguchi, H. *et al.* Novel exomic rare variants associated with venous thrombosis. *Br J Haematol* **190**, 783-786 (2020). https://doi.org/10.1111/bjh.16613

240 Deguchi, H. *et al.* Prothrombotic skeletal muscle myosin directly enhances prothrombin activation by binding factors Xa and Va. *Blood* **128**, 1870-1878 (2016). https://doi.org/10.1182/blood-2016-03-707679

241 Morla, S. *et al.* Skeletal muscle myosin promotes coagulation by binding factor XI via its A3 domain and enhancing thrombin-induced factor XI activation. *J Biol Chem* **298**, 101567 (2022). https://doi.org/10.1016/j.jbc.2022.101567

242 Zilberman-Rudenko, J. *et al.* Cardiac Myosin Promotes Thrombin Generation and Coagulation *In vitro* and *In vivo*. *Arterioscler Thromb Vasc Biol* **40**, 901-913 (2020). https://doi.org/10.1161/atvbaha.120.313990

243 Coleman, J. R. *et al.* Full-length plasma skeletal muscle myosin isoform deficiency is associated with coagulopathy in acutely injured patients. *J Thromb Haemost* **20**, 1385-1389 (2022). https://doi.org/10.1111/jth.15695

244 Kolev, K. *et al.* Myosin: a noncovalent stabilizer of fibrin in the process of clot dissolution. *Blood* **101**, 4380-4386 (2003). https://doi.org/10.1182/blood-2002-10-3227

245 Peterson, D. F. *et al.* Role of single-dose intravenous iron therapy for the treatment of anaemia after orthopaedic trauma: protocol for a pilot randomised controlled trial. *BMJ Open* **13**, e069070 (2023). https://doi.org/10.1136/bmjopen-2022-069070

246 Coleman, J. R. *et al.* Cardiac and Skeletal Muscle Myosin Exert Procoagulant Effects. *Shock* **52**, 554-555 (2019). https://doi.org/10.1097/shk.0000000000001426

247 McCall, J. R., Jacocks, H. M., Baden, D. G. & Bourdelais, A. J. Development of a competitive fluorescence-based synaptosome binding assay for brevetoxins. *Harmful Algae* **19**, 85-91 (2012). https://doi.org/10.1016/j.hal.2012.06.003

248 Hulme, E. C. & Trevethick, M. A. Ligand binding assays at equilibrium: validation and interpretation. *Br J Pharmacol* **161**, 1219-1237 (2010). https://doi.org/10.1111/j.1476-5381.2009.00604.x

249 Eble, J. A. Titration ELISA as a Method to Determine the Dissociation Constant of Receptor Ligand Interaction. *J Vis Exp* (2018). https://doi.org/10.3791/57334

250 Du, J. *et al.* Insight into the mechanism of myosin-fibrin gelation induced by non-disulfide covalent cross-linking. *Food Res Int* **156**, 111168 (2022). https://doi.org/10.1016/j.foodres.2022.111168

251 Regoeczi, E. Occlusion of plasma proteins by human fibrin: studies using trace-labelled proteins. *Br J Haematol* **14**, 279-290 (1968). https://doi.org/10.1111/j.1365-2141.1968.tb01498.x

252 Janmey, P. A., Lamb, J. A., Ezzell, R. M., Hvidt, S. & Lind, S. E. Effects of actin filaments on fibrin clot structure and lysis. *Blood* **80**, 928-936 (1992).

253 Du, J., Hu, Z. & Mitch, W. E. Molecular mechanisms activating muscle protein degradation in chronic kidney disease and other catabolic conditions. *Eur J Clin Invest* **35**, 157-163 (2005). https://doi.org/10.1111/j.1365-2362.2005.01473.x

254 Moore, H. B. *et al.* Defining trauma-induced coagulopathy with respect to future implications for patient management: Communication from the SSC of the ISTH. *J Thromb Haemost* **18**, 740-747 (2020). https://doi.org/10.1111/jth.14690

255 Brohi, K., Singh, J., Heron, M. & Coats, T. Acute traumatic coagulopathy. *J Trauma* **54**, 1127-1130 (2003). https://doi.org/10.1097/01.Ta.0000069184.82147.06

256 Cohen, M. J. *et al.* Critical role of activated protein C in early coagulopathy and later organ failure, infection and death in trauma patients. *Ann Surg* **255**, 379-385 (2012). https://doi.org/10.1097/SLA.0b013e318235d9e6

257 Cohen, M. J. *et al.* Clinical and mechanistic drivers of acute traumatic coagulopathy. *J Trauma Acute Care Surg* **75**, S40-47 (2013). https://doi.org/10.1097/TA.0b013e31828fa43d

258 Chapman, M. P. *et al.* Overwhelming tPA release, not PAI-1 degradation, is responsible for hyperfibrinolysis in severely injured trauma patients. *J Trauma Acute Care Surg* **80**, 16-23; discussion 23-15 (2016). https://doi.org/10.1097/ta.0000000000000885

259 Warren, J. D., Blumbergs, P. C. & Thompson, P. D. Rhabdomyolysis: a review. *Muscle Nerve* **25**, 332-347 (2002). https://doi.org/10.1002/mus.10053

260 Chatzizisis, Y. S., Misirli, G., Hatzitolios, A. I. & Giannoglou, G. D. The syndrome of rhabdomyolysis: complications and treatment. *Eur J Intern Med* **19**, 568-574 (2008). https://doi.org/10.1016/j.ejim.2007.06.037

261 Vicedo-Cabrera, A. M. *et al.* The burden of heat-related mortality attributable to recent human-induced climate change. *Nat Clim Chang* **11**, 492-500 (2021). https://doi.org/10.1038/s41558-021-01058-x

262 Epstein, Y. & Yanovich, R. Heatstroke. *N Engl J Med* **380**, 2449-2459 (2019). https://doi.org/10.1056/NEJMra1810762

263 Leon, L. R. & Helwig, B. G. Heatstroke: role of the systemic inflammatory response. *J Appl Physiol (1985)* **109**, 1980-1988 (2010). https://doi.org/10.1152/japplphysiol.00301.2010

264 Iba, T., Connors, J. M., Levi, M. & Levy, J. H. Heatstroke-induced coagulopathy: Biomarkers, mechanistic insights, and patient management. *EClinicalMedicine* **44**, 101276 (2022). https://doi.org/10.1016/j.eclinm.2022.101276

265 Coughlin, S. R. How the protease thrombin talks to cells. *Proc Natl Acad Sci U S A* **96**, 11023-11027 (1999). https://doi.org/10.1073/pnas.96.20.11023

266 Kahn, M. L. *et al.* A dual thrombin receptor system for platelet activation. *Nature* **394**, 690-694 (1998). https://doi.org/10.1038/29325

267 Minami, T. *et al.* Thrombin and phenotypic modulation of the endothelium. *Arterioscler Thromb Vasc Biol* **24**, 41-53 (2004). https://doi.org/10.1161/01.Atv.0000099880.09014.7d

268 Xu, Q. *et al.* Heat stress-induced disruption of endothelial barrier function is via PAR1 signaling and suppressed by Xuebijing injection. *PLoS One* **10**, e0118057 (2015). https://doi.org/10.1371/journal.pone.0118057

269 Griffin, J. H., Zlokovic, B. V. & Mosnier, L. O. Activated protein C: biased for translation. *Blood* **125**, 2898-2907 (2015). https://doi.org/10.1182/blood-2015-02-355974

270 Mosnier, L. O., Zlokovic, B. V. & Griffin, J. H. The cytoprotective protein C pathway. *Blood* **109**, 3161-3172 (2007). https://doi.org/10.1182/blood-2006-09-003004

271 Mosnier, L. O., Sinha, R. K., Burnier, L., Bouwens, E. A. & Griffin, J. H. Biased agonism of protease-activated receptor 1 by activated protein C caused by noncanonical cleavage at Arg46. *Blood* **120**, 5237-5246 (2012). https://doi.org/10.1182/blood-2012-08-452169

272 Soh, U. J. & Trejo, J. Activated protein C promotes protease-activated receptor-1 cytoprotective signaling through β-arrestin and dishevelled-2 scaffolds. *Proc Natl Acad Sci U S A* **108**, E1372-1380 (2011). https://doi.org/10.1073/pnas.1112482108

273 Finigan, J. H. *et al.* Activated protein C protects against ventilator-induced pulmonary capillary leak. *Am J Physiol Lung Cell Mol Physiol* **296**, L1002-1011 (2009). https://doi.org/10.1152/ajplung.90555.2008

274 Wang, J., Yang, L., Rezaie, A. R. & Li, J. Activated protein C protects against myocardial ischemic/reperfusion injury through AMP-activated protein kinase signaling. *J Thromb Haemost* **9**, 1308-1317 (2011). https://doi.org/10.1111/j.1538-7836.2011.04331.x

275 Bouchama, A., Hammami, M. M., Haq, A., Jackson, J. & al-Sedairy, S. Evidence for endothelial cell activation/injury in heatstroke. *Crit Care Med* **24**, 1173-1178 (1996). https://doi.org/10.1097/00003246-199607000-00018

276 Hagiwara, S. *et al.* High-dose antithrombin III prevents heatstroke by attenuating systemic inflammation in rats. *Inflamm Res* **59**, 511-518 (2010). https://doi.org/10.1007/s00011-009-0155-y

277 Chen, C. M. *et al.* Activated protein C therapy in a rat heatstroke model. *Crit Care Med* **34**, 1960-1966 (2006). https://doi.org/10.1097/01.Ccm.0000224231.01533.B1

278 Hagiwara, S. *et al.* Recombinant thrombomodulin prevents heatstroke by inhibition of high-mobility group box 1 protein in sera of rats. *Shock* **34**, 402-406 (2010). https://doi.org/10.1097/SHK.0b013e3181d492e4

279 Cantwell, A. M. & Di Cera, E. Rational design of a potent anticoagulant thrombin. *J Biol Chem* **275**, 39827-39830 (2000). https://doi.org/10.1074/jbc.C000751200

280 Berny-Lang, M. A. *et al.* Thrombin mutant W215A/E217A treatment improves neurological outcome and reduces cerebral infarct size in a mouse model of ischemic stroke. *Stroke* **42**, 1736-1741 (2011). https://doi.org/10.1161/strokeaha.110.603811

281 Gruber, A., Cantwell, A. M., Di Cera, E. & Hanson, S. R. The thrombin mutant W215A/E217A shows safe and potent anticoagulant and antithrombotic effects *in vivo*. *J Biol Chem* **277**, 27581-27584 (2002). https://doi.org/10.1074/jbc.C200237200

282 Tucker, E. I. *et al.* The protein C activator AB002 rapidly interrupts thrombus development in baboons. *Blood* **135**, 689-699 (2020). https://doi.org/10.1182/blood.2019002771

283 Verbout, N. G. *et al.* Cytoprotective WE thrombin reduces disease severity in a murine model of relapsing-remitting multiple sclerosis. *Am J Physiol Cell Physiol* **326**, C40-c49 (2024). https://doi.org/10.1152/ajpcell.00377.2023

284 Verbout, N. G. *et al.* Thrombin mutant W215A/E217A treatment improves neurological outcome and attenuates central nervous system damage in experimental autoimmune encephalomyelitis. *Metab Brain Dis* **30**, 57-65 (2015). https://doi.org/10.1007/s11011-014-9558-8

285 Tsai, H. Y. *et al.* Pharmacological Activation Of Aldehyde Dehydrogenase 2 Protects Against Heatstroke-Induced Acute Lung Injury by Modulating Oxidative Stress and Endothelial Dysfunction. *Front Immunol* **12**, 740562 (2021). https://doi.org/10.3389/fimmu.2021.740562

Biographical sketch

Chih-Jen Yang was born on October 14, 1985, in Kaohsiung, Taiwan, to Li-Hua Yang. He earned his Doctor of Medicine degree from the National Defense Medical Center in 2011 and completed postgraduate and residency training in Emergency Medicine at Tri-Service General Hospital in Taipei, Taiwan.

From 2011 to 2013, Chih-Jen served as a military physician at the Infantry Training Center. He became a board-certified Emergency Medicine physician in 2018 and served as an attending physician at Tri-Service General Hospital from 2019 to 2021, with additional certification as an Emergency Medical Service physician in New Taipei City.

In the Fall of 2021, Chih-Jen began doctoral training in Biomedical Engineering at Oregon Health & Science University under the mentorship of Dr. Owen J. T. McCarty. His research focuses on coagulation and inflammation, particularly the contact pathway and trauma-associated coagulopathy, integrating molecular mechanisms with clinically relevant pathophysiology.

Chih-Jen has received several honors, including the National Innovation Award in Taiwan (2019), the Philadelphia Congress Local Organizing Committee Legacy Fund Award (2024), and the ISTH Early Career Award (2025). He also serves as a reviewer for the American Journal of Emergency Medicine and is ECFMG certified. He plans to pursue an academic career bridging translational research with clinical emergency medicine when he is back in Taiwan. His publications and presentations are listed below.

EDUCATION / TRAINING

2021 - 2026 Oregon Health & Science University, Ph.D., Biomed Engineering

2004 - 2011 National Defense Medical Center, M.D.

CERTIFICATE / LICENSE

2025 - Certificate, Educational Commission for Foreign Medical Graduates, USA

2018 - Diplomate, Emergency Medicine, Taiwan.

2018 - Emergency Medical Service Physician, New Taipei City, Taiwan

WORK EXPERIENCE

2019 - 2021 Attending Physician in Emergency Medicine, Tri-Service General Hospital, Taiwan.

2014 - 2018 Resident Physician in Emergency Medicine, Tri-Service General Hospital, Taiwan.

RESEARCH EXPERIENCE

2021 - 2026 Molecular mechanisms of coagulation across physiological and injury states, Department of Biomedical Engineering, PI: Owen J.T. McCarty, PhD, Oregon Health & Science University, Portland, OR.

2017 The protective effect of heat shock protein in heatstroke induced acute lung injury and the modulated mechanism of microRNA-424, Department of Emergency Medicine, PI: Shih-Hung Tsai, MD PhD. Tri-Service General Hospital, Taiwan.

REVIEWER

2023 - Journal of Acute Medicine

2020 - American Journal of Emergency Medicine

AWARDS & HONORS

2025 ISTH Early Career Award

2024 Philadelphia Congress Local Organizing Committee Legacy Fund Award

2019 National Innovation Award, Taiwan

RESEARCH PUBLICATIONS

1. **CJ Yang**, Rodolf AA, Garay JP, et al. J Trauma Acute Care Surg (Accepted)
2. Peterson DF, McKibben NS, Duke VR, Hutchison CE, **Yang CJ**, Curtis C, et al. Intravenous iron therapy mitigates patient-reported fatigue, inflammation, and platelet dysfunction following orthopaedic trauma: evidence from a pilot randomized clinical trial. Bone Research (submitted)
3. CW Hong, **CJ Yang**, SJ Chen, YL Shih, FW Chang, JC Wang. Comparing Performance Outcomes of Emergency Medicine-Trained vs. Non-Emergency Medicine-Trained Physicians in Emergency Departments. J Acute Med. 2025 Jun 1;15(2):58-65.
4. **Yang CJ**, Shorey-Kendrick LE, Puy C, et al. Characterization of the procoagulant phenotype of amniotic fluid across gestation in rhesus macaques and humans. Res Pract Thromb Haemost. 2025 Jan 9;9(1):102676.
5. Zhang Y, **Yang CJ**, Melrose AR, et al. Pharmacological effects of small molecule BCR-ABL tyrosine kinase inhibitors on platelet function. J Pharmacol Exp Ther. 2025 Jan;392(1):100020.
6. Cheng SY, Lin TY, **Yang CJ**. Respiratory Distress After Wisdom Tooth Extraction. J Emerg Med. 2023 Aug;65(2):e144-e145
7. Peterson DF, McKibben NS, Hutchison CE, Lancaster K, **Yang CJ**, et al. Role of single-dose intravenous iron therapy for the treatment of anaemia after orthopaedic trauma: protocol for a pilot randomised controlled trial. BMJ Open. 2023 Mar 21;13(3):e069070.
8. Lin CH, Lin HY, **Yang CJ**, Chen SJ. Man on Noninvasive Positive Airway Pressure Ventilation With Throat Pain. J Acute Med. 2022 Dec 1;12(4):158-160.
9. Lin CH, **Yang CJ**, Tsai YD, et al. Young Man with Epigastric Pain. Ann Emerg Med. 2022 Sep;80(3):e25-e26.
10. Elstrott BK, Lakshman HHS, Melrose AR, Jordan KR, Martens KL, **Yang CJ**, et al. Platelet reactivity and platelet count in women with iron deficiency treated with intravenous iron. Res Pract Thromb Haemost. 2022 Mar 23;6(2):e12692.
11. Lin CH, Li LY, Tsai SH, Lin CY, **Yang CJ**. Male with Dyspnea. Ann Emerg Med. 2019 Sep;74(3):454-461
12. **Yang CJ**, Tsai SH, Wang JC, Chang WC, Lin CY, Tang ZC, Hsu HH. Association between acute aortic dissection and the distribution of aortic calcification. PLoS One. 2019 Jul 11;14(7):e0219461.
13. **Yang CJ**, Tsai SH, Chien WC, Chung CH, Dai NT, Tzeng YS, Chen SJ, Wu DC, Chen CJ. The crowd-out effect of a mass casualty incident: Experience from a dust explosion with multiple burn injuries Medicine (Baltimore). 2019 May;98(18):e15457
14. **Yang CJ**, Chung CH, Chen SJ, Liao WI, Tsai YD, Wang JJ, Chien WC. Association between Aortic Aneurysm and Ulcerative Colitis: A Nationwide Taiwanese Retrospective Cohort Study. J Med Sci 2019;39(2):74-80
15. An YC, **Yang CJ**, Chen CY, Kuo CY, Tsai YD. Man with Sore Throat and Dyspnea. Ann Emerg Med. 2019 May;73(5):e73-e74

16. Hong CW, **Yang CJ**, Tsai SH. Woman with Abdominal Pain. Ann Emerg Med. 2019 Apr;73(4):e39-e40
17. An YC, **Yang CJ**, Chang KH, Yeh KM, Tsai SH. Young Male with Low Back Pain. Ann Emerg Med. 2019 Apr;73(4):e43-e44
18. **Yang CJ**, Shih CC, Lin CH. Middle Aged Male with Acute Abdominal Pain. Ann Emerg Med. 2019 Mar;73(3):e17-e18
19. Lu MC, **Yang CJ**, Tsai SH, Hung CC, Chen SJ. Intraperitoneal hemorrhage after cupping therapy. Hong Kong Journal of Emergency Medicine https://doi.org/10.1177/1024907918784076
20. Chiu FH, **Yang CJ**, Huang CK, Lin CY, Tsai SH. Spontaneous chordae tendineae rupture during peripartum. American Journal of Emergency Medicine. 2018 Jun;36(6):1127. e1-1127.e3
21. Huang CK, **Yang CJ**, Shih CC, Tsai SH. Elderly Female with Dyspnea. Ann Emerg Med. 2017 Dec;70(6):e51-e52
22. **Yang CJ**, Liao WI, Tang ZC, Wang JC, Lee CH, Chang WC, Hsu CW, Tang SE, Tsai SH. Glycated hemoglobin A1c-based adjusted glycemic variables in patients with diabetes presenting with acute exacerbation of chronic obstructive pulmonary disease. Int J Chron Obstruct Pulmon Dis. 2017 Jul 3;12:1923-1932
23. Cheng SY, **Yang CJ**, Lee CH, Liu SC, Kuo CY, Lee JC, Shih CP. The association of superior attachment of uncinate process with pneumatization of middle turbinate: a computed tomographic analysis European Archives of Otorhinolaryngology. 2017 Apr; 274(4):1905-1910
24. **Yang CJ**, Liao WI, Wang JC, Tsai CL, Lee JT, Peng GS, Lee CH, Hsu CW, Tsai SH. Usefulness of glycated hemoglobin A1c-based adjusted glycemic variables in diabetic patients presenting with acute ischemic stroke. Am J Emerg Med. 2017 Sep;35(9):1240-1246
25. **Yang CJ**, Cheng SY, Cheng CC, Tang CT, Tsai SH. Vertebral artery ruptures manifesting as hoarseness Braz J Otorhinolaryngol. 2020 Dec;86 Suppl 1(Suppl 1):11-13.
26. **Yang CJ**, Chen PC, Lin CS, Tsai CL, Tsai SH. Thrombolytic therapy-associated acute myocardial infarction in patients with acute ischemic stroke: A treatment dilemma. Am J Emerg Med. 2017 May;35(5):804. e1-804.e3

RESEARCH ABSTRACTS & PRESENTATIONS

1. Activated Coagulation Factor XI Generates Kininogen Cleavage Products to Activate Immune Cells. (Poster) ISTH 2025.
2. Characterization of Interactions Between Skeletal Muscle Myosin and Activated Factor XI. (Oral) ISTH 2024.
3. Role of Circulating Phosphatidylserine in the Procoagulant Activity of Amniotic Fluid. (Poster) ISTH 2024
4. Effects of Intravenous Iron Infusion on Platelet Function in Orthopedic Trauma Patients. (Poster) ISTH 2024.